Catalog of Earthquake Hypocenters at Alaskan Volcanoes: January 1 through December 31, 2005

By James P. Dixon[1], Scott D. Stihler[2], John A. Power[1], Guy Tytgat[2], Steve Estes[2], and Stephen R. McNutt[2]

Open-File Report 2006-1264

2006

U.S. DEPARTMENT OF THE INTERIOR
U.S. GEOLOGICAL SURVEY

[1] U. S. Geological Survey Alaska Science Center, Alaska Volcano Observatory
4200 University Drive, Anchorage, AK 99508-4667
[2] University of Alaska Fairbanks - Geophysical Institute,
903 Koyukuk Drive, Fairbanks, AK 99775-7320

CONTENTS

Introduction

The Alaska Volcano Observatory (AVO), a cooperative program of the U.S. Geological Survey, the Geophysical Institute of the University of Alaska Fairbanks, and the Alaska Division of Geological and Geophysical Surveys, has maintained seismic monitoring networks at historically active volcanoes in Alaska since 1988 (Figure 1). The primary objectives of the seismic program are the real-time seismic monitoring of active, potentially hazardous, Alaskan volcanoes and the investigation of seismic processes associated with active volcanism. This catalog presents calculated earthquake hypocenters and seismic phase arrival data, and details changes in the seismic monitoring program for the period January 1 through December 31, 2005. A list of previous catalogs can be found in Appendix G.

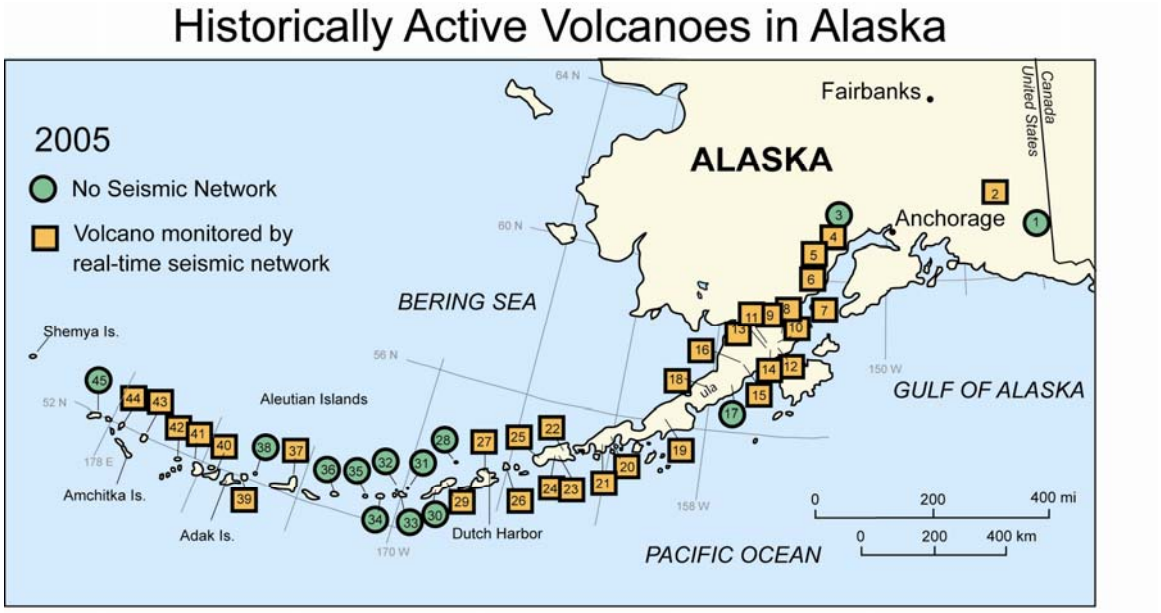

Figure 1. Orange squares show the location of all Alaskan volcanoes seismically instrumented by AVO as of 2005. Volcanoes with no documented historical unrest but still considered hazardous, based on late Holocene eruptive activity are italicized.

The AVO seismograph network was used to monitor the seismic activity at thirty-two volcanoes within Alaska in 2005 (Figure 1). The network was augmented by two new subnetworks to monitor the Semisopochnoi Island volcanoes and Little Sitkin Volcano. Seismicity at these volcanoes was still being studied at the end of 2005 and has not yet been added to the list of permanently monitored volcanoes in the AVO weekly update. Following an extended period of monitoring to determine the background seismicity at the Mount Peulik, Ukinrek Maars, and Korovin Volcano, formal monitoring of these volcanoes began in 2005. AVO located 9,012 earthquakes in 2005 (Table 1).

Table 1: Number of earthquakes located per year by AVO for the last ten years.

Year	Earthquakes located per year	Volcanoes with seismograph networks
1996	6,466	15
1997	2,930	17
1998	2,873	19
1999	2,769	21
2000	1,551	21
2001	1,427	23
2002	7,242	24
2003	3,911	27
2004	6,928	28
2005	9,012	32

Monitoring highlights in 2005 include: (1) seismicity at Mount Spurr remaining above background, starting in February 2004, through the end of the year and into 2006; (2) an increase in seismicity at Augustine Volcano starting in May 2005, and continuing through the end of the year into 2006; (3) volcanic tremor and seismicity related to low-level strombolian activity at Mount Veniaminof in January to March and September; and (4) a seismic swarm at Tanaga Volcano in October and November (Table 2).

This catalog includes: (1) descriptions and locations of seismic instrumentation deployed in the field in 2005; (2) a description of earthquake detection, recording, analysis, and data archival systems; (3) a description of seismic velocity models used for earthquake locations; (4) a summary of earthquakes located in 2005; and (5) an accompanying UNIX tar-file with a summary of earthquake origin times, hypocenters, magnitudes, phase arrival

times, and location quality statistics; daily station usage statistics; and all HYPOELLIPSE (Lahr, 1999) files used to determine the earthquake locations in 2005.

Table 2: Highlights of Alaskan volcanic seismicity in 2005.

Dates	Volcano	Event
January –December 2005	Spurr	Continuing increased seismicity
May-December 2005	Augustine	Increased seismicity
Jan–March, and Sept 2005	Veniaminof	Minor ash bursts recorded in seismic data
October-November 2005	Tanaga	Increased seismicity

Instrumentation

In 2005, the AVO seismograph network was expanded to 187 permanent seismograph stations (Appendix B, C). The AVO seismograph network is composed of 23 subnetworks with 4-20 seismograph stations per subnetwork, and nine regional seismograph stations. Two new subnetworks were installed in September to monitor Mount Cerberus on Semisopochnoi Island and Little Sitkin Volcano. In response to continued increased seismic activity at Mount Spurr, 11 temporary broadband stations were installed in June and removed three months later (Appendix B). Five regional stations (CNP, HOM, NNL, SYI, XLV), reported in previous earthquake catalogs, have been removed from the AVO inventory since they were inaccurately listed as AVO stations in the past.

Of the 187 permanent seismograph stations (265 different components) operated by AVO, 150 were short-period vertical-component seismograph stations. All these stations had either Mark Products L4 or Teledyne-Geotech S13 seismometers with a one-second natural period. AVO also operated 23 three-component, short-period instruments during the catalog period. The instruments used at sites with three component sensors were Mark Products L22 seismometers with a 0.5-second period, Mark Products L4-3D seismometers with a one-second period and Teledyne-Geotech S13 seismometers with a one-second natural period. A total of 15 broadband stations were operated with either Guralp CMG-40T seismometers (frequency range: 0.102Hz to 50 Hz) or Guralp CMG-6TD seismometers (frequency range: 0.033Hz to 50 Hz).

The majority of the short-period stations were digitized at 100 samples/second (sps). The Semisopochnoi and Little Sitkin subnetworks were recorded at 50 sps due to limitations in the broadband telemetry between the recording hub and Anchorage. Broadband stations were digitized at 50 sps. Typical calibration curves for seismometers used in the AVO seismograph network are shown in Figures 2-6.

Data from short-period seismograph stations were telemetered using voltage-controlled oscillators (VCOs) to transform the signals generated by the seismometer in response to ground velocity from a voltage to a frequency-modulated carrier suitable for transmission over a radio link or telephone circuit. AVO primarily used McVCO (McChesney, 1999) to modulate signals in the field. In rare cases, other VCO models were used instead of the McVCO but these are being replaced by McVCOs as stations are visited. These signals were transmitted via UHF and VHF radio to communication hubs located in Adak, Akutan, Amchitka Island, Anchorage, Cold Bay, Dutch Harbor, Homer, Kenai, King Cove, King Salmon, Port Heiden, Sourdough, and Tolsona. Data were then digitized at the Adak, Amchitka Island, Dutch Harbor, Homer, Kenai and King Salmon communication

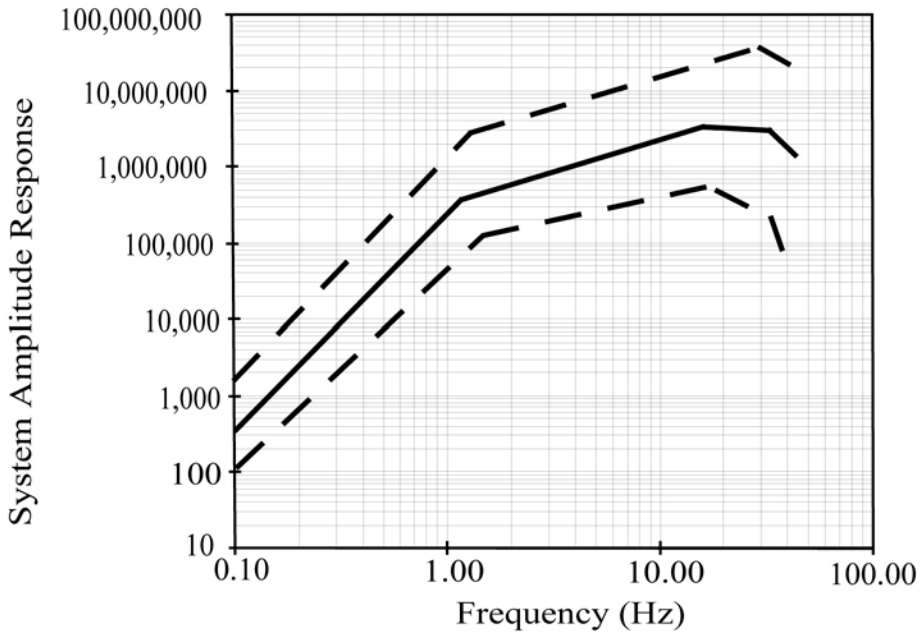

Figure 2. Representative displacement response curves for the 138 short-period stations using a Mark Products L4 or L4-3D seismometer. The solid line illustrates the typical calibration curve and the dashed lines show the range of calibration curves for all AVO stations using an L4 or L4-3D seismometer.

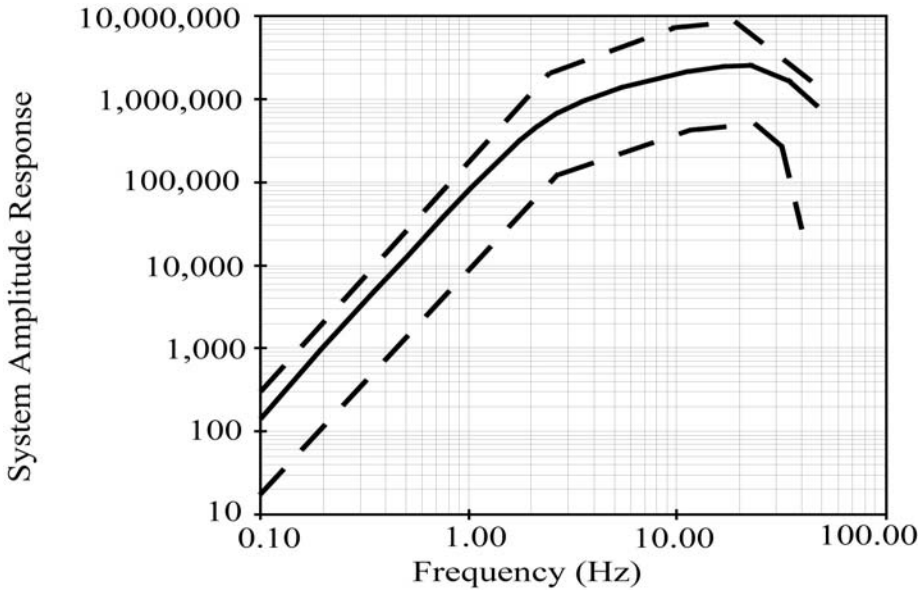

Figure 3. Representative displacement response curves for the 17 short-period stations using a Mark Products L22 seismometer. The solid line illustrates the typical calibration curve and the dashed lines show the range of calibration curves for all AVO stations using an L22 seismometer.

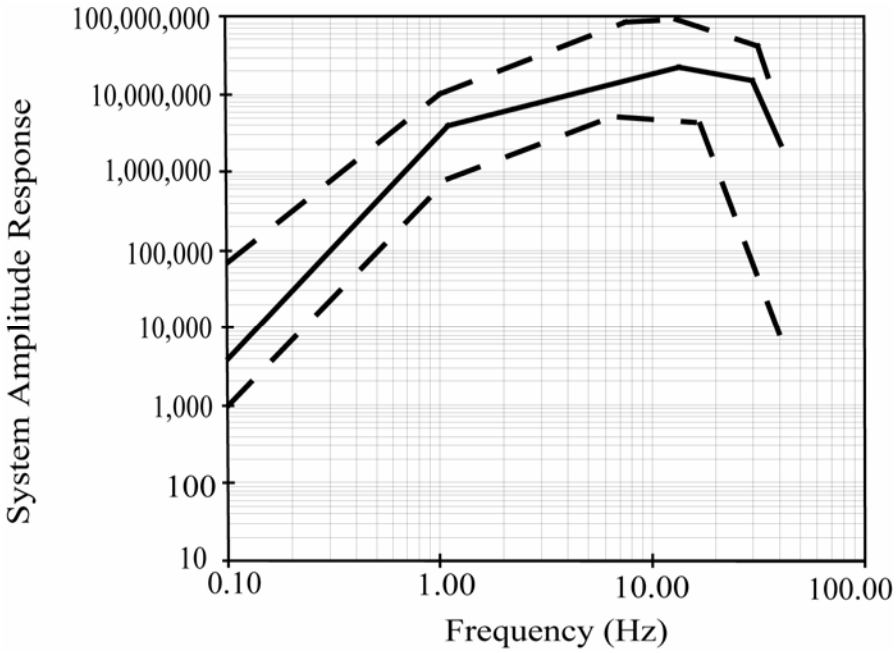

Figure 4. Representative displacement response curves for the 16 short-period stations using a Teledyne-Geotech S13 seismometer. The solid line illustrates the typical calibration curve and the dashed lines show the range of calibration curves for all AVO stations using an S13 seismometer.

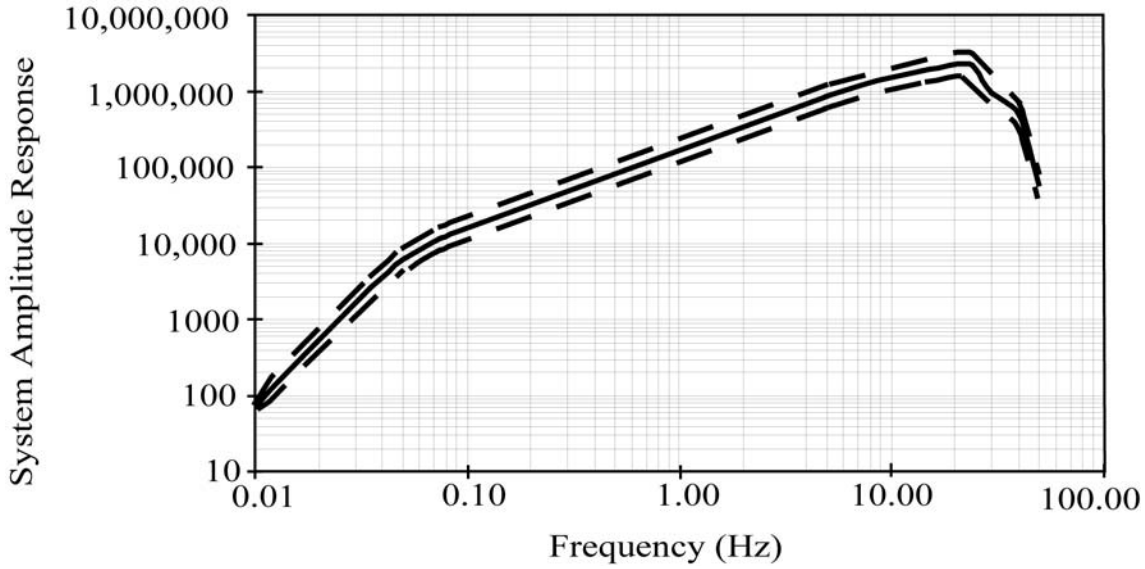

Figure 5. Representative displacement response curves for the two broadband stations using a Guralp CMG-40T seismometer. The solid line illustrates the typical calibration curve and the dashed lines show the range of calibration curves for all AVO stations using a Guralp CMG-40T seismometer.

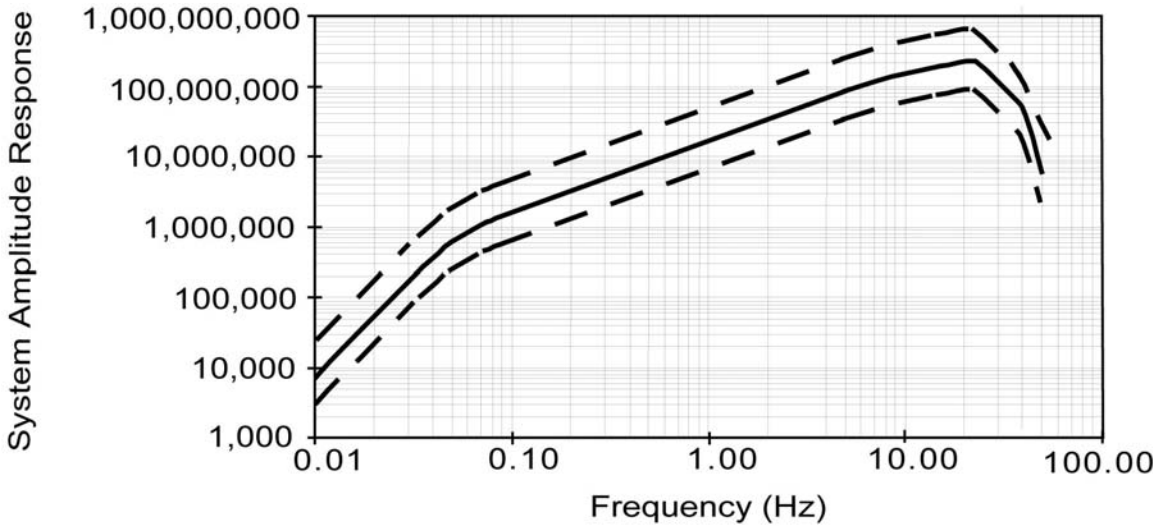

Figure 6. Representative displacement response curves for the 24 broadband stations using a Guralp CMG-6TD seismometer. The solid line illustrates the typical calibration curve and the dashed lines show the range of calibration curves for all AVO stations using a Guralp CMG-6TD seismometer.

hubs and directed to AVO offices via high speed digital circuits. From all other hubs, signals were relayed via leased telephone circuits to AVO offices in Anchorage and Fairbanks where the signals were digitized. Data from broadband seismograph stations were digitized at the seismograph station site and transmitted digitally using spread-spectrum radios to communication hubs in Akutan, Anchorage, Dutch Harbor, Homer, and King Salmon. These data were forwarded to AVO offices in Fairbanks and Anchorage via leased telephone circuits.

Locations and descriptions for all AVO stations operated during 2005 are contained in Appendix B. Maps showing the locations of permanent stations with respect to individual volcanoes are contained in Appendix C. Estimates of each station's operational status for the catalog period are shown in Appendix D. Other station information, such as calibration information contained in the file CALDATA.PRM, is available within the associated compressed UNIX tar-file.

Data Acquisition and Reduction

Data acquisition for the AVO seismograph network was accomplished with duplicate EARTHWORM systems (Johnson, 1995) located at AVO offices in Anchorage and Fairbanks, providing a backup in case of failure at either location. Data were recorded in continuous and event detected modes. Event detected data were collected using the EARTHWORM modules, ‘Carlstatrig’ and ‘Carlsubtrig’. The ‘Carlstatrig’ parameters were set as follows: Long-term-average (LTA) time = 8 seconds, Ratio = 2.3, and Quiet = 4. ‘Carlsubtrig’ was modified such that a two-letter code was appended to the filename of each trigger to identify which subnetwork triggered or if the event was a regional trigger. If four or more subnetworks triggered on the same event, all data were saved in a single trigger. These network codes are summarized in Table 3. All data are saved in Seismic Analysis Code (SAC) (Goldstein and others, 1999) format.

Event triggers were processed daily using the interactive seismic data analysis program XPICK (Robinson, 1990), and the earthquake location program HYPOELLIPSE (Lahr, 1999). Each event trigger was visually inspected and false triggers were deleted.

Table 3: Volcano Subnetwork Designators

Volcano Subnetwork	Network Code
Akutan	ak
Aniakchak	an
Augustine	au
Semisopochnoi	ce
Dutton	dt
Iliamna	il
Gareloi	ga
Great Sitkin	gs
Kanaga	ki
Katmai	ka
Volcano	ko
Little Sitkin	ls
Makushin	ma
Okmok	ok
Pavlof	pv
Peulik	pl
Redoubt	rd
Regional Event	rg
Shishaldin	sh
Spurr	sp
Tanaga	ta
Veniaminof	vn
Westdahl	we
Wrangell	wa

Each subsequent event was identified by a classification code (Table 4) and stored as a comment in the event location pick file. This classification system was modeled after that described by Lahr and others (1994). Earthquakes with a P and S-wave separation of greater than five seconds on the closest station were assumed to come from non-volcanic sources and were typically discarded. Each hypocenter was checked using a computer algorithm that identified events that did not meet the following minimum parameters: three P-phases, two S-phases, and standard hypocentral errors less than 15 km. If upon revaluation, the minimum parameters could not be met, the event was removed from the final catalog listing. For all the 2005 earthquakes in the AVO catalog, the average root-mean-square travel-time error was 0.126 seconds.

Table 4: Classification codes

Event Classification	Classification Code
Volcano-Tectonic (VT)	a
Low-Frequency (LF)	b
Hybrid	h
Regional-Tectonic	E
Teleseismic	T
Shore-Ice	i
Calibrations	C
Other non-seismic	o
Cause unknown	x

Seismic Velocity Models

During 2005, AVO employed 11 local seismic velocity models and one regional seismic velocity model (Appendix E) to locate earthquakes at monitored volcanoes. All velocity models were one-dimensional models utilizing horizontal layers to approximate the local seismic velocity structures. Each model, with one exception, assumed a series of constant velocity layers. The single exception was the Akutan velocity model (Power and others, 1996), which had a velocity gradient in the top layer overlying a half-space of constant velocity.

One or more vertical cylinders were used to model the volcanic source zones on all volcanoes where a local volcano-specific velocity model was used. Earthquakes within these cylindrical volumes were located with a local model and earthquakes outside of the cylindrical volumes were located with the regional model. All cylindrical volumes had a radius of 20 km with the exception of the cylinders centered on Shishaldin Volcano and Mount Veniaminof. The cylinder centered on Shishaldin Volcano had a radius of 30 km in order to encompass Isanotski Peaks. The cylinder centered on Mount Veniaminof also had a radius of 30 km because of the large size of the volcanic edifice. The top of each cylinder is set at three km above sea level and the bottom is set at a depth of 50 km with respect to sea level.

The Akutan, Augustine (Power, 1988), Iliamna (Roman and others, 2001), Tanaga (Power, personal communication, 2005), Veniaminof (Sánchez, 2005) and Westdahl (Dixon, 2005) velocity models were used to locate hypocenters that fell within cylindrical

volumes described above, centered on each respective volcano. The Cold Bay velocity model (McNutt and Jacob, 1986) was used to locate earthquakes that fell within single cylindrical volumes centered on Mount Dutton and Pavlof Volcano. Earthquakes on Fisher Caldera, Isanotski Peaks, and Shishaldin Volcano that fell within the cylindrical regions centered on Shishaldin Volcano were also located using the Cold Bay velocity model. Five overlapping cylinders defined the area in which the Spurr velocity model (Jolly and others, 1994) was used, four overlapping cylinders defined the area in which the Redoubt velocity model (Lahr and others, 1994) was used, and four overlapping cylinders defined the area in which the Katmai model (Searcy, 2003) was used. The Andreanof velocity model (Toth and Kisslinger, 1984) was used to locate earthquakes within a volume defined by three cylinders centered on Kanaga Volcano, Mount Moffet, and Great Sitkin Volcano. Specific velocity models for Aniakchak Crater, Mount Gareloi, Korovin Volcano, Makushin Volcano, Okmok Volcano, Mount Peulik, and Mount Wrangell were not available in 2005 and the regional velocity model (Fogleman and others, 1993) was used to locate earthquakes near these volcanoes. The cylindrical model parameters, regional velocity model, and volcano-specific models used to locate earthquakes in this report are summarized in Appendix E. Figures showing the volcanic source zones modeled by multiple cylinders are shown in Appendix F.

Seismicity

The 9,012 earthquakes located in 2005 represent the highest annual total determined by AVO in the last ten calendar years and an increase from the 6,928 earthquakes located in 2004 (Dixon, 2005). Of the earthquakes located in the last two years, a total of 6,105 earthquakes in 2004 and 8,146 earthquakes in 2005 were located within 20 km of an active volcanic center. The numbers of located events at volcanic centers in the last two years, by seismograph subnetwork, are shown in Table 5.

Using the 2005 earthquake catalog, the magnitude of completeness (Mc) for each subnetwork was calculated (Table 5). The Mc is the lowest magnitude at which we are reasonably certain that all events with a magnitude greater than or equal to the Mc were detected. The Mc was determined using a maximum likelihood estimate of the inflection

point in the frequency magnitude distribution using the seismology analysis software ZMAP (Weimer, 2001).

Four volcanoes, Mount Spurr, Augustine Volcano, Mount Veniaminof and Tanaga Volcano, showed significant unrest in 2005 and the level of concern color code for each was raised above green. Of these volcanic centers, Mount Veniaminof and Mount Spurr did not have an increased level of activity compared to the seismicity in 2004. At Mount

Table 5: Number of earthquakes located for each seismograph subnetwork in 2004 and 2005 within 20 km of the volcanic centers in each subnetwork. The totals for 2005 are broken into three event types: volcanic-tectonic (VT), low-frequency (LF) and other (all other possible event types shown in Table 4). Magnitude of completeness (Mc) for AVO seismograph subnetworks used the 2005 catalog. The Semisopochnoi, Dutton, Little Sitkin subnetworks were not included because there were too few earthquakes in 2005 to calculate a Mc.

Volcano Subnetwork	Earthquakes located in 2004	Earthquakes located in 2005	2005 VT	2005 LF	2005 Other	2005 Mc
Akutan	120	100	99	1	0	0.3
Aniakchak	5	33	4	29	0	1.0
Augustine	241	1,204	1,180	11	13	-0.9
Semisopochnoi	n/a	6	6	0	0	n/a
Dutton	40	13	13	0	0	n/a
Gareloi	376	580	61	519	0	1.0
Great Sitkin	65	51	50	1	0	0.3
Iliamna	805	979	920	59	0	-0.4
Kanaga	32	42	42	0	0	0.9
Katmai Cluster	976	1,084	1,072	11	1	0.6
Korovin	n/a	74	74	5	0	0.7
Little Sitkin	n/a	15	15	0	0	n/a
Makushin	233	135	133	2	0	0.6
Okmok	44	71	66	5	0	0.9
Pavlof	58	32	14	18	0	1.5
Peulik	5	48	47	1	0	0.8
Redoubt	94	70	68	2	0	0.1
Shishaldin	98	208	11	197	0	0.9
Spurr	2,616	2,317	1,980	320	17	0.2
Tanaga	11	925	920	4	1	1.0
Veniaminof	21	24	24	0	0	1.1
Westdahl	166	27	24	3	0	0.9
Wrangell	99	106	15	91	0	0.7
Totals	6,105	8,146	6,833	1,279	34	0.7

Veniaminof, the seismic activity is dominated by non-locatable tremor and low-frequency events. The seismicity in 2005 at Mount Spurr is similar to that in 2004 (Power, 2004) because the volcanic unrest started in mid 2004 and continued through 2005. At Augustine Volcano an increase in the seismicity above background was first noted in May 2005. By the end of 2005 the seismicity was well above background due to an episode of unrest continuing into 2006. The majority of the seismicity at Tanaga Volcano occurred in October and November 2005. By the end of 2005, the level of seismicity at Tanaga Volcano had returned to background levels.

The subnetworks at Iliamna and Aniakchak showed increased seismic activity. The number of earthquakes was elevated for Iliamna compared to background for the first half of 2005 but remained at background for the last part of 2005. At Aniakchak Crater, there were three small burst of activity (one in January, two in December) accounting for the increased seismicity at this volcanic center. The seismicity at Shishaldin Volcano and Mount Gareloi also increased from that in 2004. The seismicity at both volcanic centers is dominated by low-frequency events that are near the limits of detection. Small changes in factors like background noise or volcanic activity can cause widely varying apparent seismicity rates.

The seismicity in the Katmai volcanic cluster for 2005 was similar to that in 2004. Several volcanic centers (Trident Volcano, Mount Katmai and Mount Martin) showed elevated seismic activity at times in 2005. The seismicity at Trident Volcano was consistently higher than normal through most of 2005. Declines in seismicity were noted at Novarupta, Mount Martin and Mount Mageik in regular AVO staff reports. Novarupta was the only volcanic center that consistently showed lower levels of seismicity in 2005. Seismicity rates at the Wrangell, Redoubt, Pavlof, Akutan, Okmok, Kanaga, and Great Sitkin subnetworks, were also similar to that in 2004.

Seismicity at Mount Dutton, Makushin Volcano and Westdahl Peak in 2005 declined compared to that in 2004. Near Mount Dutton, the rate of seismicity is low but highly variable. No station outages are responsible for the apparent decrease in seismicity. The decrease in seismicity at Makushin Volcano is related in part to several long-lived station outages lasting six months or longer. The seismicity at Westdahl Peak would show

no change to the previous year if a cluster of activity in January 2004 is removed from the earthquake totals.

The subnetwork at Mount Peulik was installed in mid-2004 and the subnetworks at Korovin, Semisopochnoi and Little Sitkin were established in 2005. No comparisons could be made for these four subnetworks.

Summary

Between January 1 and December 31, 2005, AVO located 9,012 earthquakes of which 8,146 occurred at or near volcanoes in Alaska. Monitoring highlights in 2005 include: elevated seismicity and low level tremor at Mount Veniaminof, and an increase in seismicity at Mount Spurr, Augustine Volcano and Tanaga Volcano, all related to episodes of volcanic unrest. New seismic subnetworks were installed on Semisopochnoi Island and Little Sitkin Volcano.

Available for download with this report is a compressed Unix tar-file containing a summary listing of earthquake hypocenters and all the necessary HYPOELLIPSE input files to recalculate the hypocenters including station locations and calibrations, seismic velocity models, and phase information. The reader should refer to Lahr (1999) for information on file formats and instructions for configuring and running the location program HYPOELLIPSE. Archives of waveform data are maintained on DVD-ROM at AVO offices in Fairbanks and Anchorage.

Acknowledgements

The contents of this report reflect a great deal of hard work by a large number of people including AVO, AEIC, and USGS personnel and various students, interns and volunteers. We thank Silvio DeAngelis and Mike Thorne for formal reviews of the text and figures.

References

Dixon, J. P., J. A. Power, and S. D. Stihler (2005). Seismic Observations of Westdahl volcano and Western Unimak Island Alaska: 1999-2005, *Eos Trans. AGU*, **86**, no. 52, Fall Meeting Suppl. Abstract S11b-0169.

Fogleman, K. A., J. C. Lahr, C. D. Stephens, and R. A. Page (1993). Earthquake locations determined by the southern Alaska seismograph network for October 1971 through May 1989, *U.S. Geol. Surv. Open-File Rept. 93-309*, 54 p.

Goldstein, P., D. Dodge, and M. Firpo (1999). SAC2000: Signal processing and analysis tools for seismologists and engineers, in *International Handbook of Engineers and Engineering Seismology*, Lee W.H.K , Kanamori, H., Jennings, P.P, Kisslinger, C. (Editors), v. 81B, Academic Press, San Diego, CA, 1613-1614.

Johnson, C. E., A. Bittenbinder, D. Bogaert, L. Dietz, and W. Kohler (1995). EARTHWORM: A Flexible Approach to Seismograph network Processing, *IRIS Newsletter*, **14**, no. 2, 1-4.

Jolly, A. D., R. A. Page, and J. A. Power (1994). Seismicity and stress in the vicinity of Mt. Spurr volcano, south-central Alaska, *J. Geophys. Res.*, 99, 15305-15318.

Lahr, J. C, B. A. Chouet, C. D. Stephens, J. A. Power, and R. A. Page (1994). Earthquake classification, location, and error analysis in a volcanic environment: Implications for the magmatic system of the 1989-90 eruptions at Redoubt Volcano, Alaska, *J. Volc. Geotherm. Res.*, **62**, 137–152.

Lahr, J. C. (1999). HYPOELLIPSE: A Computer Program for Determining Local Earthquake Hypocentral Parameters, Magnitude, and First Motion Pattern, *U.S. Geol. Surv. Open-File Rept. 99-23*, 116 pp.

McChesney, P. J. (1999). McVCO Handbook 1999, *U.S. Geol. Surv. Open-File Rept. 99-361*, 48 p.

McNutt, S. R., and K. H. Jacob (1986). Determination of large-scale velocity structure of the crust and upper mantle in the vicinity of Pavlof volcano, Alaska: *J. of Geophys. Res.*, **91**, 5013-5022.

Power, J. A. (1988). Seismicity associated with the 1986 eruption of Augustine Volcano, Alaska, *Masters Thesis*, University of Alaska Fairbanks, 149 p.

Power, J. A., J. F. Paskievitch, D. H. Richter, R. G. McGimsey, P. Stelling, A. D. Jolly, and H. J. Fletcher (1996). 1996 seismicity and ground deformation at Akutan Volcano, *Eos Trans. AGU*, **77**, F514.

Power, J. A. (2004). Renewed unrest at Mount Spurr Volcano, Alaska, *Eos Trans. AGU*, **85**, 434.

Robinson, M. (1990). XPICK users manual, version 2.7: Seismology Lab, Geophysical Institute, University of Alaska Fairbanks, 93 p.

Rogers, J. A., S. Maslak, and J. C. Lahr (1980). A seismic electronic system with automatic calibration and crystal reference, *U.S. Geol. Surv. Open-File Rept. 80-324*, 130 p.

Roman, D. C., J. A. Power, S. C. Moran, K. V. Cashman, S. D. Stihler (2001). Unrest at Iliamna Volcano, Alaska in 1996, Evidence for a magmatic intrusion, *Eos Trans. AGU*, v. **82**, F1329.

Sánchez, J. J. (2005). Volcano Seismology from around the World: Case Studies from Mount Pinatubo (Philippines), Galeras (Columbia), Mount Wrangell and Mount Veniaminof (Alaska), *Ph.D. Dissertation*, University of Alaska Fairbanks, 208 p.

Searcy, C. K. (2003). Station Corrections for the Katmai Region Seismograph network, *U.S. Geol. Surv. Open-File Rept. 03-40*3, 16 p.

Toth, T., and C. Kisslinger (1984). Revised focal depths and velocity model for local earthquakes in the Adak seismic zone, *Bull. Seism. Soc. Am.*, **74**, 1349-1360.

Wiemer, S. (2001). A software package to analyze seismicity: ZMAP, *Seism. Res. Lett.*, **72**, 373-382.

Appendix A: Maps showing the locations of the earthquakes located in 2005.

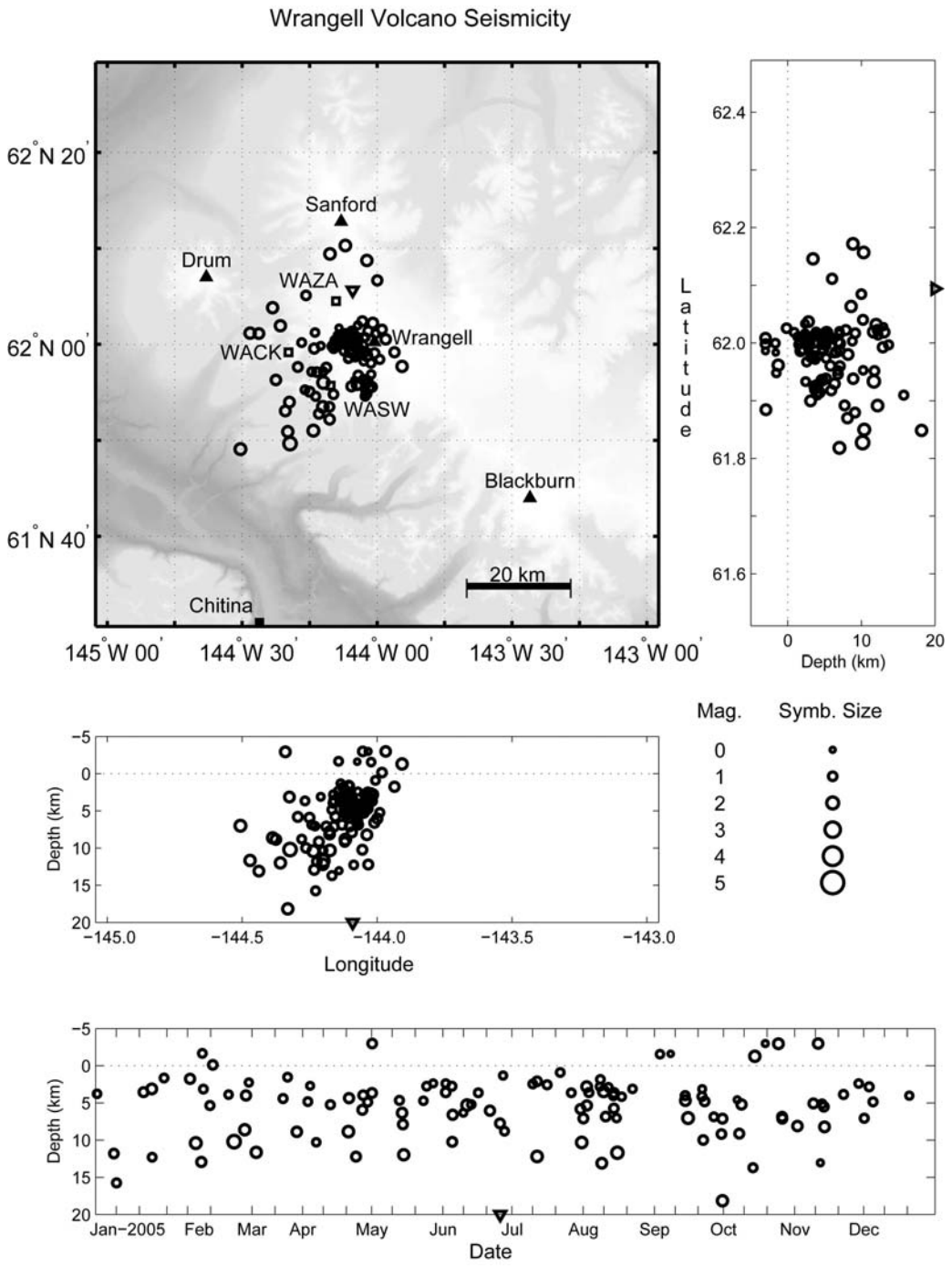

Figure A1. Summary plots of 116 earthquakes located near Mount Wrangell in 2005. Open circles show hypocenter locations shallower than 20 km and open triangles show hypocenters with depths of 20 km and deeper. Hypocenter symbols are scaled with magnitude. Seismograph stations are shown by open squares and labeled by station code. Solid triangles are used to show volcanic centers and solid squares are used to show other points of interest. See Appendix B for station information.

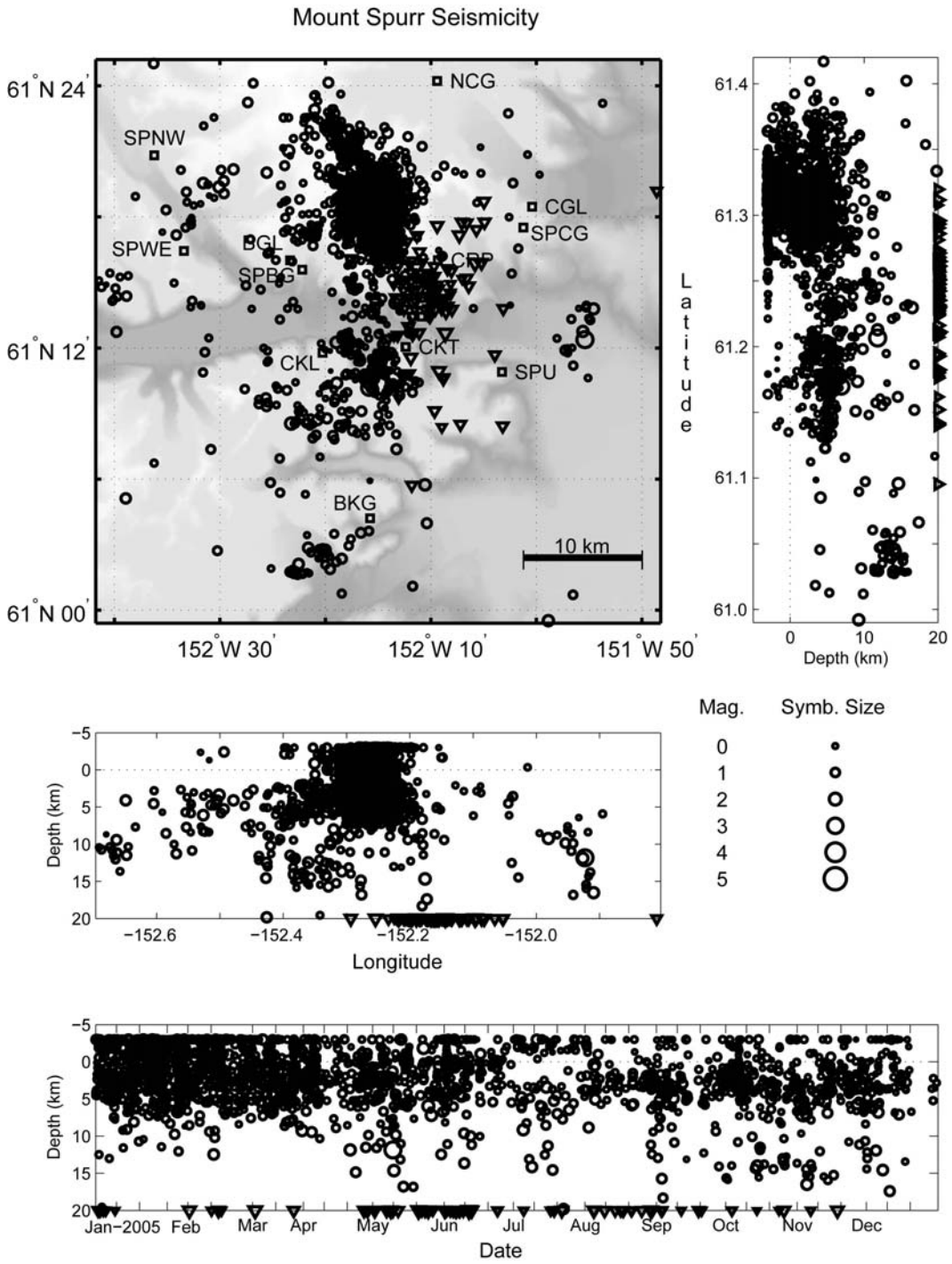

Figure A2. Summary plots of 2,386 earthquakes located near Mount Spurr in 2005. Open circles show hypocenter locations shallower than 20 km and open triangles show hypocenters with depths of 20 km and deeper. Hypocenter symbols are scaled with magnitude. Seismograph stations are shown by open squares and labeled by station code. Solid triangles are used to show volcanic centers and solid squares are used to show other points of interest. See Appendix B for station information.

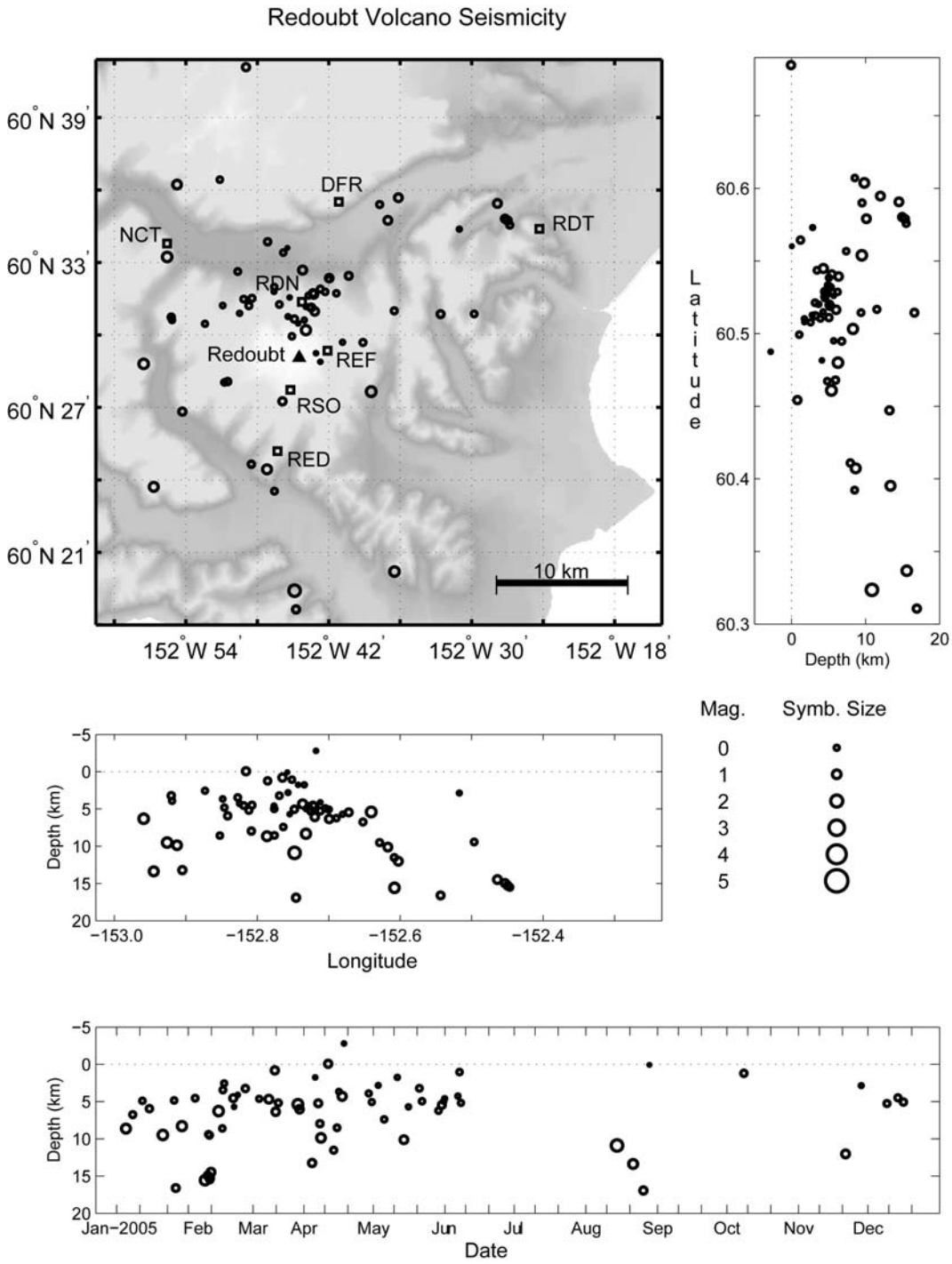

Figure A3. Summary plots of 68 earthquakes located near Redoubt Volcano in 2005. Open circles show hypocenter locations shallower than 20 km and open triangles show hypocenters with depths of 20 km and deeper. Hypocenter symbols are scaled with magnitude. Seismograph stations are shown by open squares and labeled by station code. Solid triangles are used to show volcanic centers and solid squares are used to show other points of interest. See Appendix B for station information.

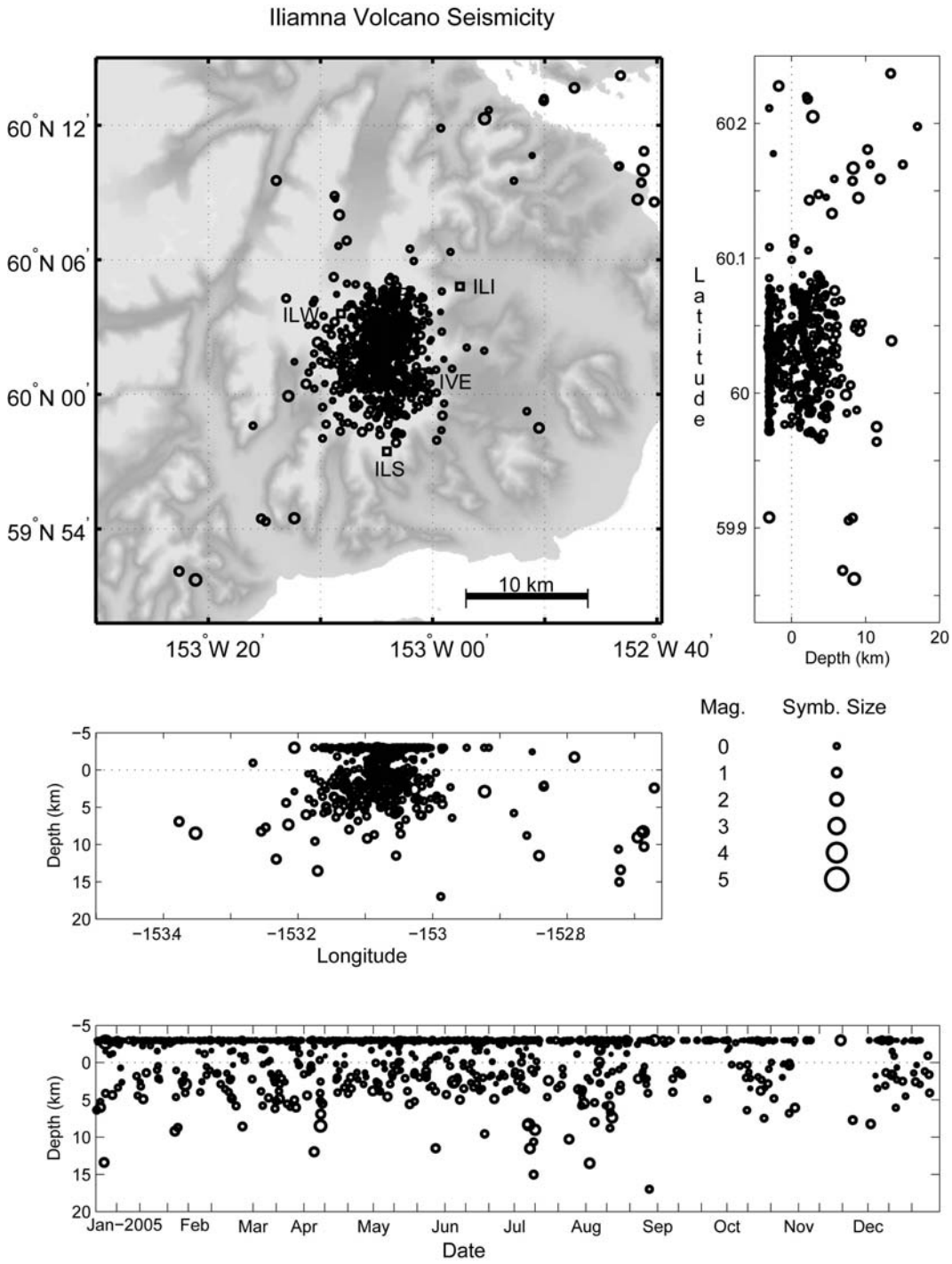

Figure A4. Summary plots of 995 earthquakes located near Iliamna Volcano in 2005. Open circles show hypocenter locations shallower than 20 km and open triangles show hypocenters with depths of 20 km and deeper. Hypocenter symbols are scaled with magnitude. Seismograph stations are shown by open squares and labeled by station code. Solid triangles are used to show volcanic centers and solid squares are used to show other points of interest. See Appendix B for station information.

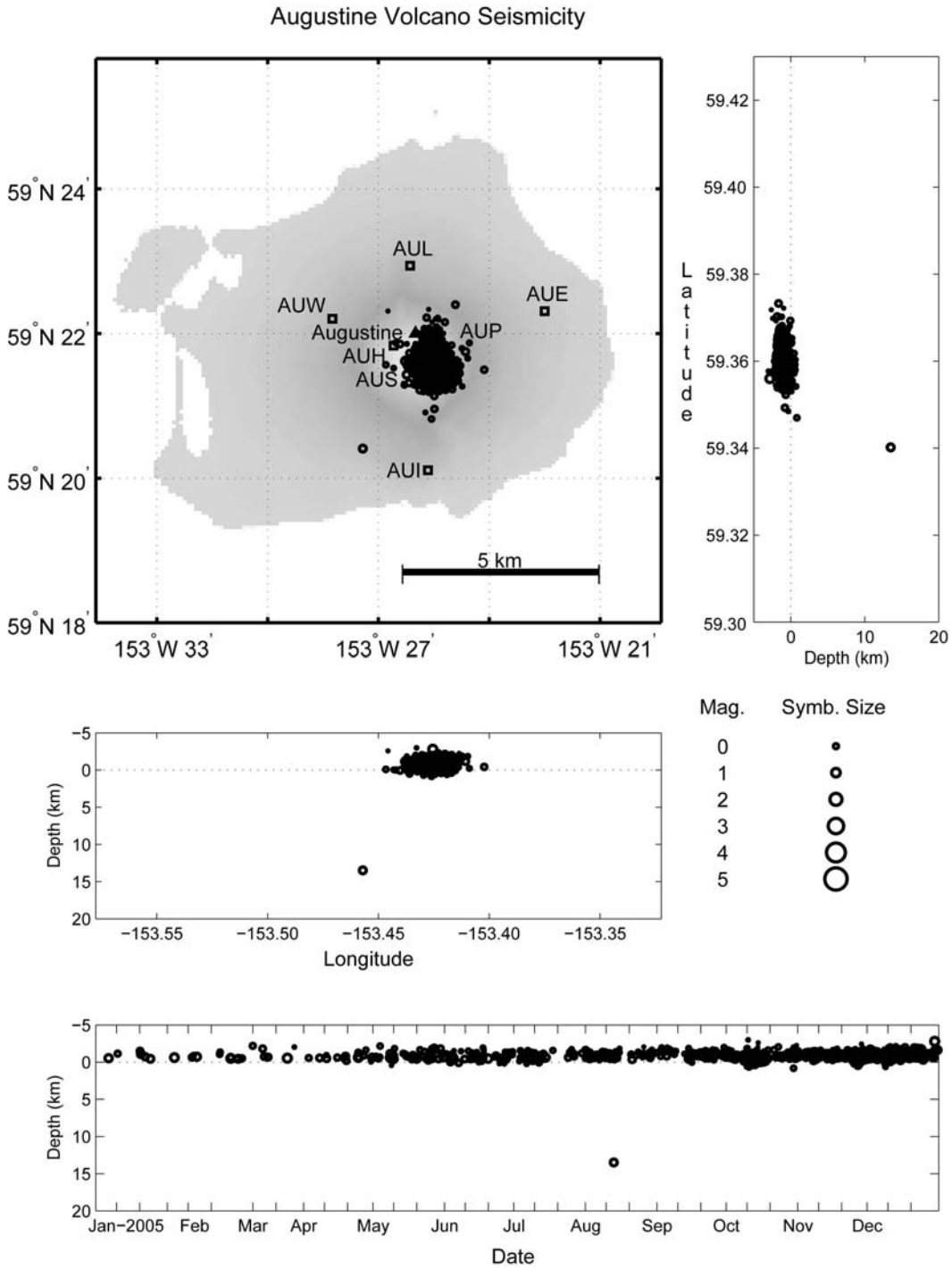

Figure A5. Summary plots of 1,189 earthquakes located near Augustine Volcano in 2005. Open circles show hypocenter locations shallower than 20 km and open triangles show hypocenters with depths of 20 km and deeper. Hypocenter symbols are scaled with magnitude. Seismograph stations are shown by open squares and labeled by station code. Solid triangles are used to show volcanic centers and solid squares are used to show other points of interest. See Appendix B for station information.

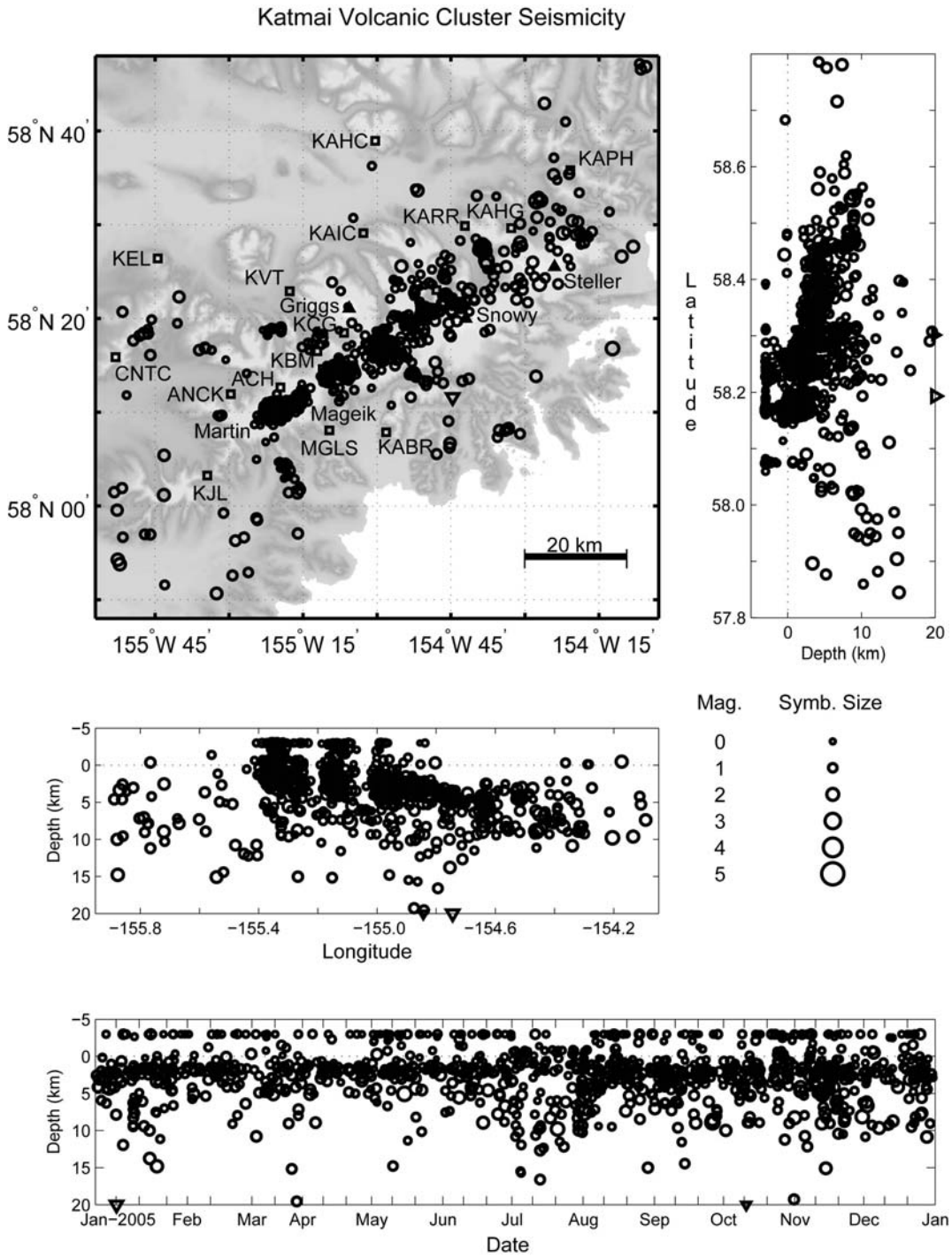

Figure A6. Summary plots of 1,138 earthquakes located near the Katmai volcanic cluster in 2005. Open circles show hypocenter locations shallower than 20 km and open triangles show hypocenters with depths of 20 km and deeper. Hypocenter symbols are scaled with magnitude. Seismograph stations are shown by open squares and labeled by station code. Solid triangles are used to show volcanic centers and solid squares are used to show other points of interest. See Appendix B for station information...

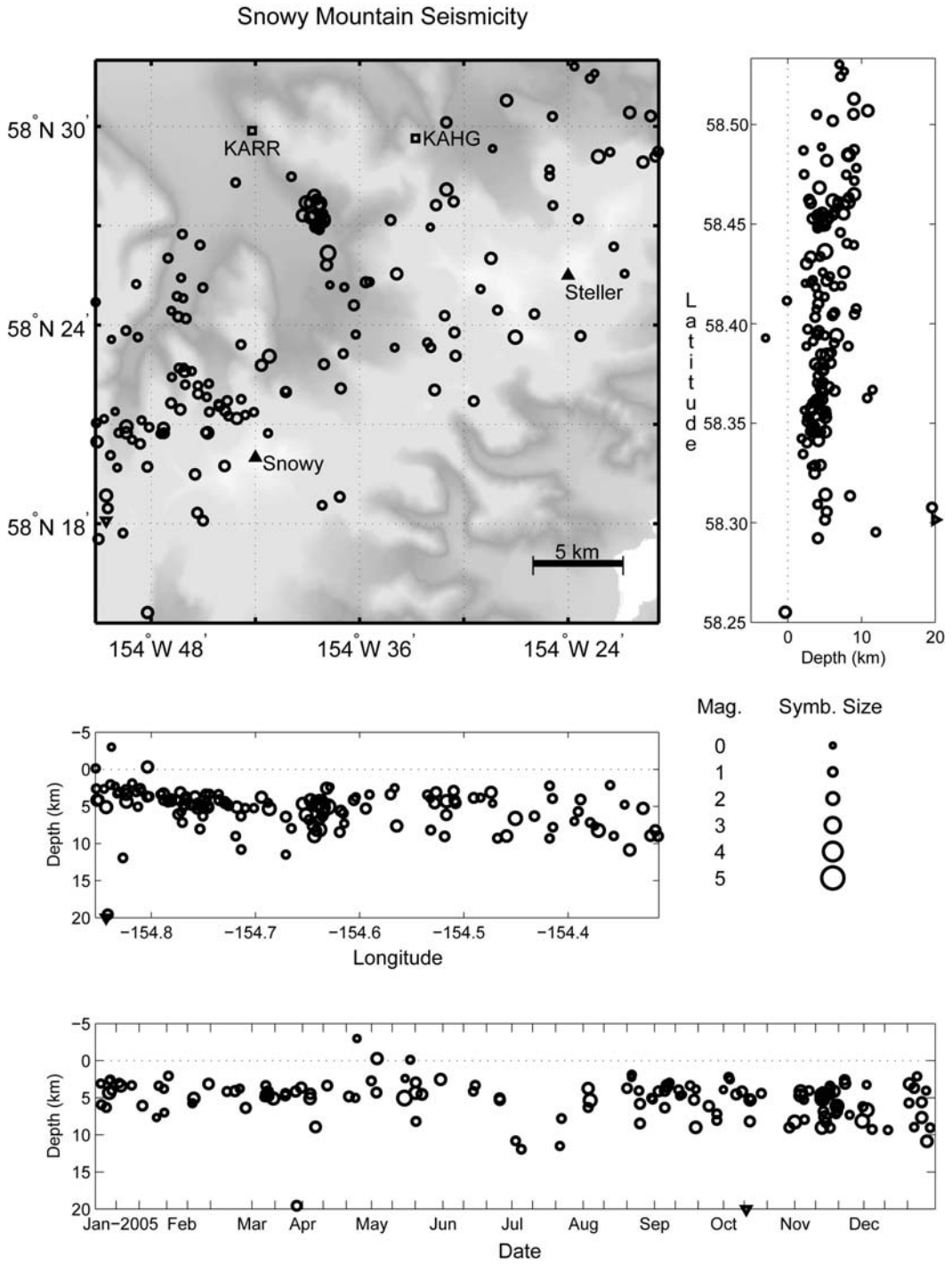

Figure A7. Summary plots of 145 earthquakes located near Snowy Mountain in the Katmai volcanic cluster in 2005. Open circles show hypocenter locations shallower than 20 km and open triangles show hypocenters with depths of 20 km and deeper. Hypocenter symbols are scaled with magnitude. Seismograph stations are shown by open squares and labeled by station code. (See Appendix B for station information). Solid triangles are used to show volcanic centers and solid squares are used to show other points of interest.

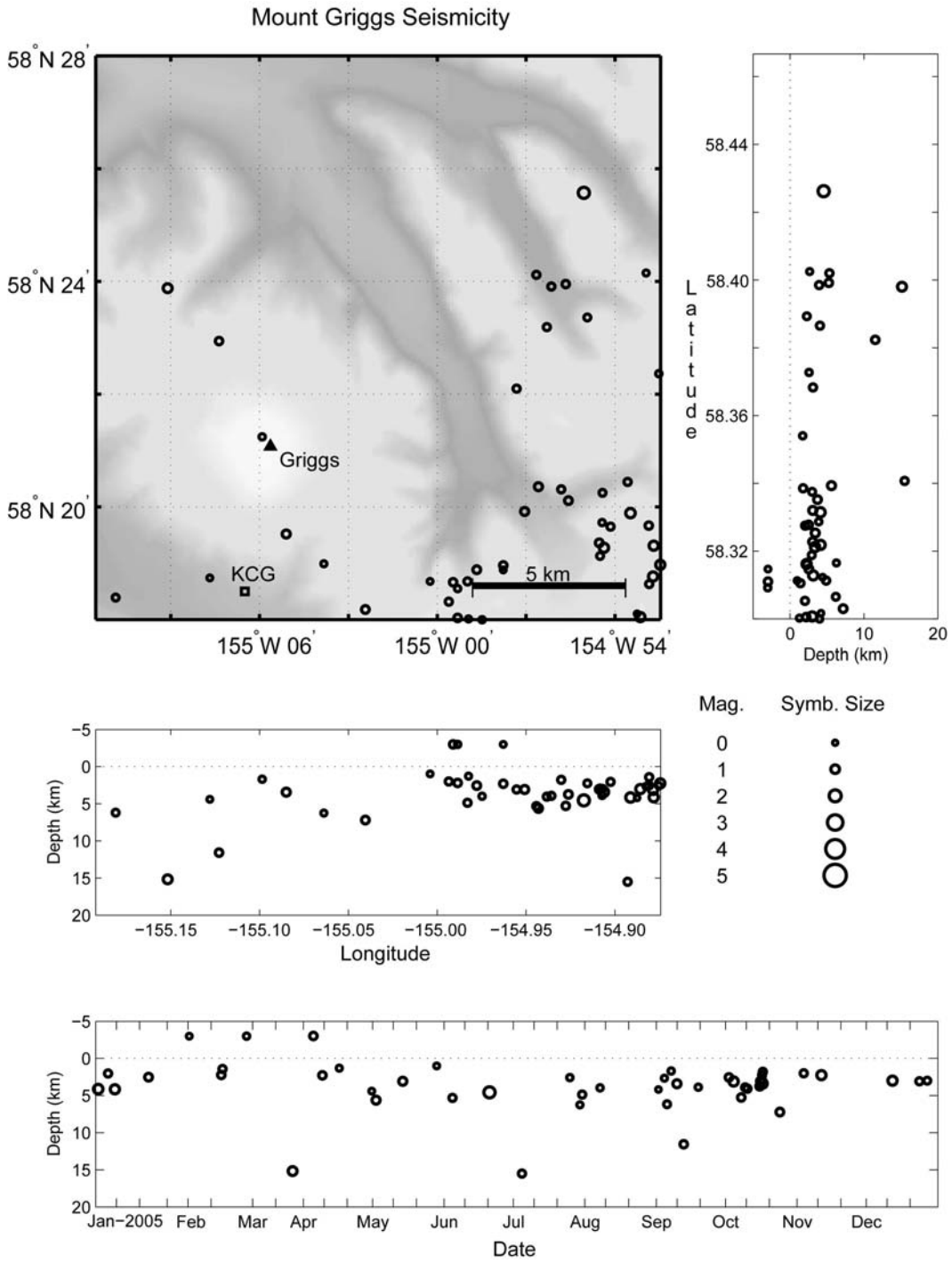

Figure A8. Summary plots of 47 earthquakes located near Mount Griggs in the Katmai volcanic cluster in 2005. Open circles show hypocenter locations shallower than 20 km and open triangles show hypocenters with depths of 20 km and deeper. Hypocenter symbols are scaled with magnitude. Seismograph stations are shown by open squares and labeled by station code. Solid triangles are used to show volcanic centers and solid squares are used to show other points of interest. See Appendix B for station information. Several earthquakes that appear on this figure appear on other figures.

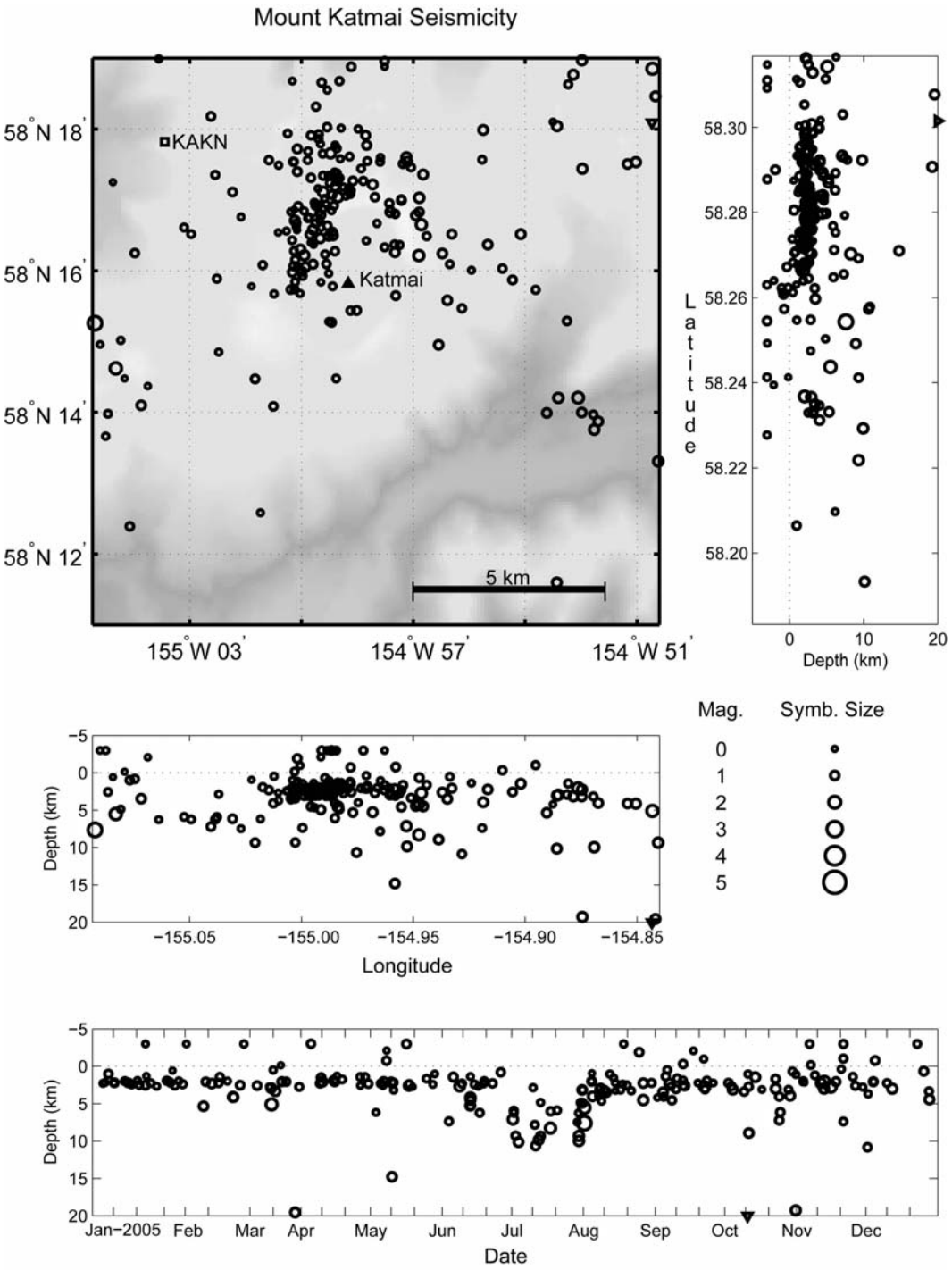

Figure A9. Summary plots of 209 earthquakes located near Mount Katmai in the Katmai volcanic cluster in 2005. Open circles show hypocenter locations shallower than 20 km and open triangles show hypocenters with depths of 20 km and deeper. Hypocenter symbols are scaled with magnitude. Seismograph stations are shown by open squares and labeled by station code. Solid triangles are used to show volcanic centers and solid squares are used to show other points of interest. See Appendix B for station information. Several earthquakes that appear on this figure appear on other figures.

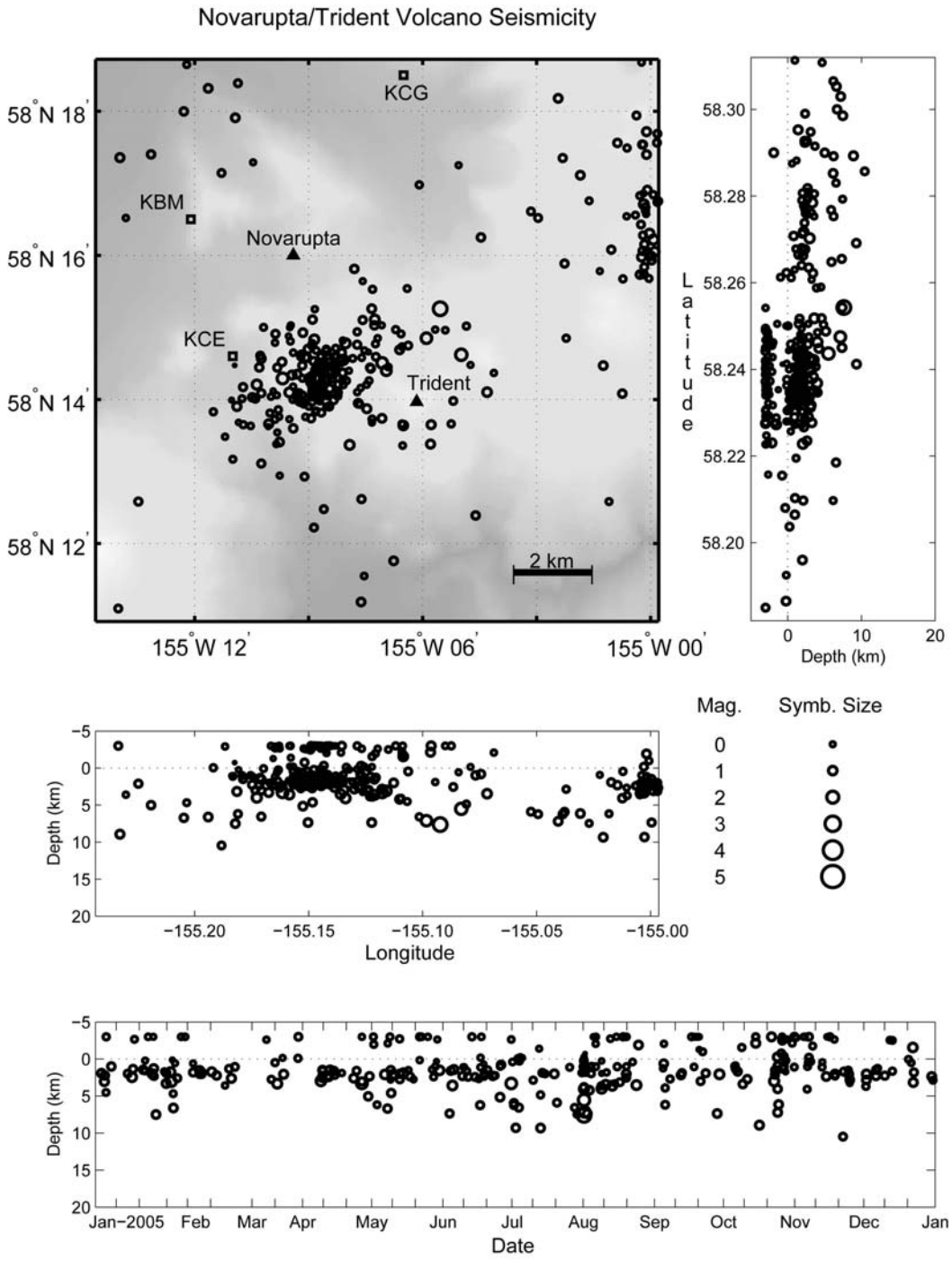

Figure A10. Summary plots of 287 earthquakes located near Novarupta and Trident Volcano in the Katmai volcanic cluster in 2005. Open circles show hypocenter locations shallower than 20 km and open triangles show hypocenters with depths of 20 km and deeper. Hypocenter symbols are scaled with magnitude. Seismograph stations are shown by open squares and labeled by station code. Solid triangles are used to show volcanic centers and solid squares are used to show other points of interest. See Appendix B for station information. Several earthquakes that appear on this figure appear on other figures.

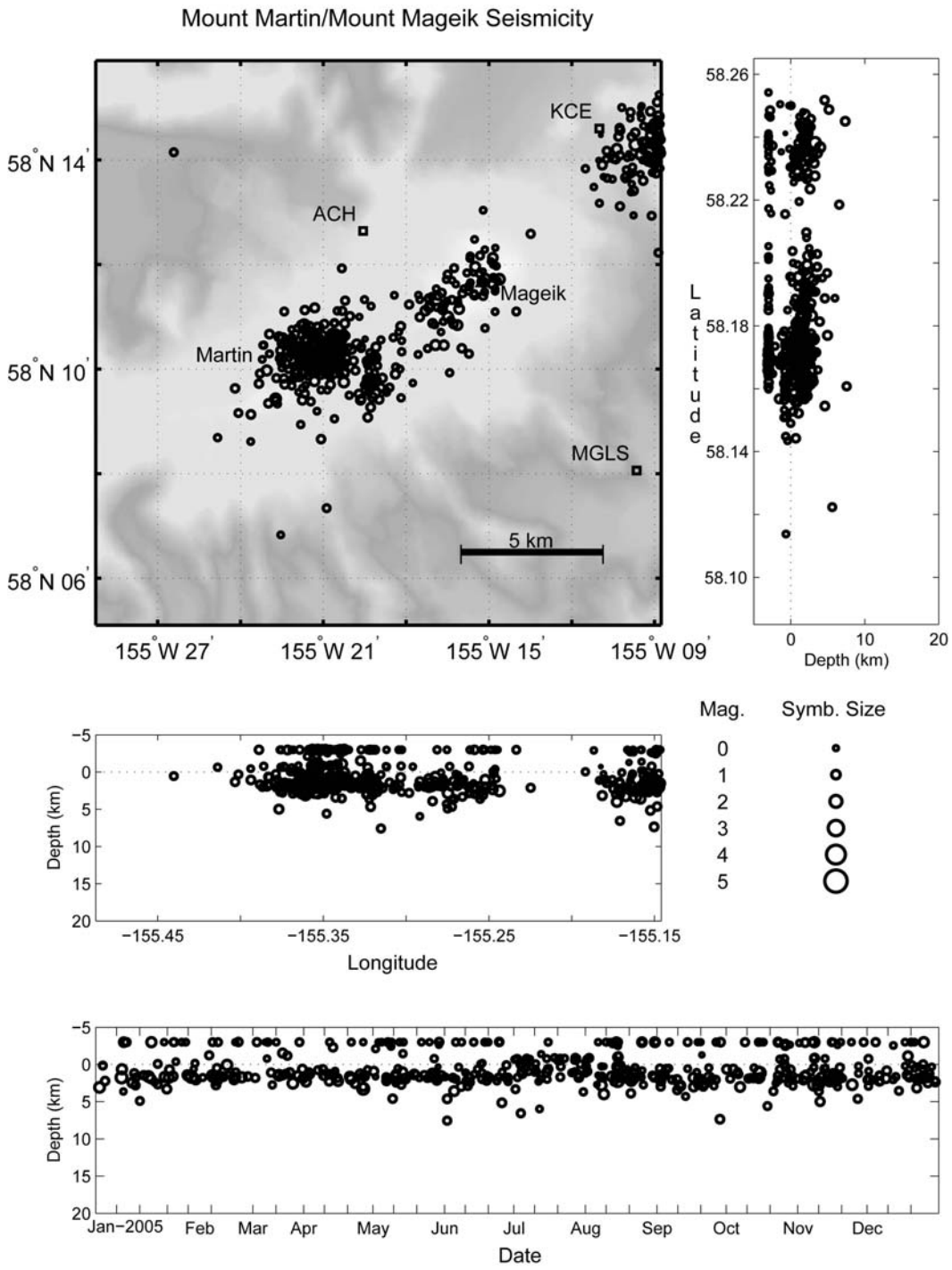

Figure A11. Summary plots of 495 earthquakes located near Mount Mageik and Mount Martin in the Katmai volcanic cluster in 2005. Open circles scaled with magnitude show hypocenter locations. Seismograph stations are shown by open squares and labeled by station code. Solid triangles are used to show volcanic centers and solid squares are used to show other points of interest. See Appendix B for station information. Several earthquakes that appear on this figure appear on other figures.

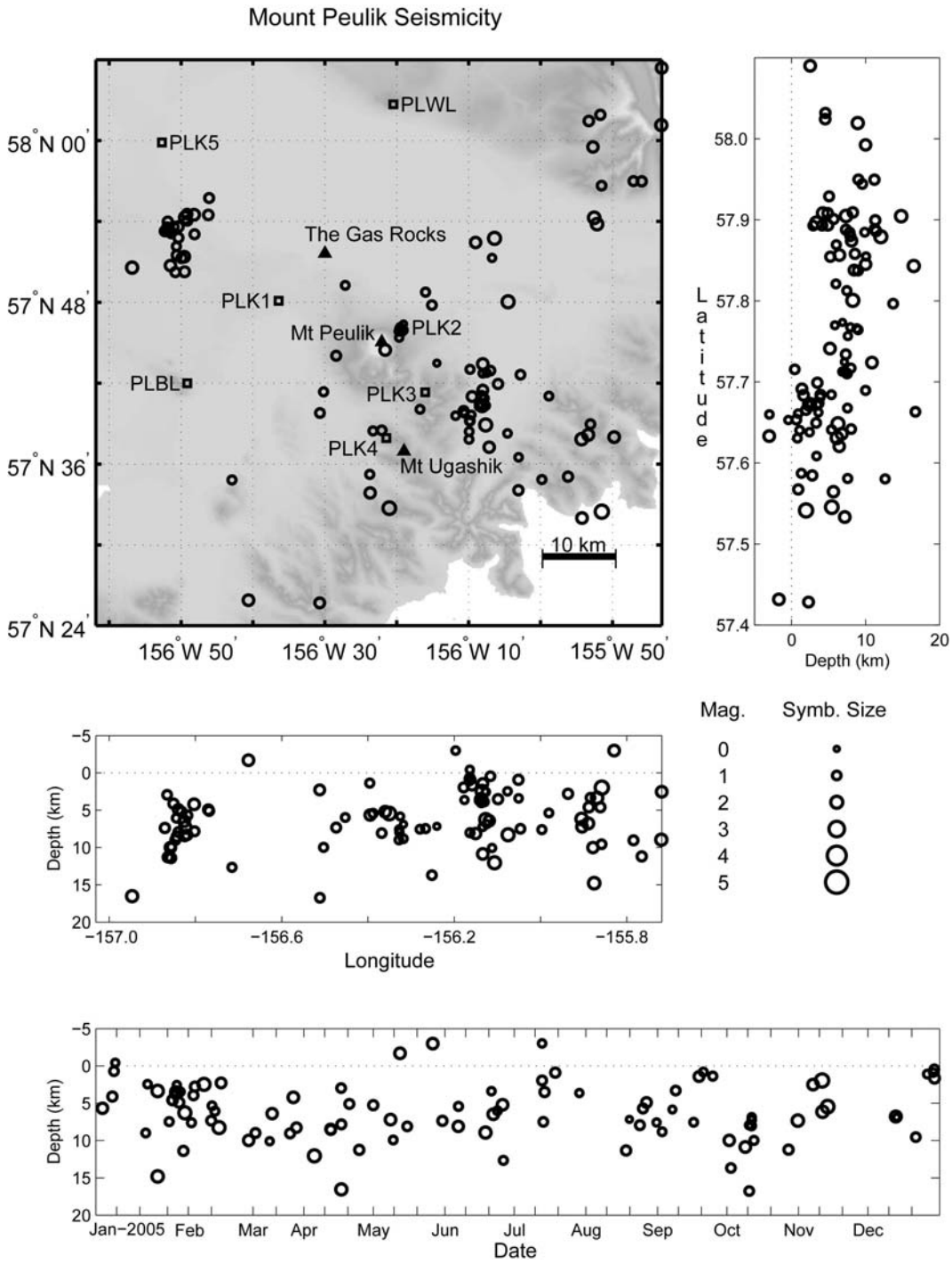

Figure A12. Summary plots of 101 earthquakes located near Mount Peulik in 2005. Open circles show hypocenter locations shallower than 20 km and open triangles show hypocenters with depths of 20 km and deeper. Hypocenter symbols are scaled with magnitude. Seismograph stations are shown by open squares and labeled by station code. Solid triangles are used to show volcanic centers and solid squares are used to show other points of interest. See Appendix B for station information.

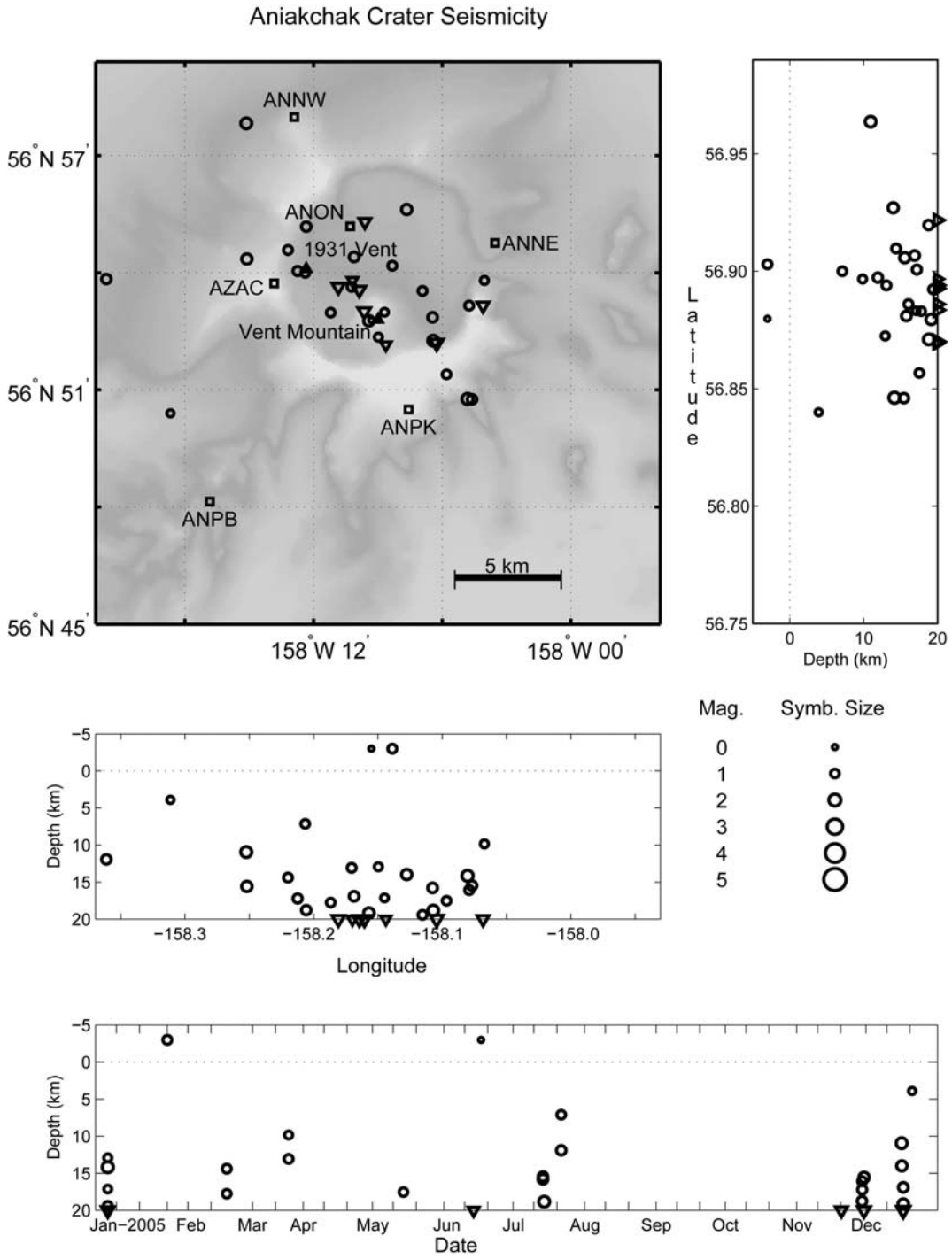

Figure A13. Summary plots of 33 earthquakes located near Aniakchak Crater in 2005. Open circles show hypocenter locations shallower than 20 km and open triangles show hypocenters with depths of 20 km and deeper. Hypocenter symbols are scaled with magnitude. Seismograph stations are shown by open squares and labeled by station code. Solid triangles are used to show volcanic centers and solid squares are used to show other points of interest. See Appendix B for station information.

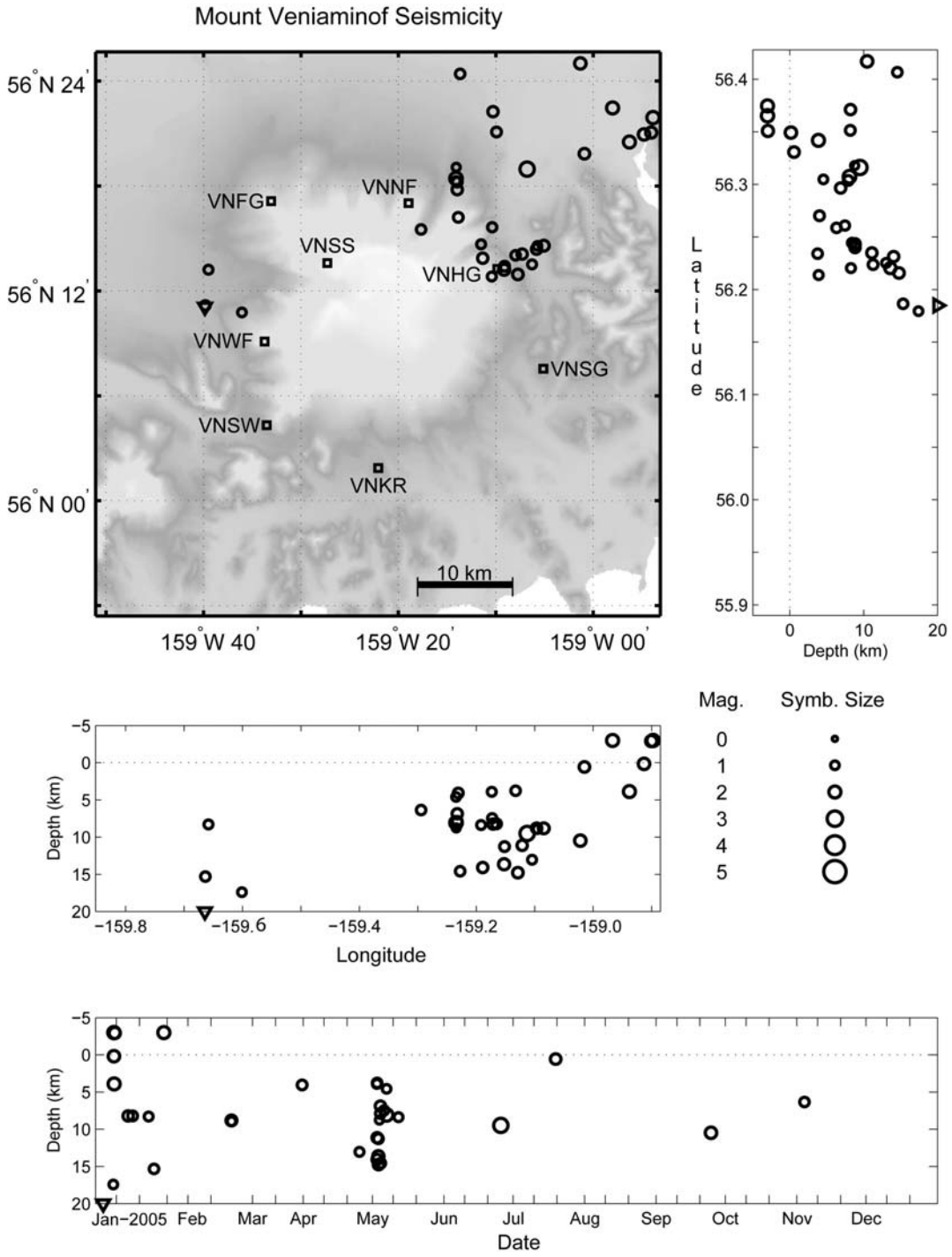

Figure A14. Summary plots of 35 earthquakes located near Mount Veniaminof in 2005. Open circles show hypocenter locations shallower than 20 km and open triangles show hypocenters with depths of 20 km and deeper. Hypocenter symbols are scaled with magnitude. Seismograph stations are shown by open squares and labeled by station code. Solid triangles are used to show volcanic centers and solid squares are used to show other points of interest. See Appendix B for station information.

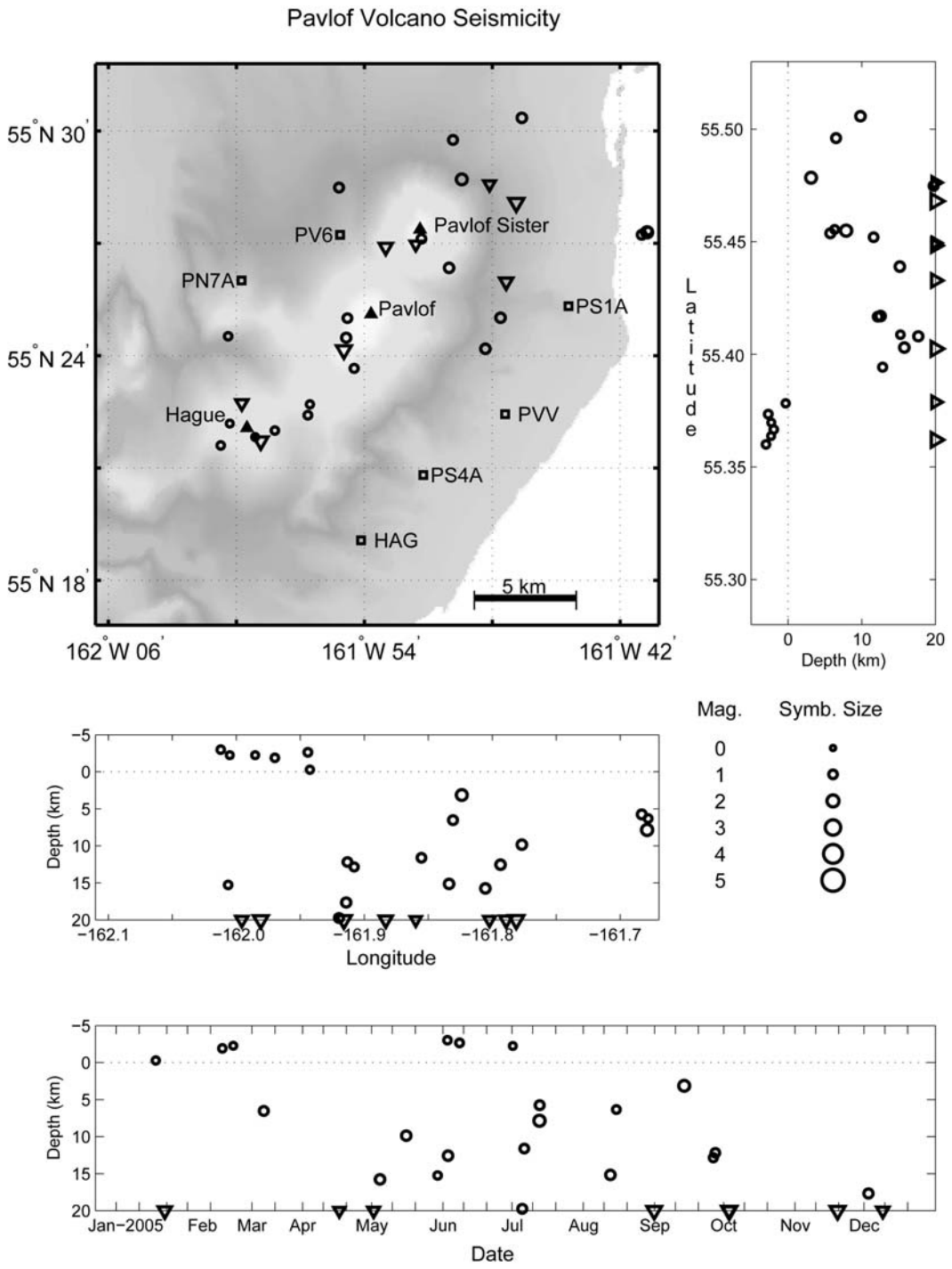

Figure A15. Summary plots of 29 earthquakes located near Pavlof Volcano in 2005. Open circles show hypocenter locations shallower than 20 km and open triangles show hypocenters with depths of 20 km and deeper. Hypocenter symbols are scaled with magnitude. Seismograph stations are shown by open squares and labeled by station code. Solid triangles are used to show volcanic centers and solid squares are used to show other points of interest. See Appendix B for station information.

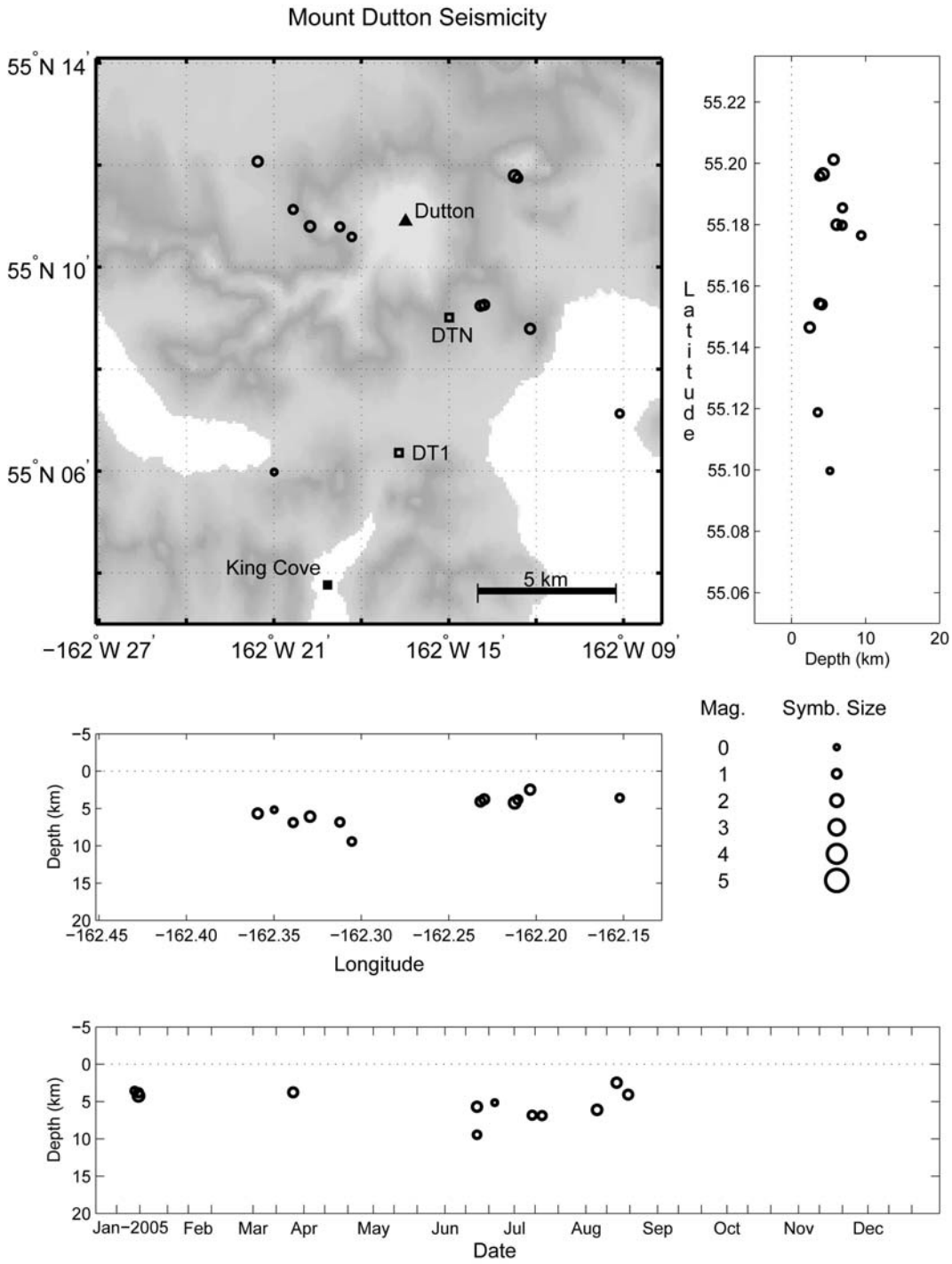

Figure A16. This summary plot shows 12 earthquakes located near Mount Dutton in 2005. Open circles show hypocenter locations shallower than 20 km and open triangles show hypocenters with depths of 20 km and deeper. Hypocenter symbols are scaled with magnitude. Seismograph stations are shown by open squares and labeled by station code. Solid triangles are used to show volcanic centers and solid squares are used to show other points of interest. See Appendix B for station information.

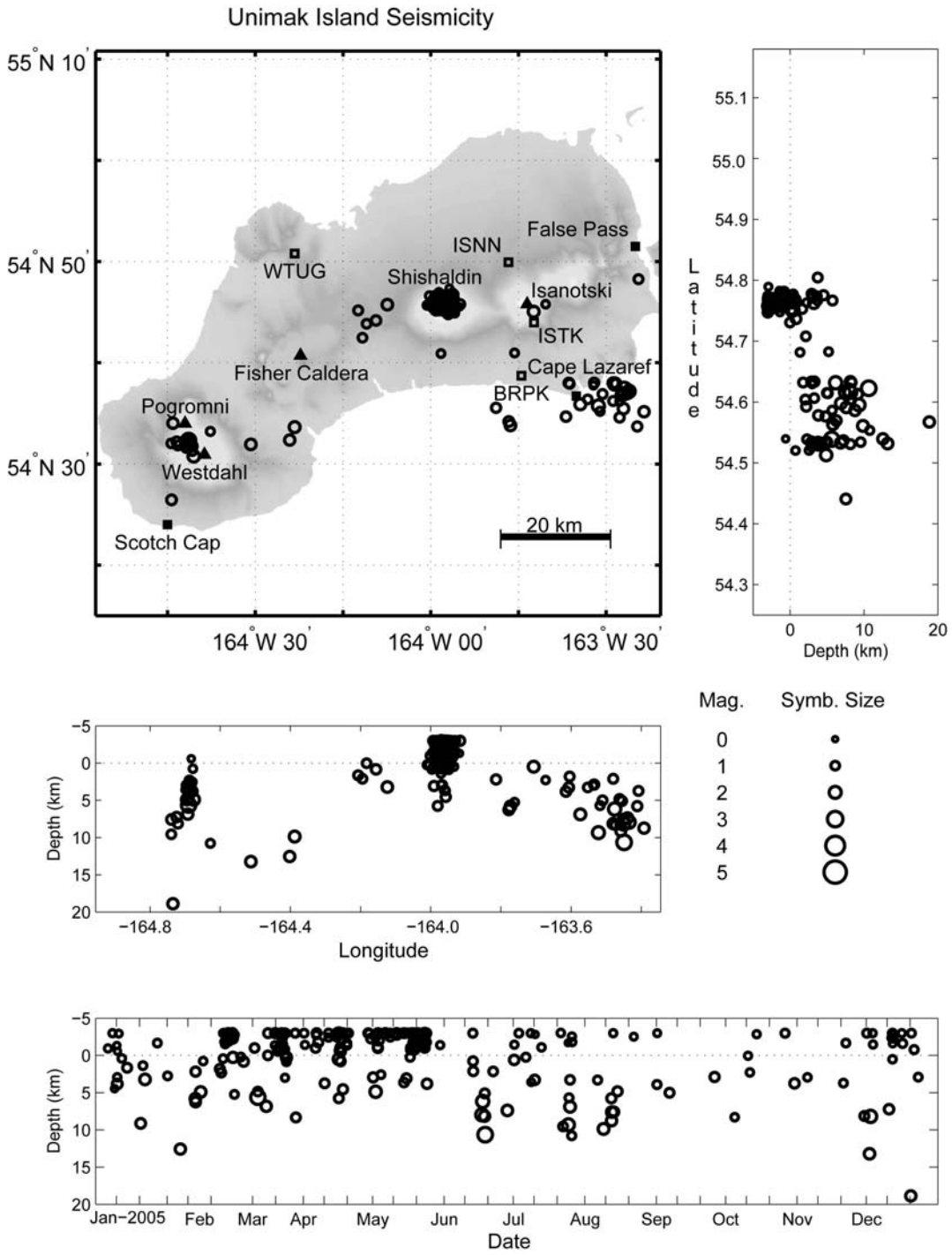

Figure A17. Summary plots of 264 earthquakes located near Unimak Island in 2005. Open circles show hypocenter locations shallower than 20 km and open triangles show hypocenters with depths of 20 km and deeper. Hypocenter symbols are scaled with magnitude. Seismograph stations are shown by open squares and labeled by station code. Solid triangles are used to show volcanic centers and solid squares are used to show other points of interest. See Appendix B for station information.

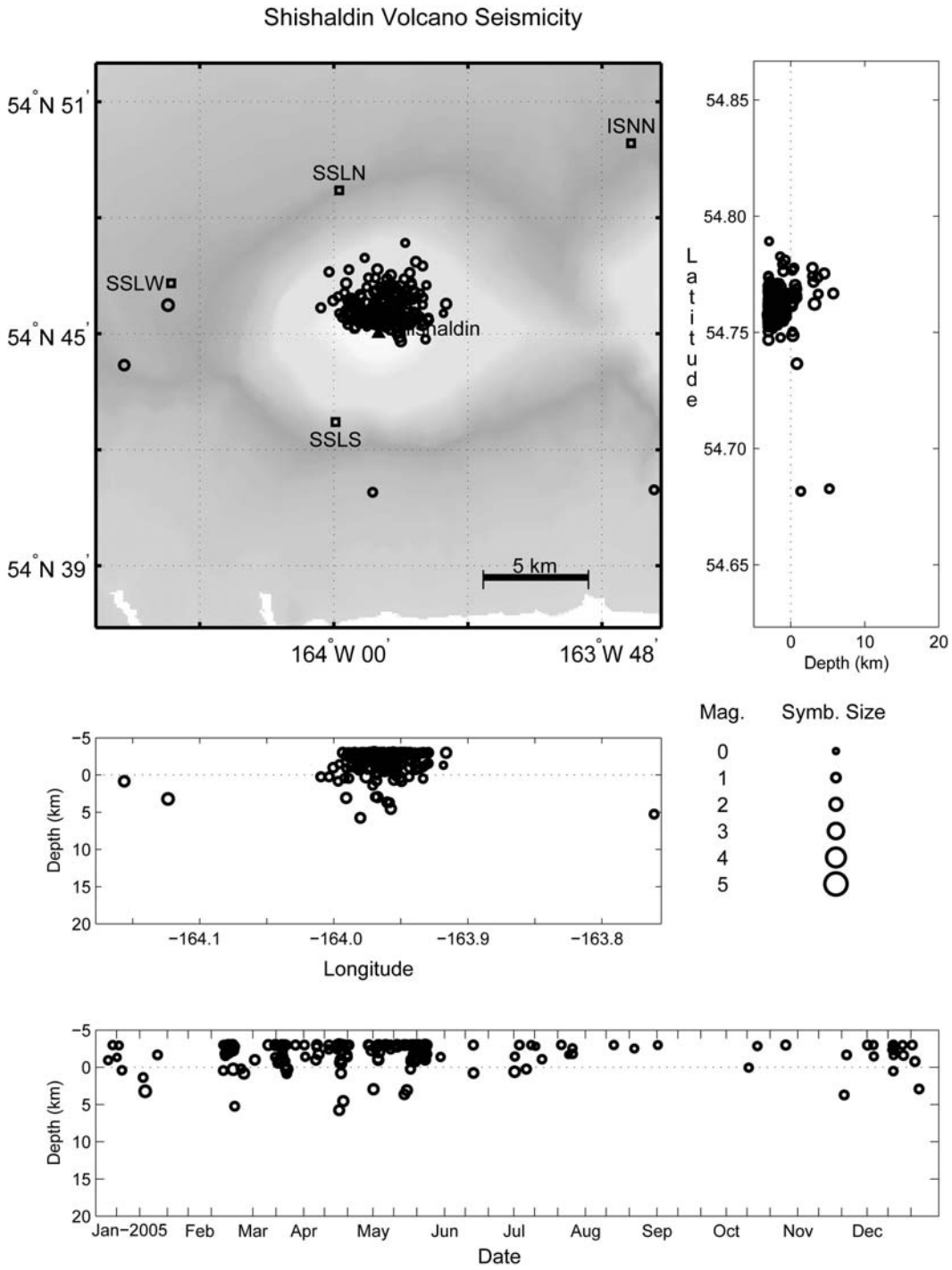

Figure A18. Summary plots of 203 earthquakes located near Shishaldin Volcano in 2005. Open circles show hypocenter locations shallower than 20 km and open triangles show hypocenters with depths of 20 km and deeper. Hypocenter symbols are scaled with magnitude. Seismograph stations are shown by open squares and labeled by station code. Solid triangles are used to show volcanic centers and solid squares are used to show other points of interest. See Appendix B for station information.

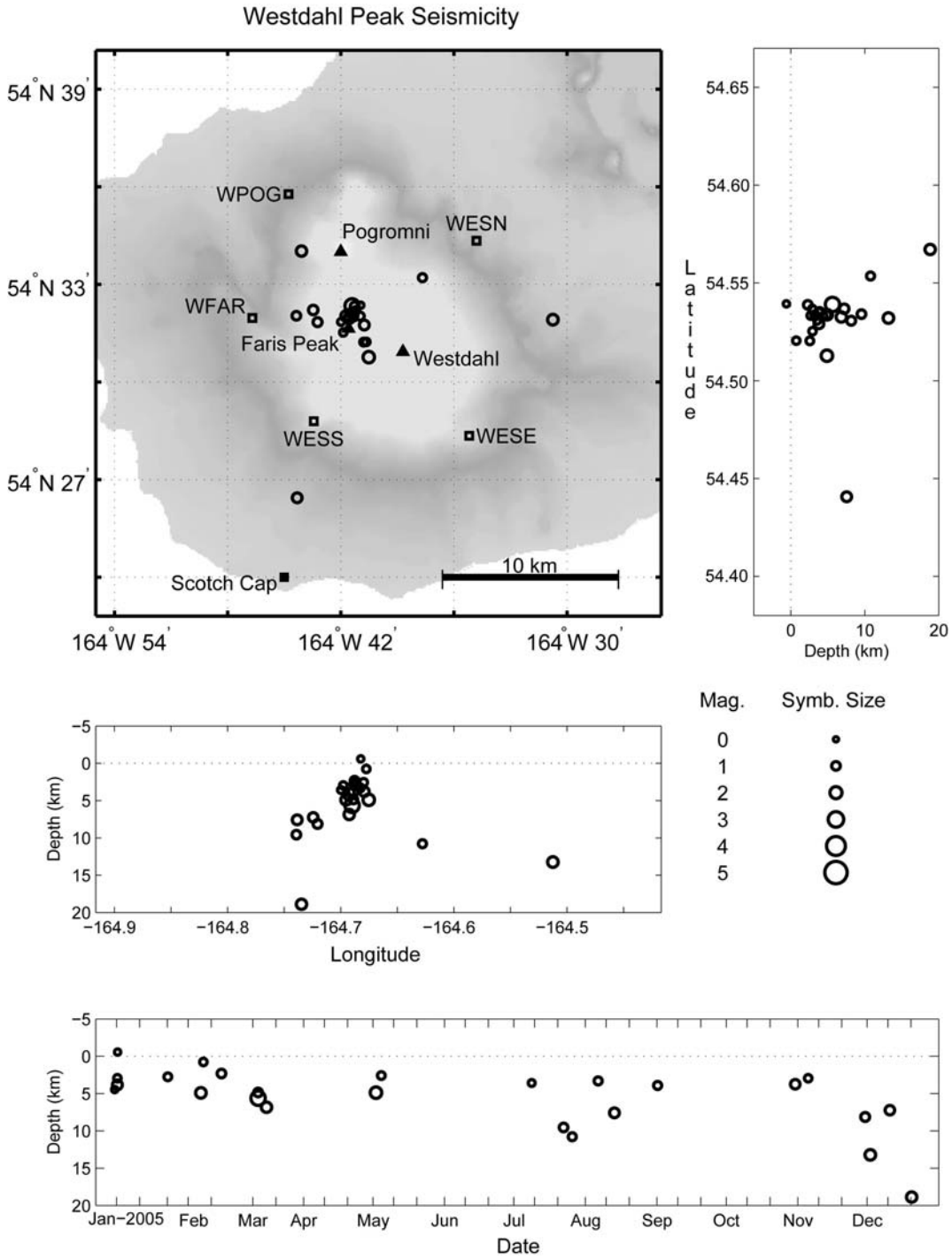

Figure A19. Summary plots of 25 earthquakes located near Westdahl Peak in 2005. Open circles show hypocenter locations shallower than 20 km and open triangles show hypocenters with depths of 20 km and deeper. Hypocenter symbols are scaled with magnitude. Seismograph stations are shown by open squares and labeled by station code. Solid triangles are used to show volcanic centers and solid squares are used to show other points of interest. See Appendix B for station information.

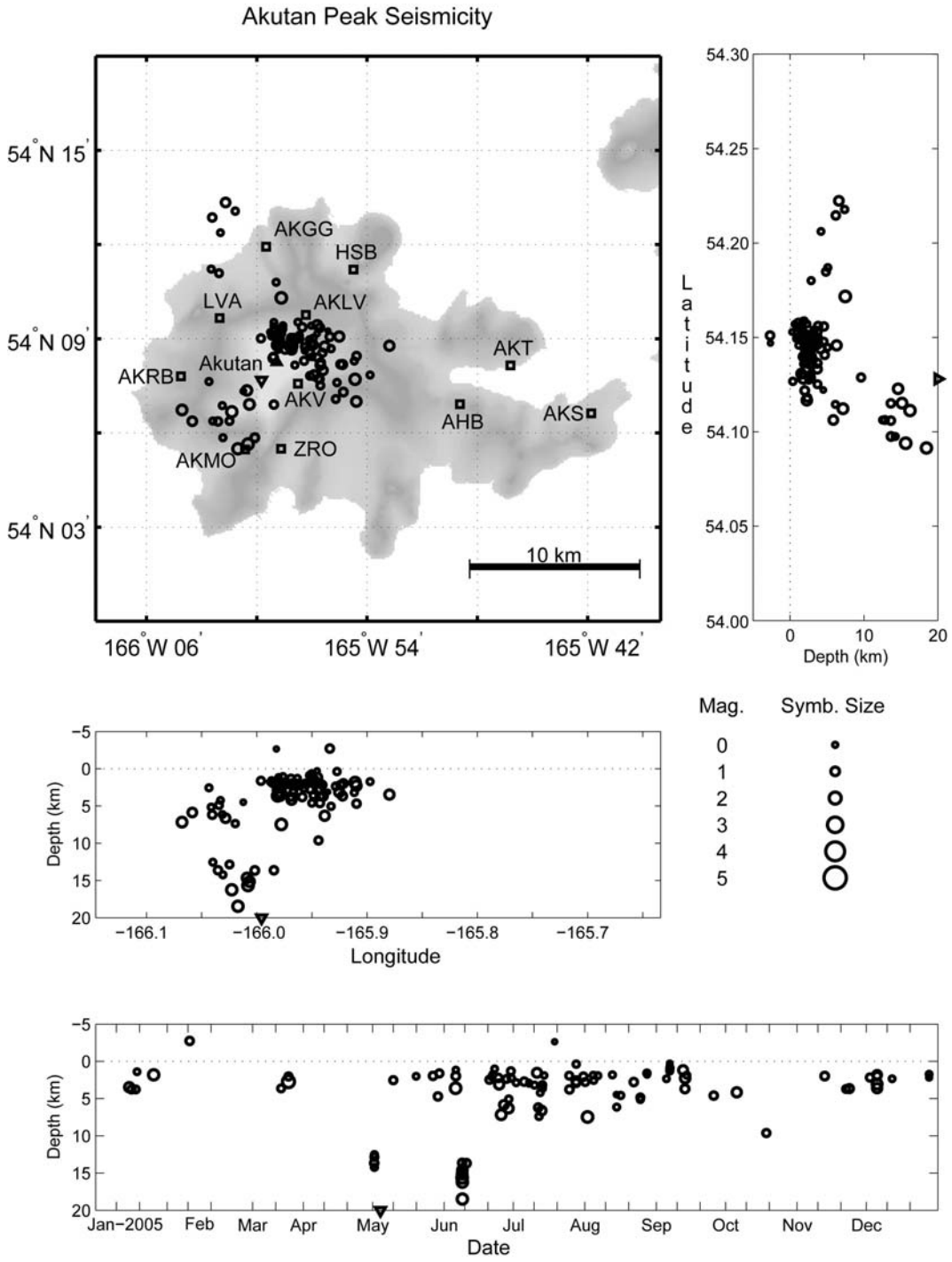

Figure A20. Summary plots of 100 earthquakes located near Akutan Peak in 2005. Open circles show hypocenter locations shallower than 20 km and open triangles show hypocenters with depths of 20 km and deeper. Hypocenter symbols are scaled with magnitude. Seismograph stations are shown by open squares and labeled by station code. Solid triangles are used to show volcanic centers and solid squares are used to show other points of interest. See Appendix B for station information.

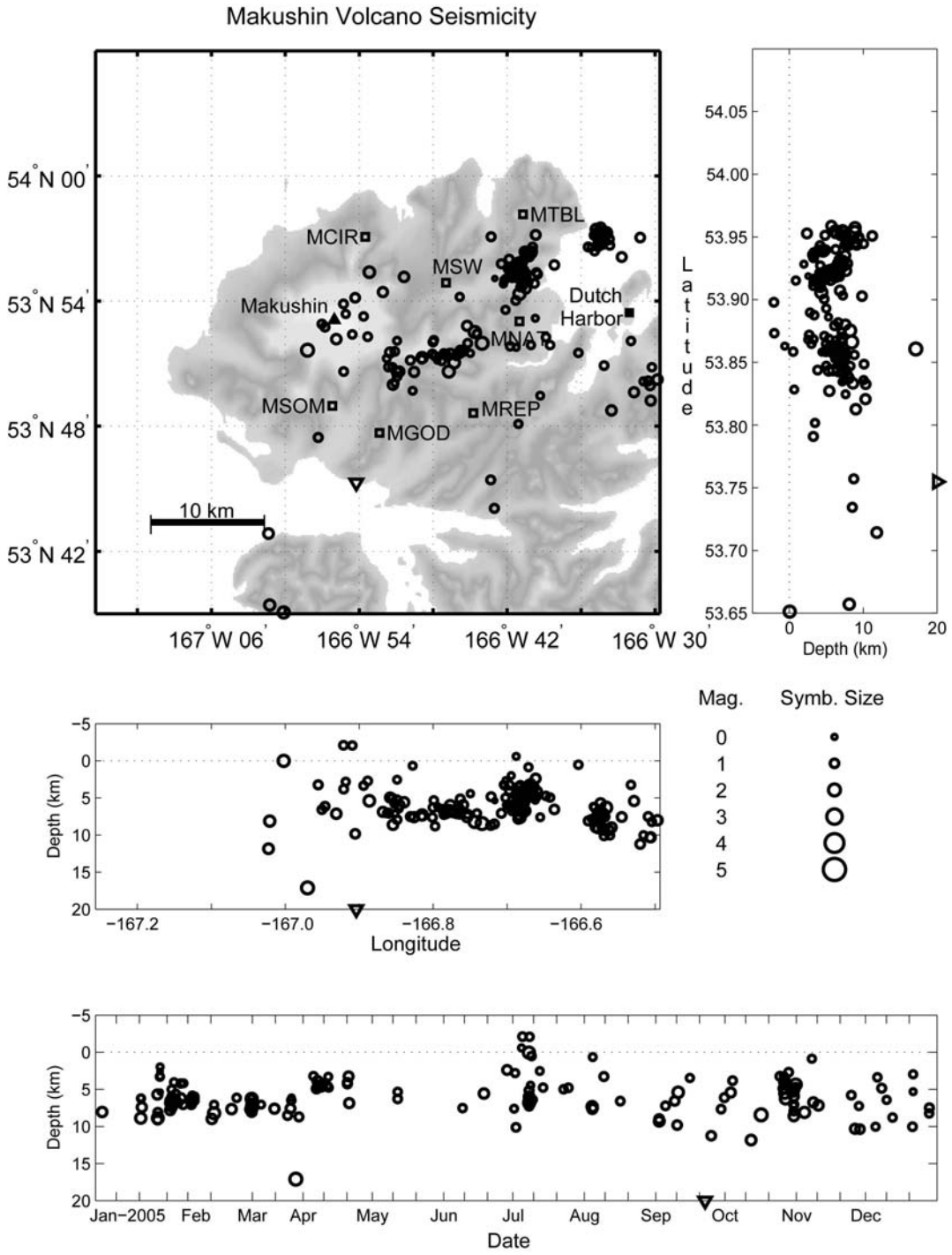

Figure A21. Summary plots of 175 earthquakes located near Makushin Volcano in 2005. Open circles show hypocenter locations shallower than 20 km and open triangles show hypocenters with depths of 20 km and deeper. Hypocenter symbols are scaled with magnitude. Seismograph stations are shown by open squares and labeled by station code. Solid triangles are used to show volcanic centers and solid squares are used to show other points of interest. See Appendix B for station information.

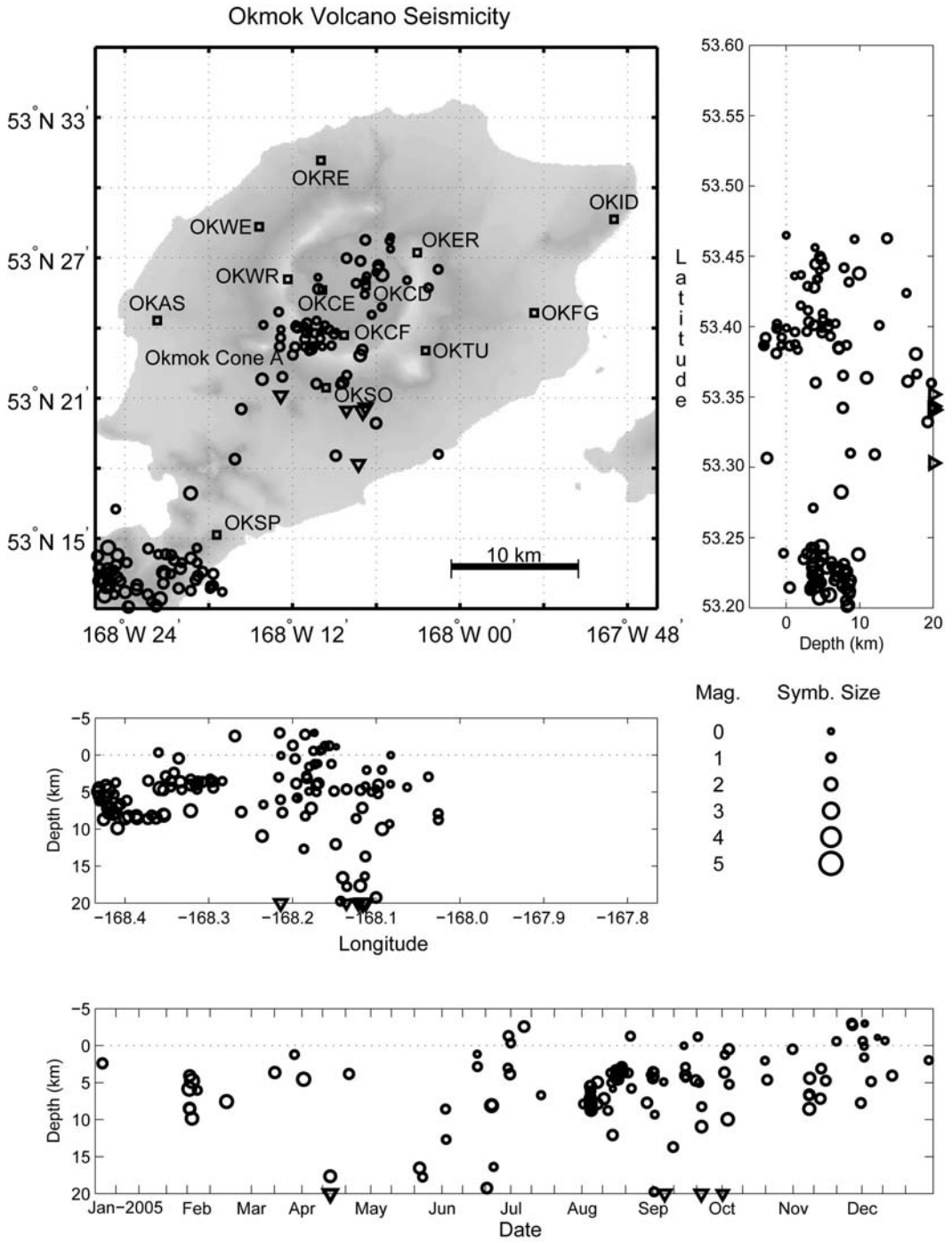

Figure A22. Summary plots of 123 earthquakes located near Okmok Caldera in 2005. Open circles show hypocenter locations shallower than 20 km and open triangles show hypocenters with depths of 20 km and deeper. Hypocenter symbols are scaled with magnitude. Seismograph stations are shown by open squares and labeled by station code. Solid triangles are used to show volcanic centers and solid squares are used to show other points of interest. See Appendix B for station information.

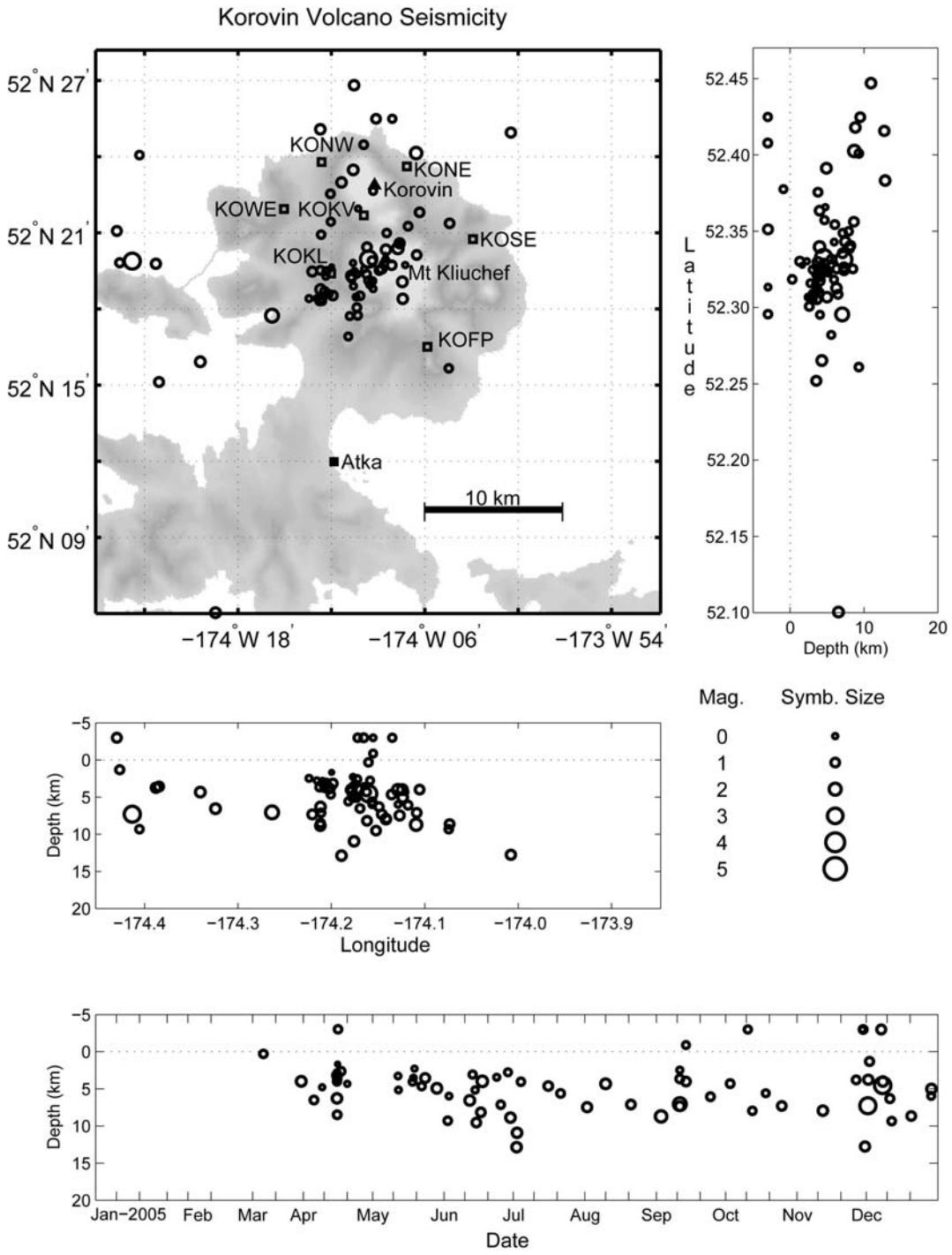

Figure A23. Summary plots of 74 earthquakes located near Korovin Volcano in 2005. Open circles show hypocenter locations shallower than 20 km and open triangles show hypocenters with depths of 20 km and deeper. Hypocenter symbols are scaled with magnitude. Seismograph stations are shown by open squares and labeled by station code. Solid triangles are used to show volcanic centers and solid squares are used to show other points of interest. See Appendix B for station information.

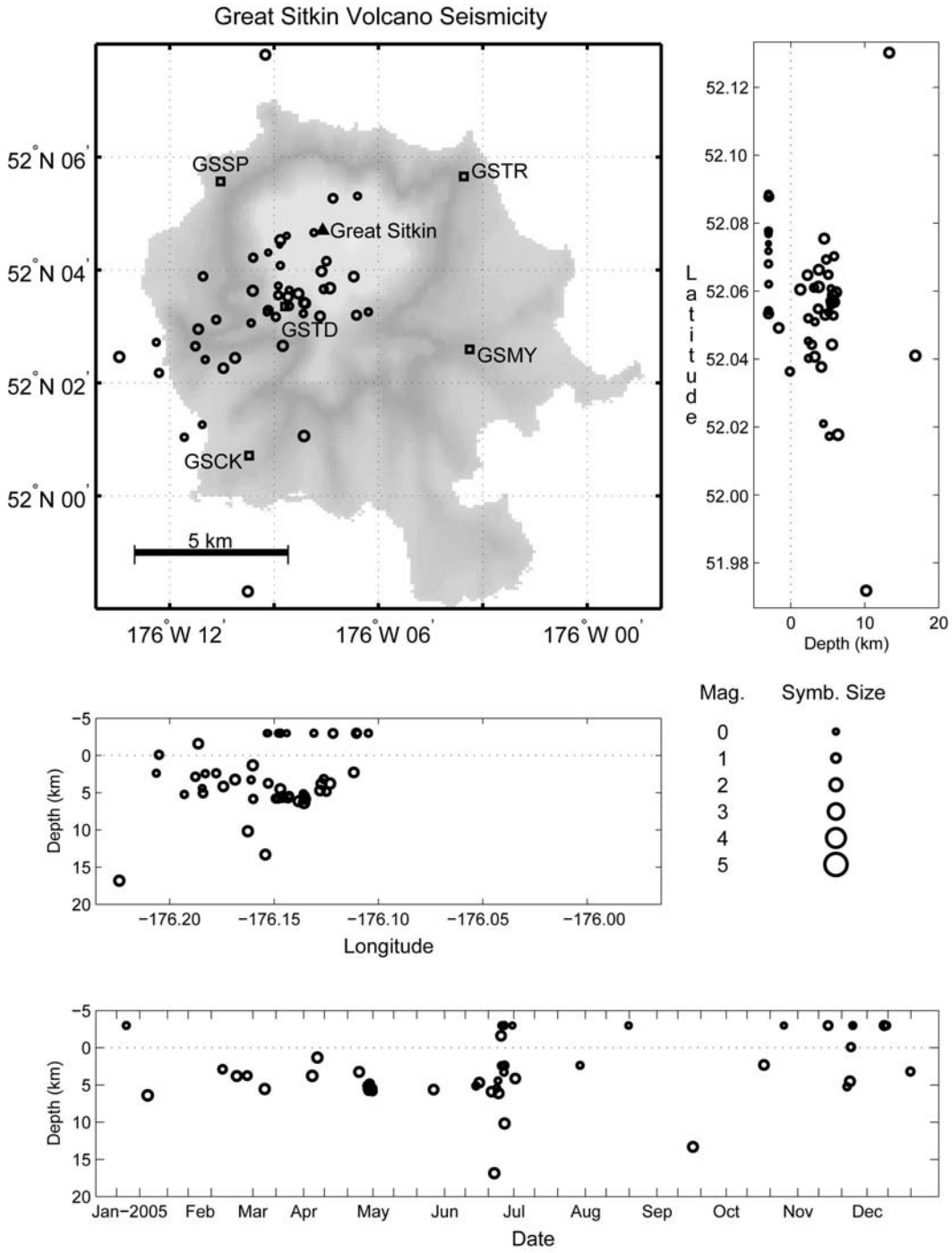

Figure A24. Summary plots of 47 earthquakes located near Great Sitkin Volcano in 2005. Open circles show hypocenter locations shallower than 20 km and open triangles show hypocenters with depths of 20 km and deeper. Hypocenter symbols are scaled with magnitude. Seismograph stations are shown by open squares and labeled by station code. Solid triangles are used to show volcanic centers and solid squares are used to show other points of interest. See Appendix B for station information.

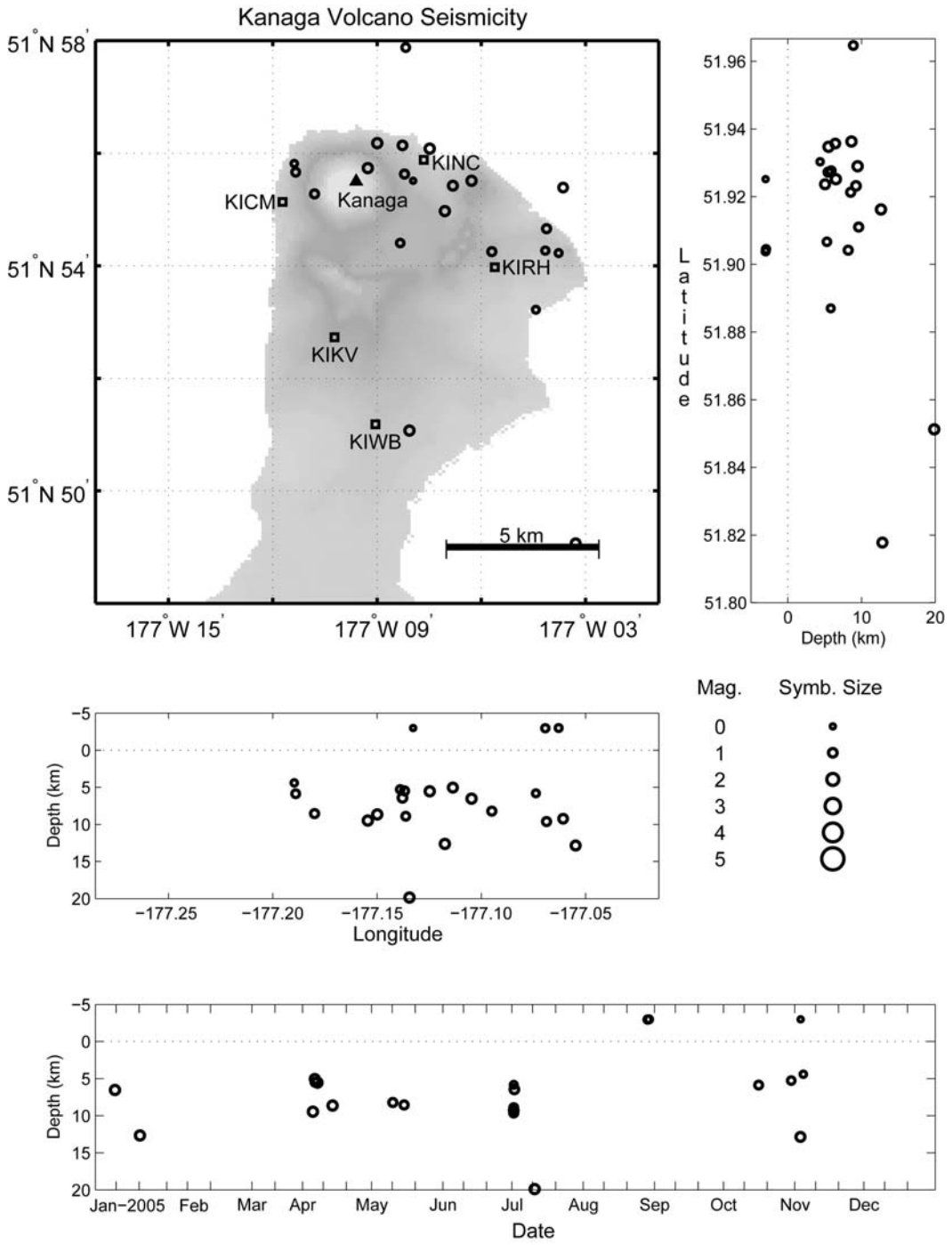

Figure A25. Summary plots of 22 earthquakes located near Kanaga Volcano in 2005. Open circles show hypocenter locations shallower than 20 km and open triangles show hypocenters with depths of 20 km and deeper. Hypocenter symbols are scaled with magnitude. Seismograph stations are shown by open squares and labeled by station code. Solid triangles are used to show volcanic centers and solid squares are used to show other points of interest. See Appendix B for station information.

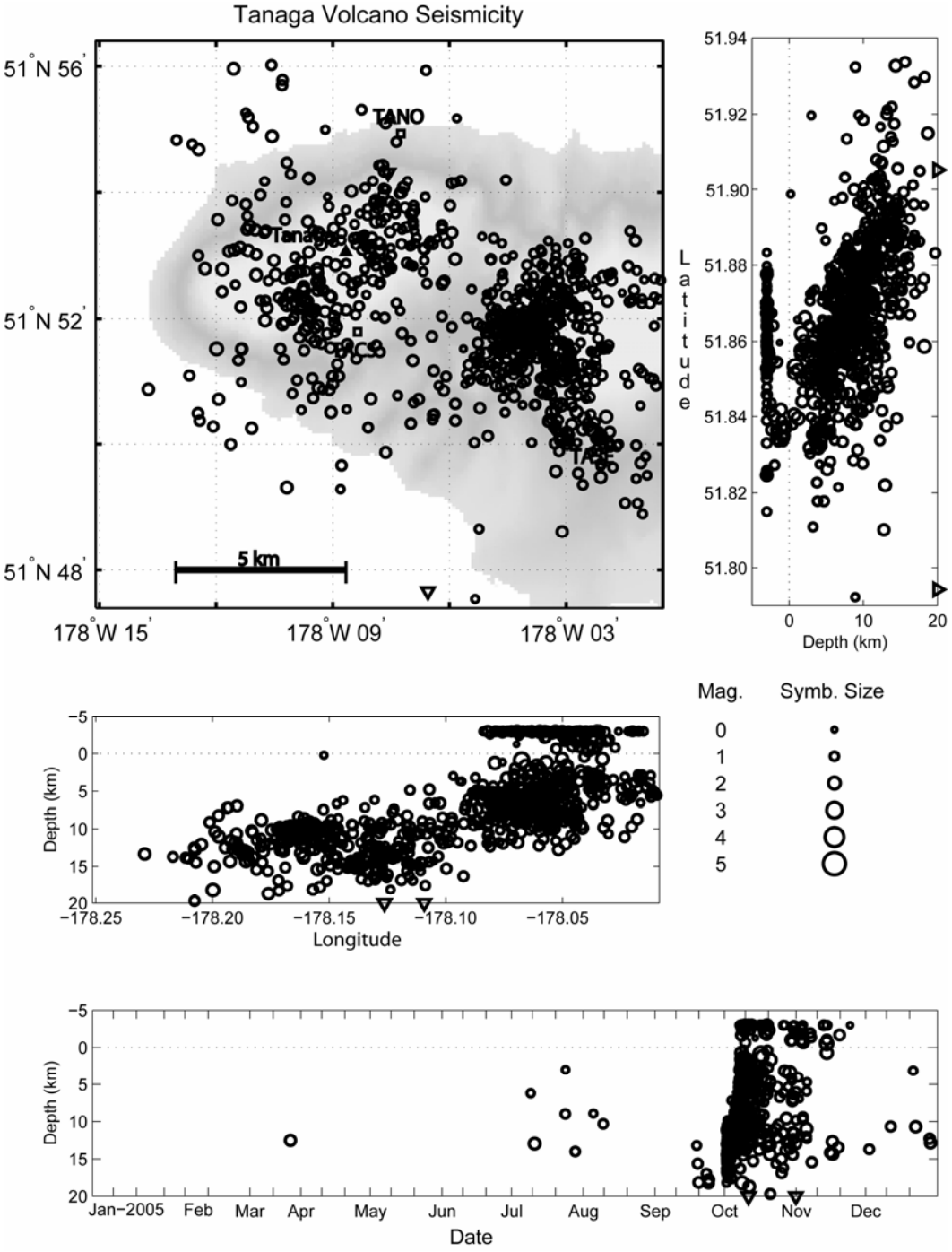

Figure A26. Summary plots of 855 earthquake located near Tanaga Volcano in 2005. Open circles show hypocenter locations shallower than 20 km and open triangles show hypocenters with depths of 20 km and deeper. Hypocenter symbols are scaled with magnitude. Seismograph stations are shown by open squares and labeled by station code. Solid triangles are used to show volcanic centers and solid squares are used to show other points of interest. See Appendix B for station information.

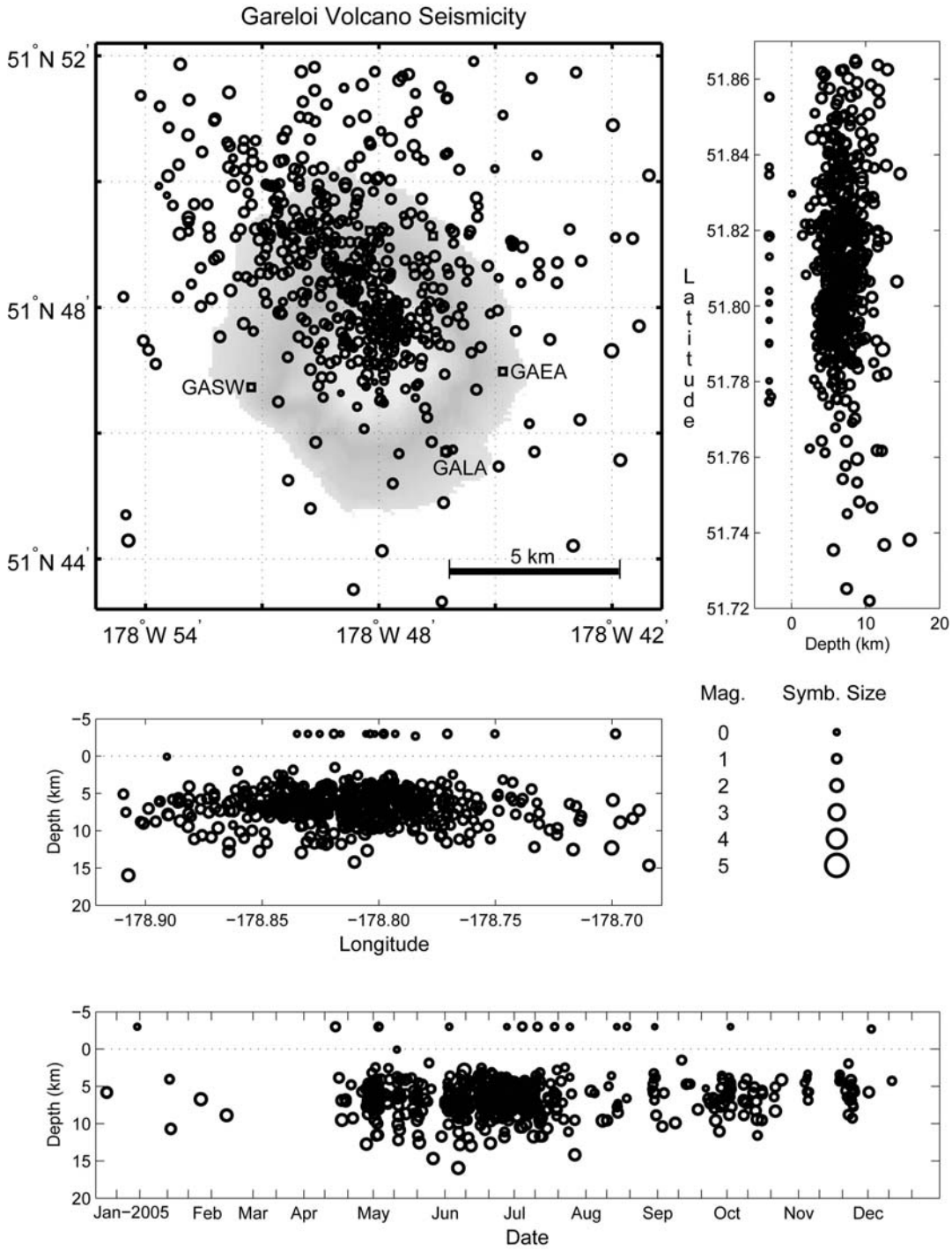

Figure A27. Summary plots of 547 earthquakes located near Mount Gareloi in 2005. Open circles show hypocenter locations shallower than 20 km and open triangles show hypocenters with depths of 20 km and deeper. Hypocenter symbols are scaled with magnitude. Seismograph stations are shown by open squares and labeled by station code. Solid triangles are used to show volcanic centers and solid squares are used to show other points of interest. See Appendix B for station information.

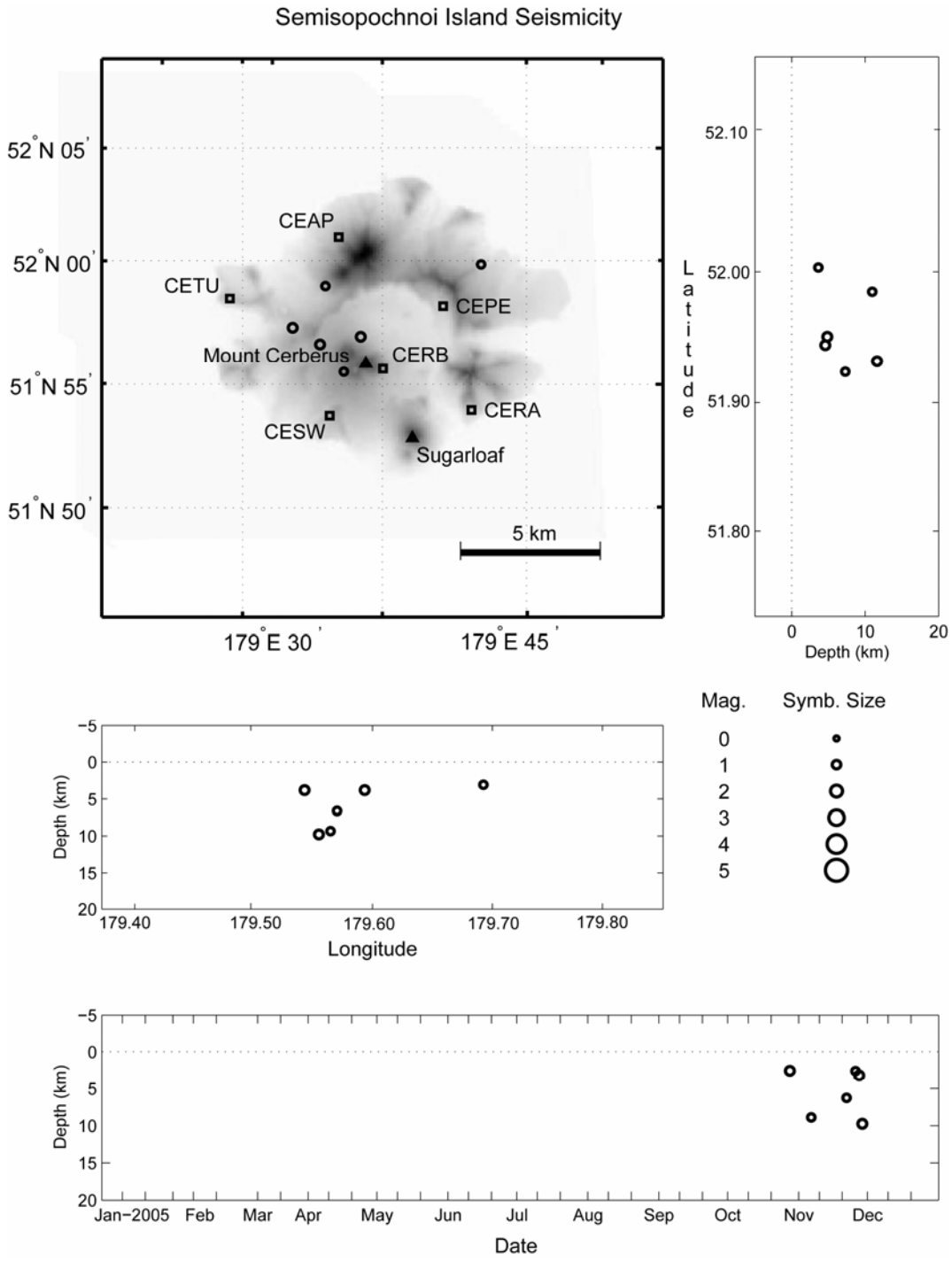

Figure A28. Summary plots of six earthquakes located on Semisopochnoi Island in 2005. Open circles show hypocenter locations shallower than 20 km and open triangles show hypocenters with depths of 20 km and deeper. Hypocenter symbols are scaled with magnitude. Seismograph stations are shown by open squares and labeled by station code. Solid triangles are used to show volcanic centers and solid squares are used to show other points of interest. See Appendix B for station information.

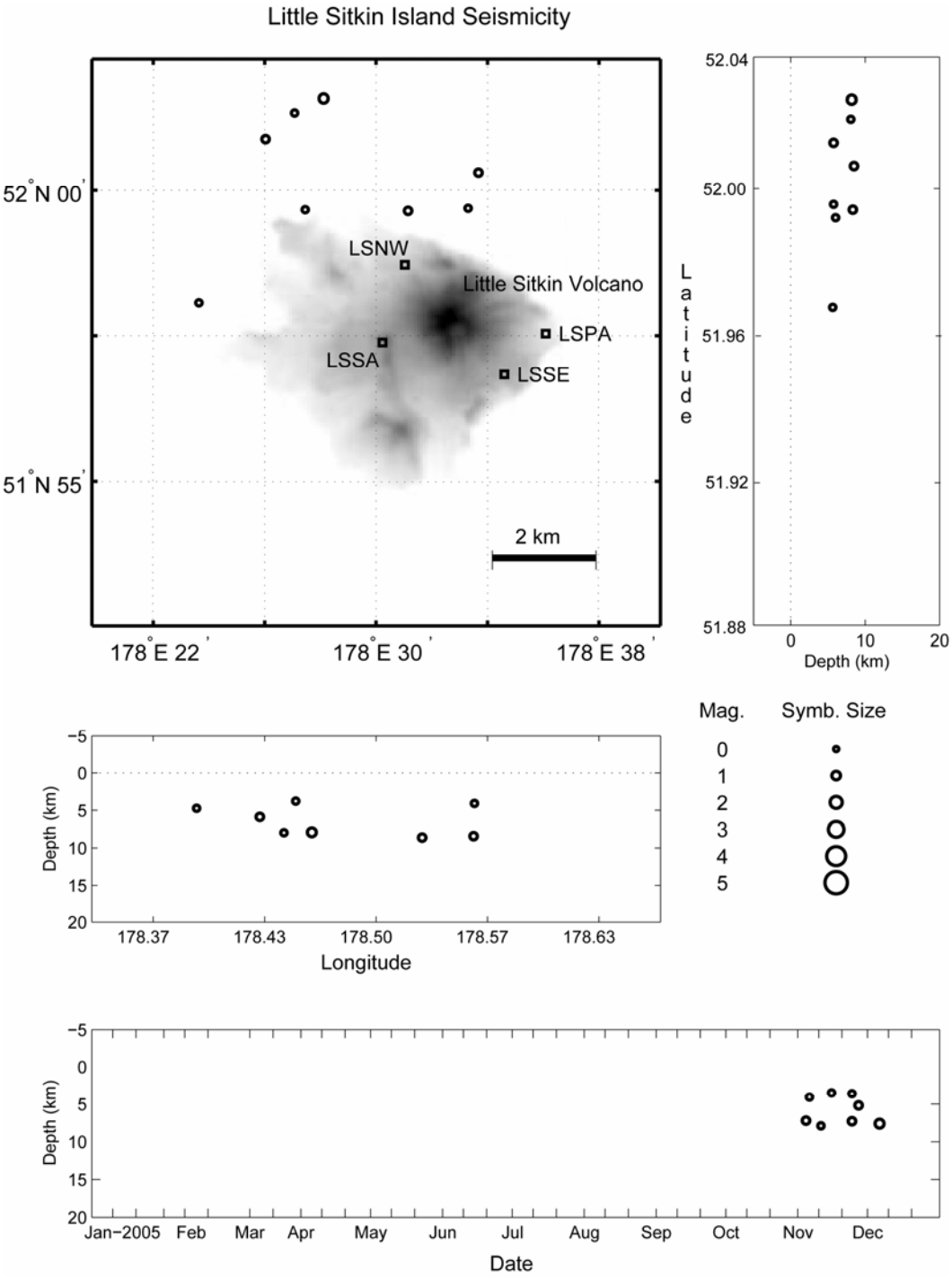

Figure A29. Summary plots of eight earthquakes located on Little Sitkin Island in 2005. Open circles show hypocenter locations shallower than 20 km and open triangles show hypocenters with depths of 20 km and deeper. Hypocenter symbols are scaled with magnitude. Seismograph stations are shown by open squares and labeled by station code. Solid triangles are used to show volcanic centers and solid squares are used to show other points of interest. See Appendix B for station information.

Appendix B: Parameters for AVO seismograph stations (datum NAD27) in 2005

Station	Latitude (N)	Longitude (E)	Elevation (m)	Seismometer	Station open date
Akutan Peak subnet (11 stations - 23 components)					
AHB	54 06.916	-165 48.943	447	L4	1996/07/24
AKGG[3]	54 11.930	-165 59.495	326	CMG-6TD	2003/06/27
AKLV[3]	54 09.762	-165 57.336	551	CMG-6TD	2003/07/02
AKMO[3]	54 05.471	-166 00.634	277	CMG-6TD	2003/06/25
AKRB[3]	54 07.803	-166 04.125	334	CMG-6TD	2003/06/29
AKS[3]	54 06.624	-165 41.803	213	L22	1996/07/24
AKT[3]	54 08.15	-165 46.2	12	CMG-40T	1996/03/18
AKV	54 07.571	-165 57.763	863	L4	1996/07/24
HSB	54 11.205	-165 54.743	497	L4	1996/07/24
LVA	54 09.655	-166 02.025	457	L4	1996/07/24
ZRO	54 05.494	-165 58.678	446	L4	1996/07/24
Aniakchak Crater subnet (6 stations - 8 components)					
ANNE	56 54.763	-158 03.534	705	L4	1997/07/18
ANNW	56 57.986	-158 12.895	816	L4	1997/07/18
ANON[3]	56 55.188	-158 10.293	445	L22	2000/07/10
ANPB	56 48.141	-158 16.847	658	L4	1997/07/18
ANPK	56 50.499	-158 07.572	972	L4	1997/07/18
AZAC	56 53.727	-158 13.841	1,057	L4	2003/07/12
Augustine Volcano subnet (8 stations - 15 components)					
AUE[3]	59 22.308	-153 22.504	168	S13	1980/10/29
AUH	59 21.833	-153 26.591	890	S13	1978/12/01
AUI[3]	59 20.11	-153 25.66	293	S13	1978/04/06
AUL	59 22.937	-153 26.142	360	S13	1980/10/29
AUL[3]	59 22.937	-153 26.142	360	CMG-40T	1997/08/27
AUP	59 21.805	-153 25.210	1,033	S13	1977/09/22
AUR	59 21.766	-153 25.876	1,225	L4	1995/11/01
AUS	59 21.599	-153 25.840	1,226	L4	1990/09/01
AUW	59 22.205	-153 28.249	276	S13	1976/10/17
Mount Dutton subnet (5 stations - 5 components)					
BLDY	55 11.670	-162 47.018	259	L4	1996/07/11
DOL	55 08.960	-161 51.683	442	L4	1996/07/11
DRR3	54 58.014	-162 15.665	457	L4	1996/07/11
DT1	55 06.427	-162 16.859	198	L4	1991/06/21
DTN	55 08.744	-162 15.419	396	S13	1988/07/16
Gareloi Volcano subnet (6 stations - 8 components)					
GAEA	51 46.980	-178 44.810	326	L4	2003/08/30
GAKI	51 33.267	-178 48.725	99	L4	2003/09/01
GALA	51 45.704	-178 46.292	315	L4	2003/08/30
GANE	51 49.135	-178 46.603	325	L4	2003/09/02
GANO	51 49.220	-178 48.230	451	L4	2003/09/02
GASW[3]	51 46.731	-178 51.276	248	L22	2003/08/30

Station	Latitude (N)	Longitude (E)	Elevation (m)	Seismometer	Station open date
Great Sitkin Volcano subnet (6 stations - 8 components)					
GSCK	52 00.712	-176 09.718	384	L4	1999/09/15
GSIG	51 59.181	-175 55.502	407	L4	1999/09/03
GSMY	52 02.594	-176 03.376	418	L4	1999/09/03
GSSP	52 05.566	-176 10.541	295	L4	1999/09/15
GSTD[3]	52 03.356	-176 08.685	873	L22	1999/09/03
GSTR	52 05.655	-176 03.546	536	L4	1999/09/03
Iliamna Volcano subnet (6 stations - 8 components)					
ILI	60 04.877	-152 57.502	771	L4	1987/09/15
ILS	59 57.454	-153 04.083	1,125	S13	1996/08/28
ILW	60 03.585	-153 08.222	1,646	S13	1994/09/09
INE	60 03.65	-153 03.75	1,585	S13	1990/08/29
IVE[3]	60 01.014	-153 00.981	1,173	S13,L22	1996/09/19
IVS	60 00.55	-153 04.85	2,332	S13	1990/08/29
Kanaga Volcano subnet (6 stations - 6 components)					
KICM	51 55.136	-177 11.718	183	L4	1999/09/15
KIKV	51 52.730	-177 10.223	411	L4	1999/09/15
KIMD	51 45.697	-177 14.093	183	L4	1999/09/15
KINC	51 55.884	-177 07.657	198	L4	1999/09/15
KIRH	51 53.976	-177 05.611	309	L4	1999/09/03
KIWB	51 51.183	-177 09.049	244	L4	1999/09/03
Katmai Volcanic Cluster subnet (20 stations - 30 components)					
ACH[3]	58 12.64	-155 19.56	960	L22	1996/07/25
ANCK	58 11.93	-155 29.64	869	L4	1996/07/25
CAHL	58 03.15	-155 18.09	807	L4	1996/07/25
CNTC	58 15.87	-155 53.02	1,158	L4	1996/07/25
KABR	58 07.87	-154 58.15	884	L4	1998/08/12
KABU[3]	58 16.225	-155 16.934	1,065	CMT-6TD	2004/08/01
KAHC	58 38.94	-155 00.36	1,250	L4	1998/10/12
KAHG	58 29.64	-154 32.78	923	L4	1998/10/12
KAIC	58 29.10	-155 02.75	734	L4	1998/10/12
KAKN[3]	58 17.819	-155 03.668	1,049	CMG-6TD	2004/08/01
KAPH[3]	58 35.81	-154 20.81	907	L22	1998/10/12
KARR	58 29.87	-154 42.20	610	L4	1998/10/12
KAWH	58 23.02	-154 47.95	777	L4	1998/10/12
KBM	58 16.50	-155 12.10	732	L4	1991/07/22
KCE	58 14.60	-155 11.00	777	L4	1991/07/22
KCG[3]	58 18.457	-155 06.684	762	L22	1988/08/01
KEL	58 26.401	-155 44.442	975	L4	1988/08/01
KJL	58 03.24	-155 34.39	792	L4	1996/07/25
KVT	58 22.90	-155 17.70	457	L4	1988/08/01
MGLS	58 08.06	-155 09.65	472	L4	1996/07/25
Korovin Volcano subnet (7 stations - 9 components)					
KOFP	53 57.08	-166 53.51	662	L4	2004/07/02
KOKL	53 47.68	-166 52.35	758	L4	2004/07/05
KOKV[3]	53 53.03	-166 41.00	776	L22	2004/07/05
KONE	53 48.629	-166 44.736	253	L4	2004/07/10
KONW	53 48.978	-166 56.187	334	L4	2004/07/04
KOSE	53 54.88	-166 46.96	625	L4	2004/07/07
KOWE	53 58.16	-166 40.71	527	L4	2004/07/06

Station	Latitude (N)	Longitude (E)	Elevation (m)	Seismometer	Station open date
Little Sitkin subnet (4 stations - 6 components)					
LSNW	51 58.232	178 31.011	290	L4	2005/09/30
LSPA[3]	51 57.413	178 34.405	335	L4-3D	2005/09/30
LSSSA	51 56.973	178 30.793	549	L4	2005/09/28
LSSE	51 55.993	178 34.139	335	L4	2005/09/27
Makushin Volcano subnet (7 stations - 9 components)					
MCIR	53 57.086	-166 53.529	800	L4	1996/07/25
MGOD	53 47.683	-166 52.561	650	L4	1996/07/25
MNAT	53 53.028	-166 41.016	397	L4	1996/07/25
MREP	53 48.629	-166 44.736	785	L4	2002/01/01
MSOM	53 48.978	-166 56.187	146	L4	1996/07/25
MSW[3]	53 54.929	-166 47.186	418	L22	1996/07/25
MTBL	53 58.136	-166 40.760	810	L4	1996/07/25
Okmok Volcano subnet (13 stations - 21 components)					
OKAS	53 24.319	-168 21.686	270	L4	2003/01/09
OKCD[3]	53 25.818	-168 06.737	459	CMG-6TD	2003/01/09
OKCE[3]	53 25.622	-168 09.858	515	CMG-6TD	2003/01/09
OKCF	53 23.749	-168 08.175	685	L4	2003/01/09
OKER	53 27.278	-168 02.960	956	L4	2003/01/09
OKFG[3]	53 24.702	-167 54.568	201	CMG-6TD	2003/01/09
OKID	53 28.645	-167 48.972	437	L4	2003/01/09
OKRE	53 31.215	-168 09.846	422	L4	2003/01/09
OKSO[3]	53 21.447	-168 09.591	460	CMG-6TD	2004/09/01
OKSP	53 15.156	-168 17.431	608	L4	2003/01/09
OKTU	53 23.035	-168 02.466	646	L4	2003/01/09
OKWE	53 28.328	-168 14.388	445	L4	2003/01/09
OKWR	53 26.084	-168 12.333	1,017	L4	2003/01/09
Pavlof Volcano subnet (7 stations - 9 components)					
BLHA	55 42.227	-162 03.907	411	L4	1996/07/11
HAG	55 19.068	-161 54.150	503	L4	1996/07/11
PN7A	55 26.020	-161 59.713	838	L4	1996/07/11
PS1A	55 25.321	-161 44.425	293	L4	1996/07/11
PS4A	55 20.811	-161 51.233	322	L4	1996/07/11
PV6[3]	55 27.217	-161 55.112	747	L22	1996/07/11
PVV	55 22.438	-161 47.396	161	L4	1996/07/11
Mount Peulik subnet (7 stations - 9 components)					
PLBL	57 41.990	-156 49.131	461	L4	2004/08/01
PLK1	57 48.114	-156 36.433	78	L4	2004/08/01
PLK2	57 45.852	-156 19.458	401	L4	2004/08/01
PLK3[3]	57 41.320	-156 16.044	494	L22	2004/08/01
PLK4	57 37.928	-156 21.464	1,031	L4	2004/08/01
PLK5	57 59.864	-156 52.662	49	L4	2004/08/01
PLWL	58 02.696	-156 20.479	585	L4	2004/08/01

Station	Latitude (N)	Longitude (E)	Elevation (m)	Seismometer	Station open date
Redoubt Volcano subnet (7 stations - 12 components)					
DFR	60 35.514	-152 41.160	1,090	L4	1988/08/15
NCT	60 33.789	-152 55.568	1,079	L4	1988/08/14
RDN	60 31.377	-152 44.273	1,400	L4	1988/08/13
RDT	60 34.394	-152 24.315	930	L4	1971/08/09
RED[3]	60 25.192	-152 46.308	1,064	L4	1990/08/30
REF[3]*	60 29.35	-152 42.10	1,801	L22	1992/07/27
RSO	60 27.73	-152 45.23	1,921	L4	1990/03/01
Semisopochnoi Island subnet (6 stations - 8 components)					
CEAP	52 00.146	179 47.018	244	L4	2005/09/17
CEPE	51 57.948	179 51.683	335	L4	2005/09/17
CERA	51 54.419	179 15.665	305	L4	2005/09/26
CERB[3]	51 55.886	179 16.859	305	L4-3D	2005/09/18
CESW	51 54.060	179 15.419	238	L4	2005/09/18
CETU	51 57.965	179 15.419	335	L4	2005/09/22
Shishaldin Volcano subnet (6 stations - 8 components)					
BRPK	54 38.730	-163 44.449	393	L4	1997/07/27
ISNN	54 49.937	-163 46.706	466	L4	1997/07/27
ISTK	54 43.929	-163 42.376	704	L4	1997/07/27
SSLN	54 48.709	-163 59.756	637	L4	1997/07/27
SSLS[3]	54 42.718	-163 59.926	817	L22	1997/07/27
SSLW	54 46.307	-164 07.282	628	L4	1997/07/27
Mount Spurr subnet (26 stations - 56 components; Perm. Stations only: 15 stations - 23 components)					
BGL	61 16.012	-152 23.340	1,127	L4	1989/08/13
BKG	61 04.21	-152 15.76	1,009	L4	1991/07/01
CGL	61 18.46	-152 00.40	1,082	L4	1981/09/22
CKL	61 11.782	-152 20.268	1,281	L4	1989/08/05
CKN	61 13.44	-152 10.89	735	L4	1991/08/19
CKT	61 12.05	-152 12.37	975	L4	1992/09/16
CP2	61 15.85	-152 14.51	1,981	L4	1992/10/23
CRP[3]	61 16.02	-152 09.33	1,622	L4	1981/08/26
NCG	61 24.22	-152 09.40	1,244	L4	1989/08/06
SP02[3]	61 10.616	-152 03.481	821	CMG-6TD	2005/06/16**
SP03[3]	61 08.208	-152 02.815	882	CMG-6TD	2005/06/16**
SP04[3]	61 08.014	-152 15.394	946	CMG-6TD	2005/06/16**
SP05[3]	61 20.793	-152 05.296	893	CMG-6TD	2005/06/16**
SP06[3]	61 15.586	-152 11.053	1,192	CMG-6TD	2005/06/16**
SP07[3]	61 20.781	-151 57.842	1,113	CMG-6TD	2005/06/16**
SP08[3]	61 19.956	-152 26.700	1,545	CMG-6TD	2005/06/16**
SP09[3]	61 14.137	-151 47.920	814	CMG-6TD	2005/06/16**
SP10[3]	61 22.465	-152 30.981	1,429	CMG-6TD	2005/06/16**
SP11[3]	61 10.780	-152 37.253	921	CMG-6TD	2005/06/16**
SP12[3]	61 23.627	-152 07.974	1,034	CMG-6TD	2005/06/16**
SPBG[3]	61 15.583	-152 22.194	1,087	CMG-6TD	2004/09/09
SPCG[3]	61 17.512	-152 01.228	1,329	CMG-6TD	2004/09/08
SPCR[3]	61 12.051	-152 12.409	984	CMG-6TD	2004/09/08
SPNW	61 20.826	-152 36.236	1,040	L4	2004/08/17
SPU	61 10.90	-152 03.26	800	L4	1971/08/10
SPWE	61 16.405	-152 33.545	1,327	L4	2004/08/18

Station	Latitude (N)	Longitude (E)	Elevation (m)	Seismometer	Station open date
Tanaga Volcano subnet (6 stations - 8 components)					
TACS	51 51.792	-178 08.363	918	L4	2003/08/28
TAFL	51 45.396	-177 53.867	186	L4	2003/08/28
TAFP[3]	51 54.003	-177 58.997	440	L22	2003/08/27
TANO	51 54.942	-178 07.249	269	L4	2003/08/24
TAPA	51 48.932	-177 48.770	640	L4	2003/08/27
TASE	51 50.099	-178 02.222	682	L4	2003/08/24
Mount Veniaminof subnet (9 stations - 9 components)					
BPBC	56 35.383	-158 27.153	584	L4	2002/10/03
VNFG	56 17.140	-159 33.066	1,068	L4	2002/02/06
VNHG	56 13.267	-159 09.853	966	L4	2002/02/06
VNKR	56 01.871	-159 22.068	620	L4	2002/02/06
VNNF	56 17.022	-159 18.961	1,153	L4	2002/06/20
VNSG	56 07.549	-159 05.121	761	L4	2002/02/06
VNSS	56 13.600	-159 27.290	1,733	L4	2002/02/06
VNSW	56 04.317	-159 33.508	716	L4	2002/06/20
VNWF	56 09.104	-159 33.733	1,095	L4	2002/02/06
Westdahl Peak subnet (6 stations - 8 components)					
WESE	54 28.389	-164 35.038	953	L4	1998/08/28
WESN	54 34.600	-164 34.703	549	L4	1998/10/17
WESS[3]	54 28.828	-164 43.333	908	L22	1998/08/28
WFAR	54 32.029	-164 46.567	640	L4	1998/08/28
WPOG	54 35.837	-164 44.606	445	L4	1998/10/17
WTUG	54 50.847	-164 23.117	636	L4	1998/10/17
Mount Wrangell subnet (4 stations - 6 components)					
WACK[3]	61 59.178	-144 19.703	2,280	L22	2000/07/31
WANC	62 00.189	-144 4.195	4,190	L4	2000/07/31
WASW	61 55.692	-144 10.346	2,196	L4	2001/08/03
WAZA	62 04.506	-144 9.132	2,531	L4	2001/08/03
Regional stations (9 stations - 9 components)					
ADAG	51 58.812	-176 36.104	286	L4	1999/09/15
BGM	59 23.56	-155 13.76	625	L4	1978/09/08
BGR	60 45.45	-152 25.06	985	L4	1991/07/01
CDD	58 55.771	-153 38.558	622	S13	1981/08/17
ETKA	51 51.712	-176 24.351	290	L4	1999/09/15
MMN	59 11.11	-154 20.20	442	S13	1981/08/22
OPT	59 39.192	-153 13.796	634	S13	1974/00/00
PDB	59 47.27	-154 11.55	305	S13	1978/09/09
STLK	61 29.926	-151 49.963	945	L4	1997/09/01

Station Codes:
[3] Three-component station
* REF also has a low-gain vertical component.
** Temporary stations removed on 2005/09/14

Seismometer Codes:

CMG-40T	Guralp CMG-40T 60 second natural period three-component broadband seismometer
CMG-6TD:	Guralp CMG-6TD 30 second natural period three-component broadband seismometer
L4	Mark Products L4 one second natural period single-component seismometer
L4-3D:	Mark Products L4-3D one second natural period three-component seismometer
L22:	Mark Products L22 0.5 second natural period three-component seismometer
S13:	Teledyne Geotech S13 one second natural period single-component seismometer

Appendix C: Figures showing the locations of the permanent AVO regional and volcano-specific seismograph stations in 2005. In all figures, closed triangles show volcanic centers and open squares show seismograph stations.

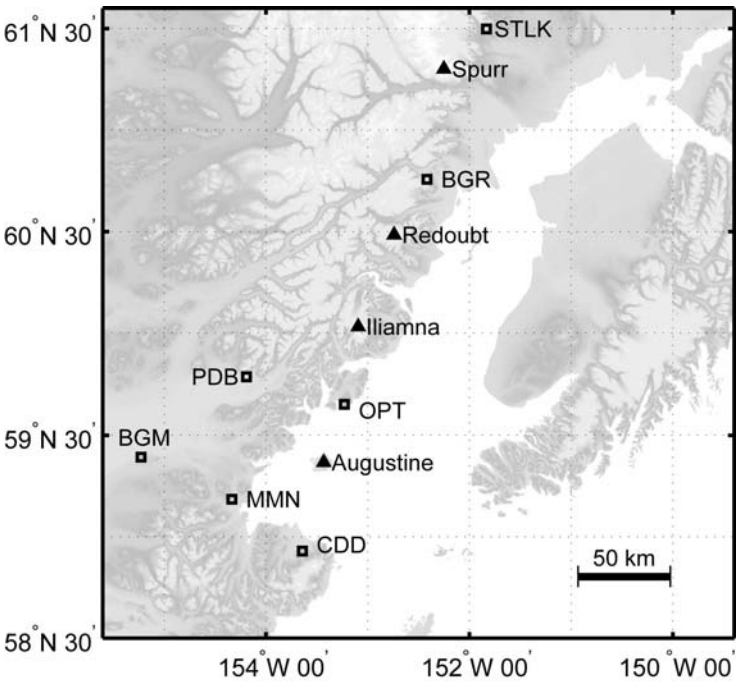

Figure C1. Regional AVO seismograph stations in Cook Inlet. Seismograph stations are shown by open squares. Closed triangles show volcanic centers.

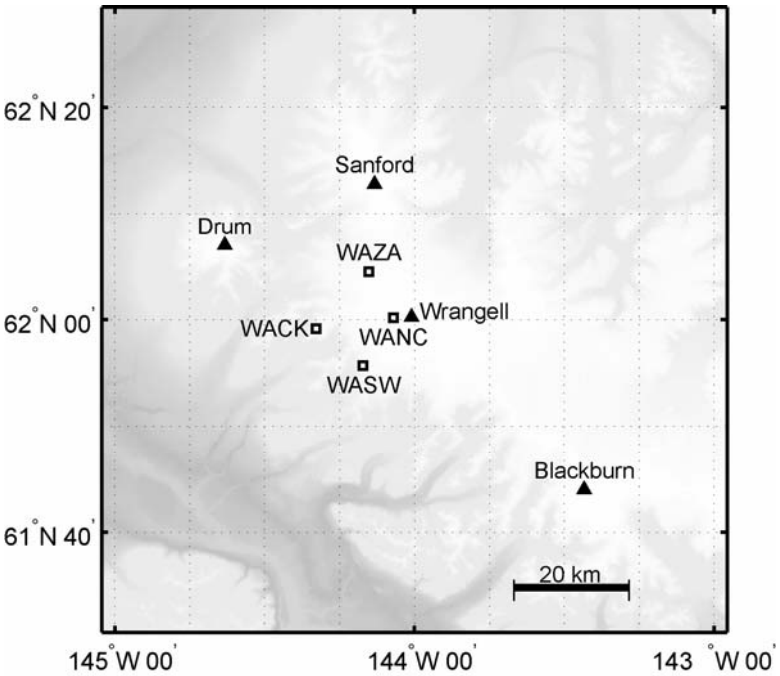

Figure C2. AVO seismograph stations near Mount Wrangell. Seismograph stations are shown by open squares. Closed triangles show volcanic centers.

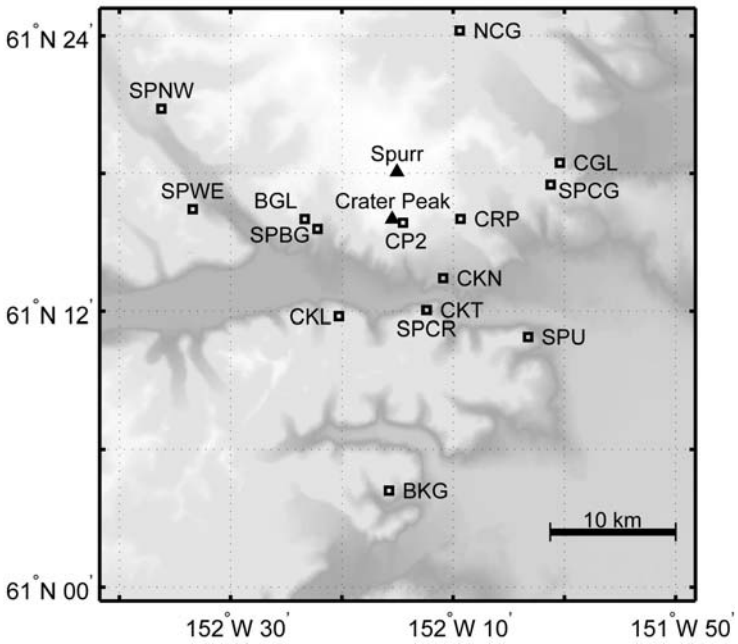

Figure C3. AVO seismograph stations near Mount Spurr. Seismograph stations are shown by open squares. Closed triangles show volcanic centers.

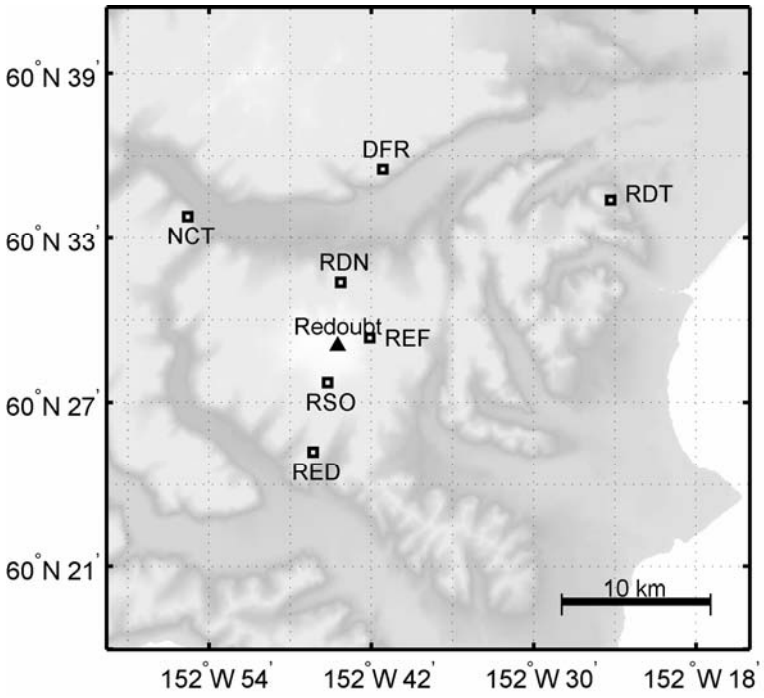

Figure C4. AVO seismograph stations near Redoubt Volcano. Seismograph stations are shown by open squares. Closed triangles show volcanic centers.

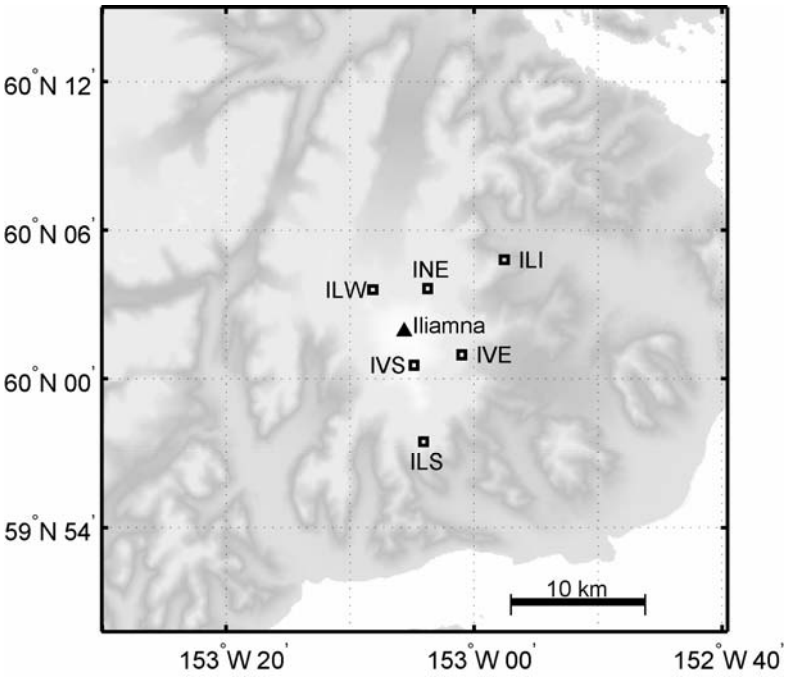

Figure C5. AVO seismograph stations near Iliamna Volcano. Seismograph stations are shown by open squares. Closed triangles show volcanic centers.

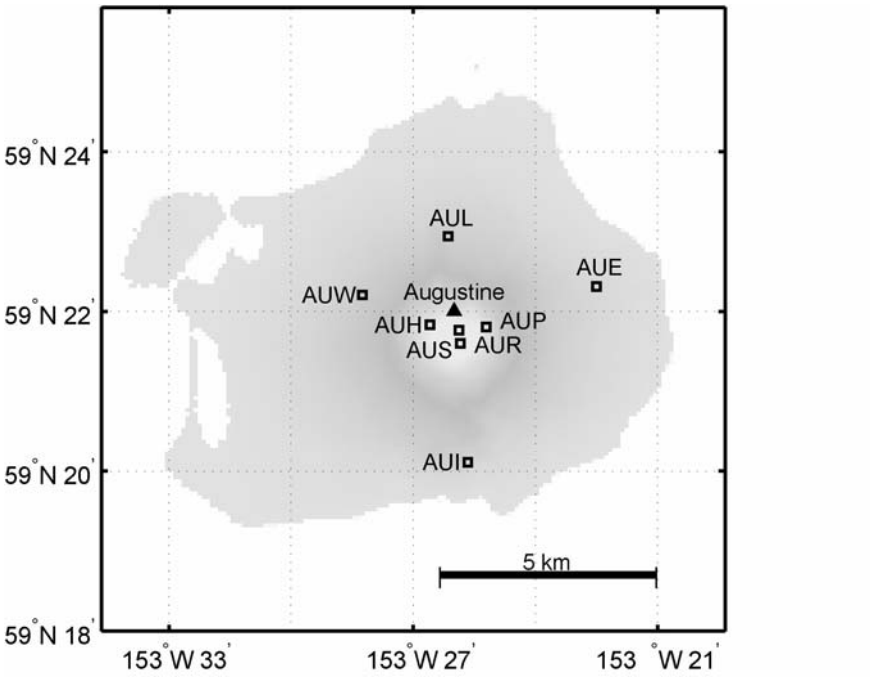

Figure C6. AVO seismograph stations near Augustine Volcano. Seismograph stations are shown by open squares. Closed triangles show volcanic centers.

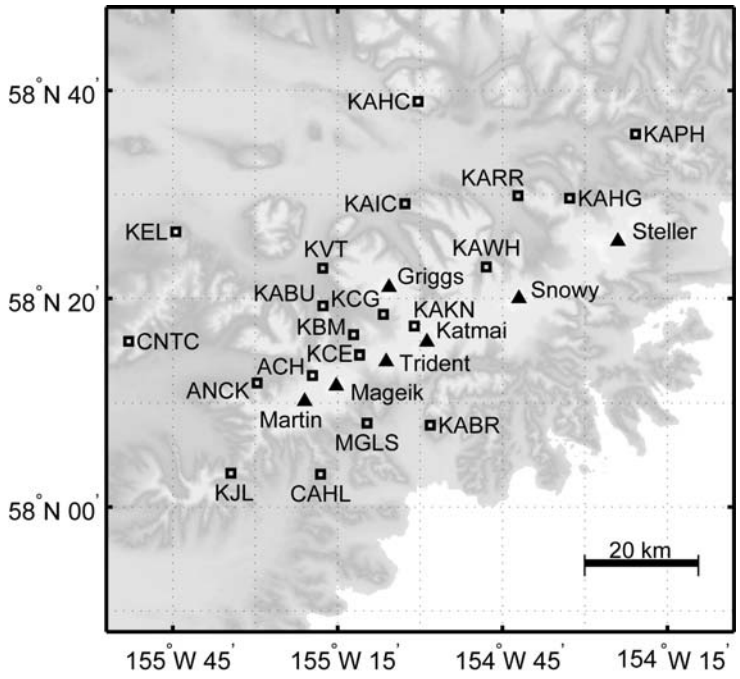

Figure C7. AVO seismograph stations near the Katmai volcanic cluster. Seismograph stations are shown by open squares. Closed triangles show volcanic centers.

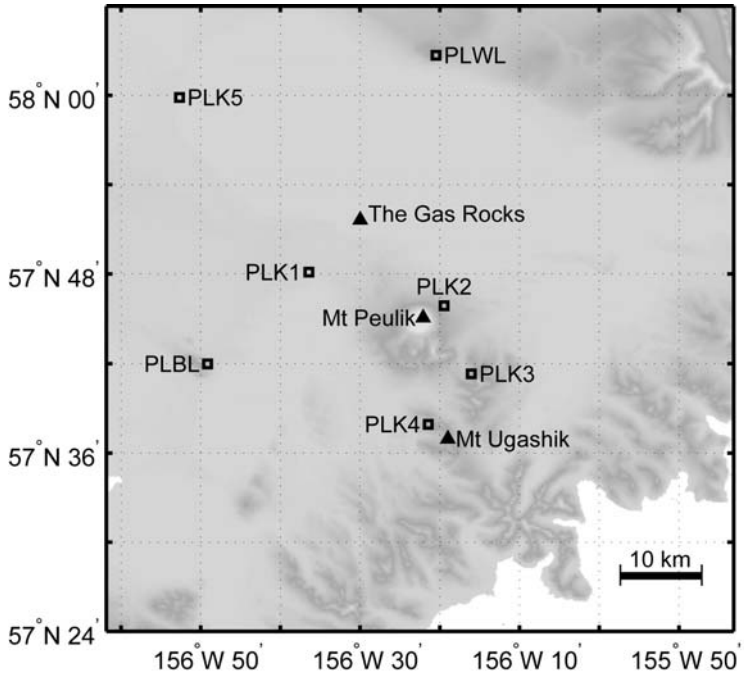

Figure C8. AVO seismograph stations near the Mount Peulik. Seismograph stations are shown by open squares. Closed triangles show volcanic centers.

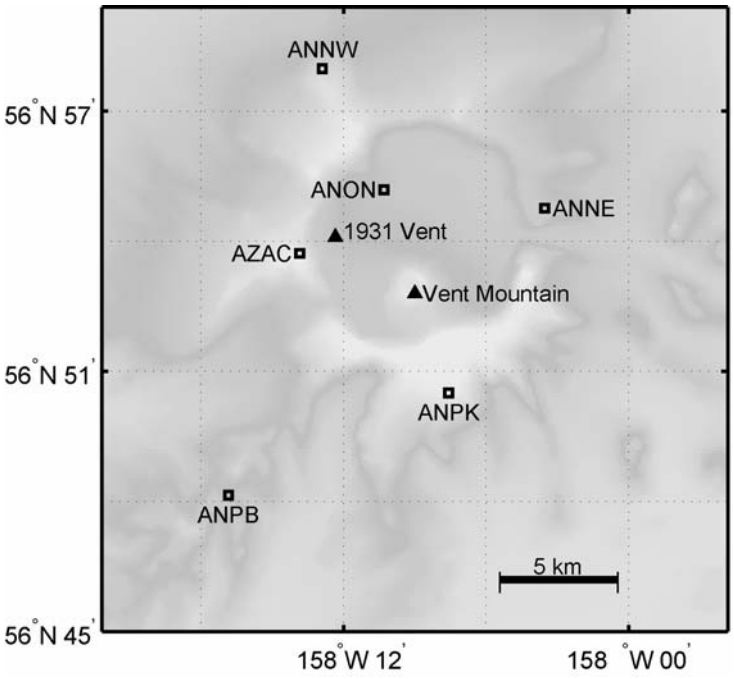

Figure C9. AVO seismograph stations near Aniakchak Crater. Seismograph stations are shown by open squares. Closed triangles show volcanic centers.

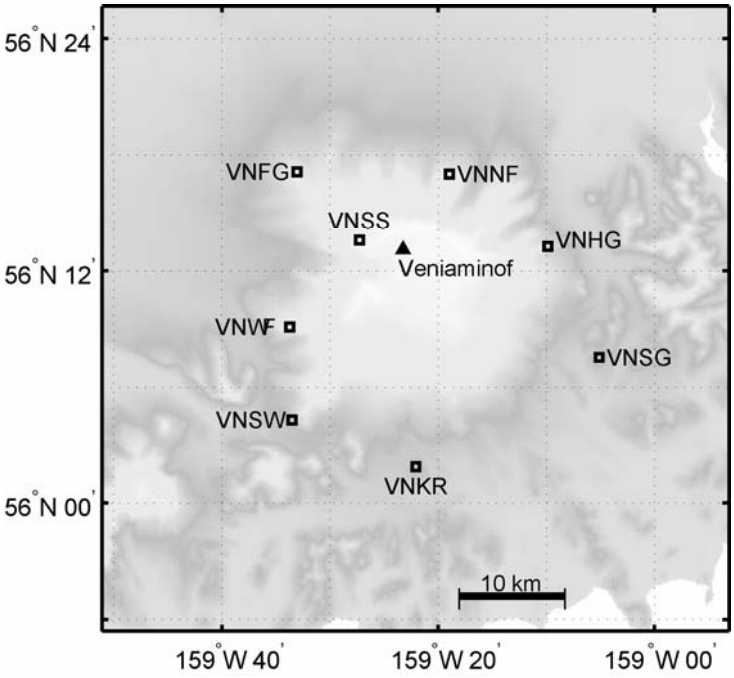

Figure C10. AVO seismograph stations near Mount Veniaminof. Seismograph station BPBC is not shown and is located 70 km northeast of Mount Veniaminof. Seismograph stations are shown by open squares. Closed triangles show volcanic centers.

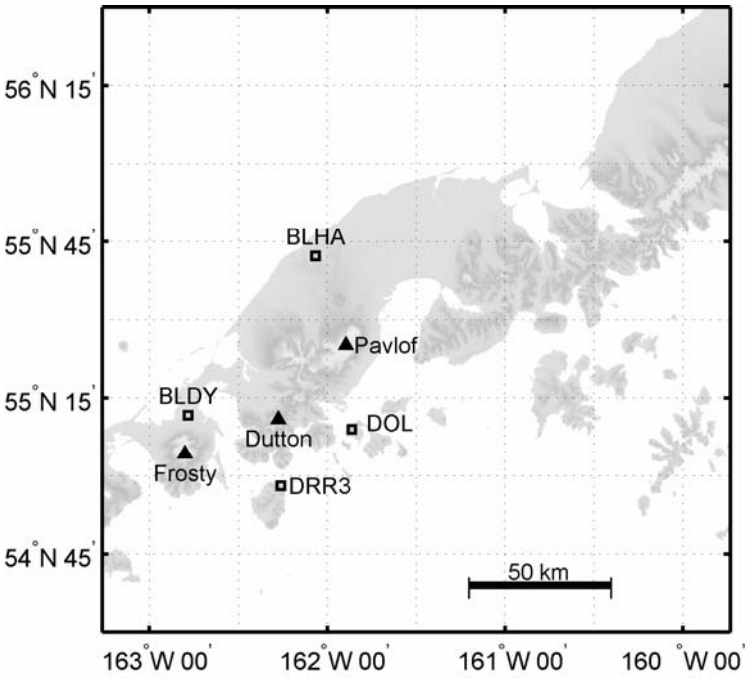

Figure C11. Regional AVO seismograph stations on the western end of the Alaska Peninsula. Seismograph stations are shown by open squares. Closed triangles show volcanic centers.

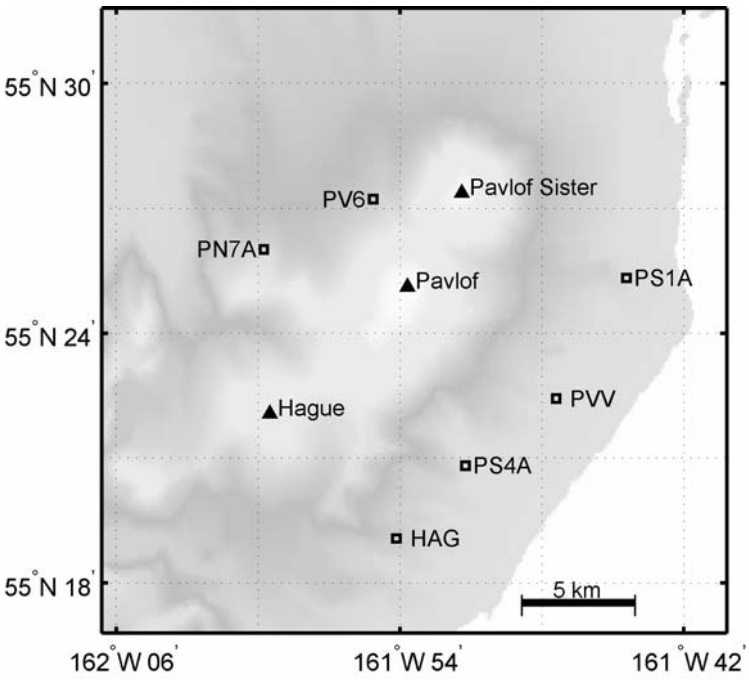

Figure C12. AVO seismograph stations near Pavlof Volcano. Seismograph stations are shown by open squares. Closed triangles show volcanic centers.

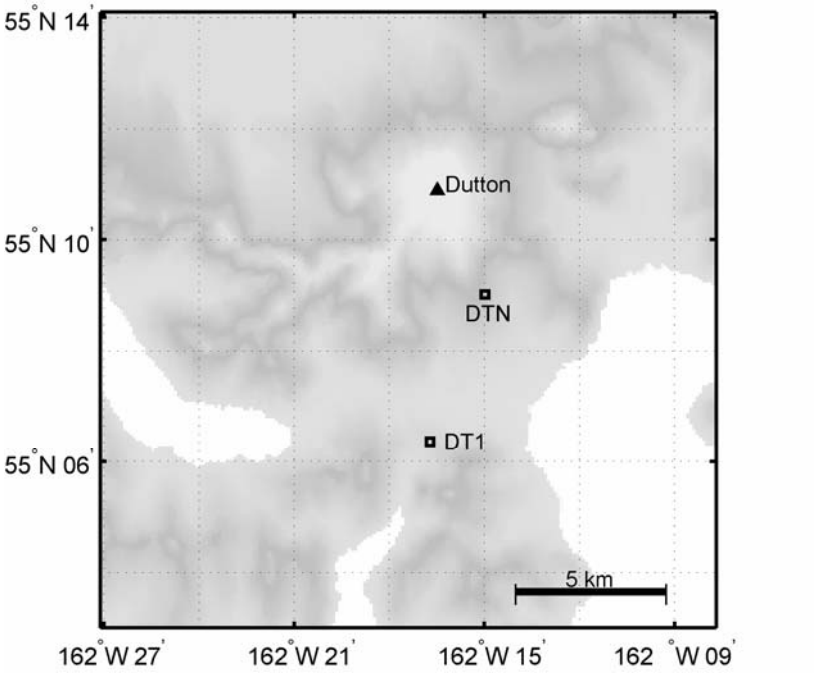

Figure C13. AVO seismograph stations near Mount Dutton. Seismograph stations are shown by open squares. Closed triangles show volcanic centers.

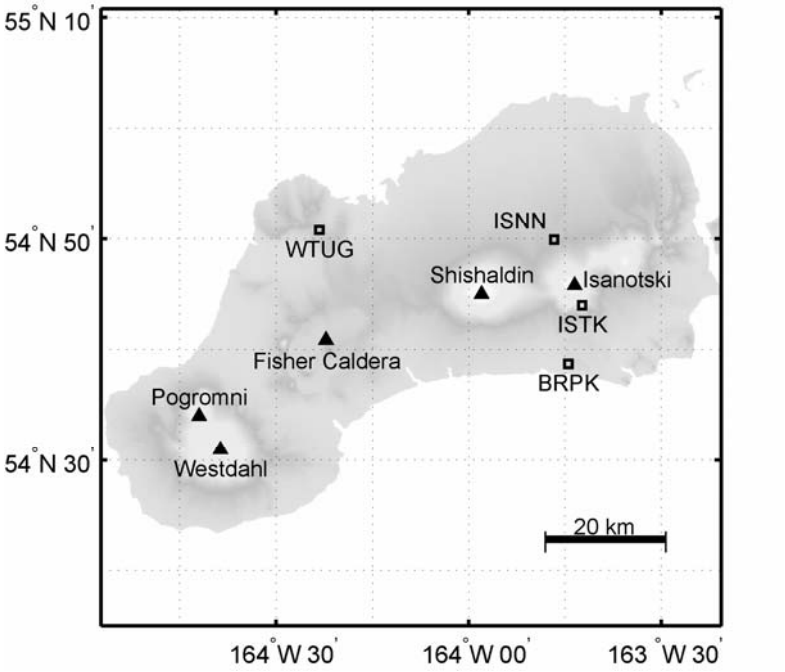

Figure C14. Regional AVO seismograph stations on Unimak Island. Seismograph stations are shown by open squares. Closed triangles show volcanic centers.

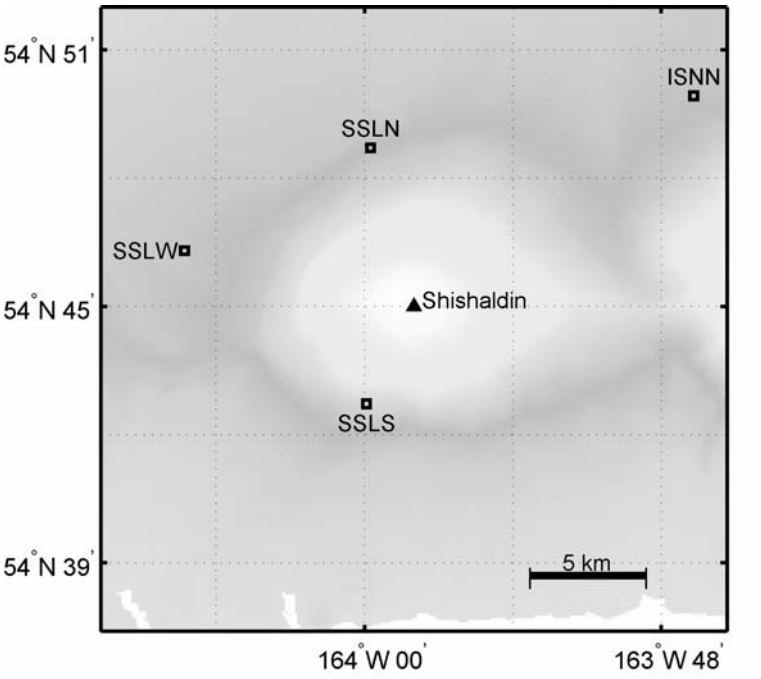

Figure C15. AVO seismograph stations near Shishaldin Volcano. Seismograph stations are shown by open squares. Closed triangles show volcanic centers.

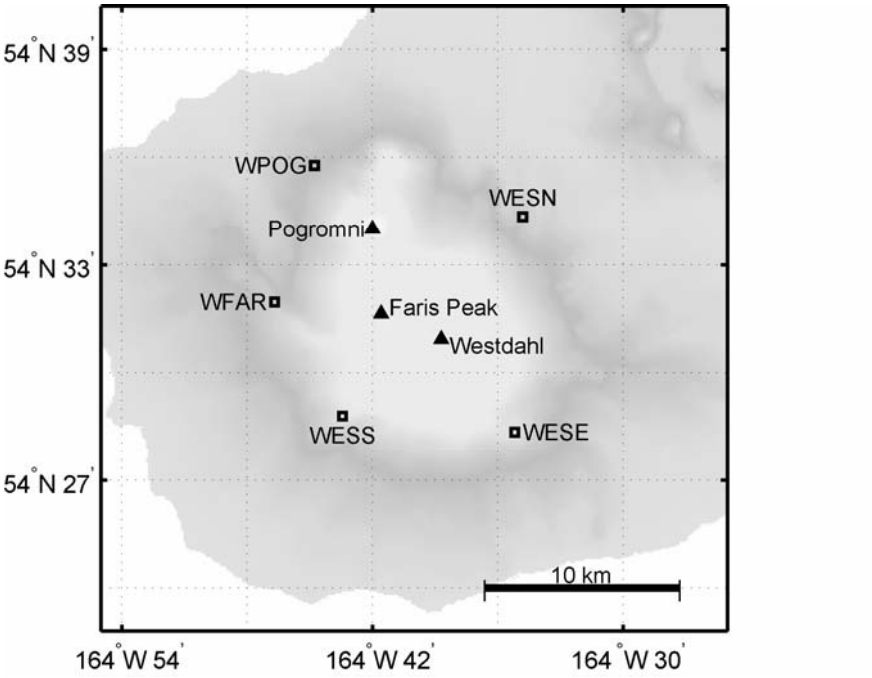

Figure C16. AVO seismograph stations near Westdahl Peak. Seismograph stations are shown by open squares. Closed triangles show volcanic centers.

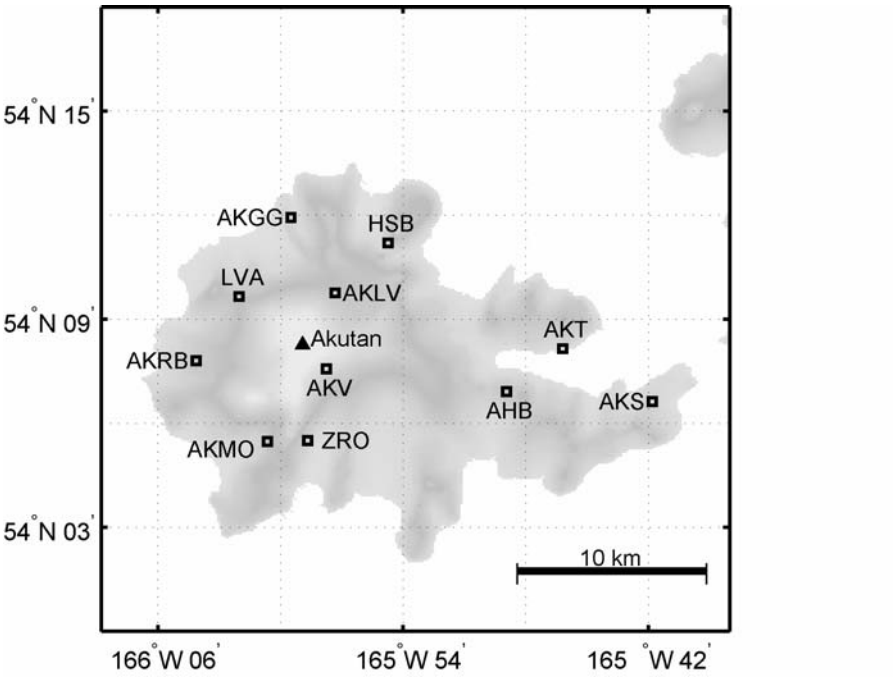

Figure C17. AVO seismograph stations near Akutan Peak. Seismograph stations are shown by open squares. Closed triangles show volcanic centers.

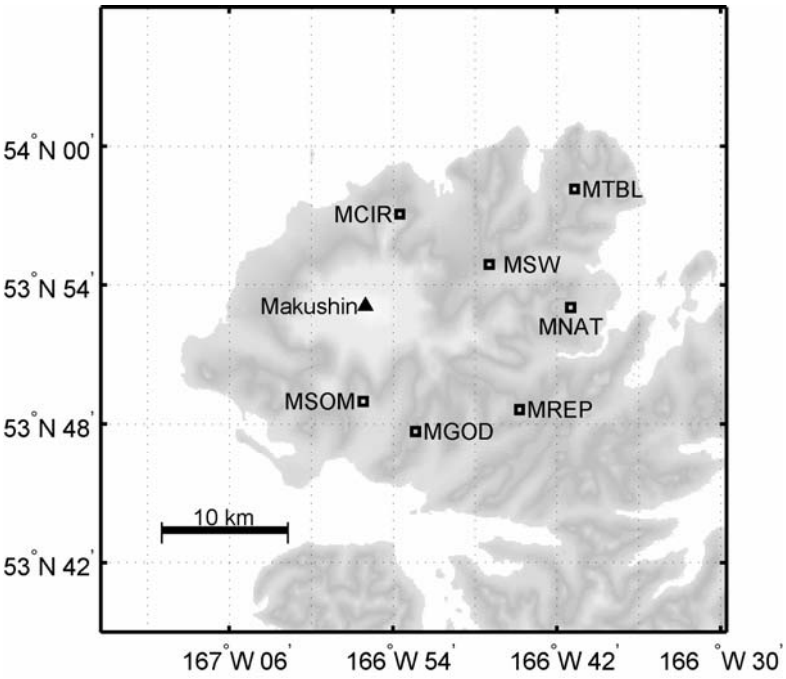

Figure C18. AVO seismograph stations near Makushin Volcano. Seismograph stations are shown by open squares. Closed triangles show volcanic centers.

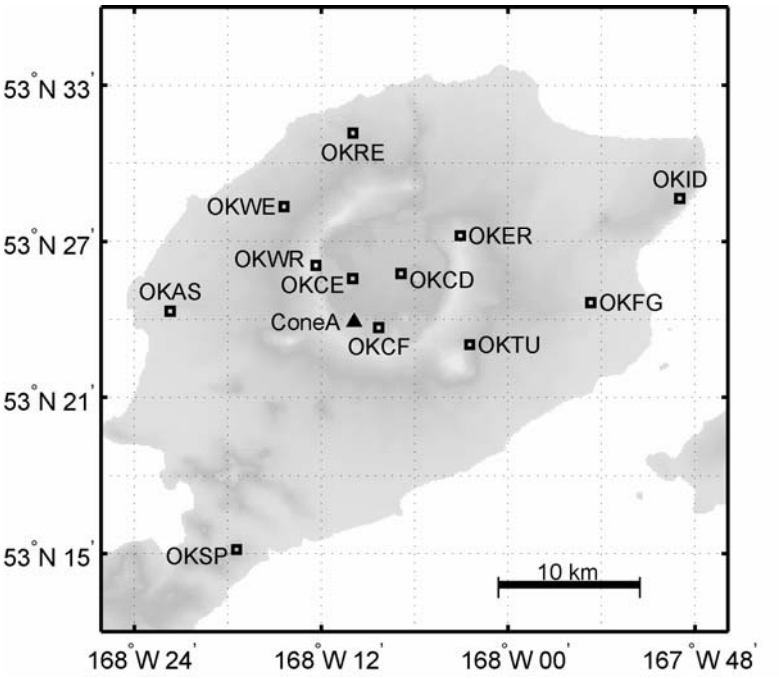

Figure C19. AVO seismograph stations near Okmok Volcano. Seismograph stations are shown by open squares. Closed triangles show volcanic centers.

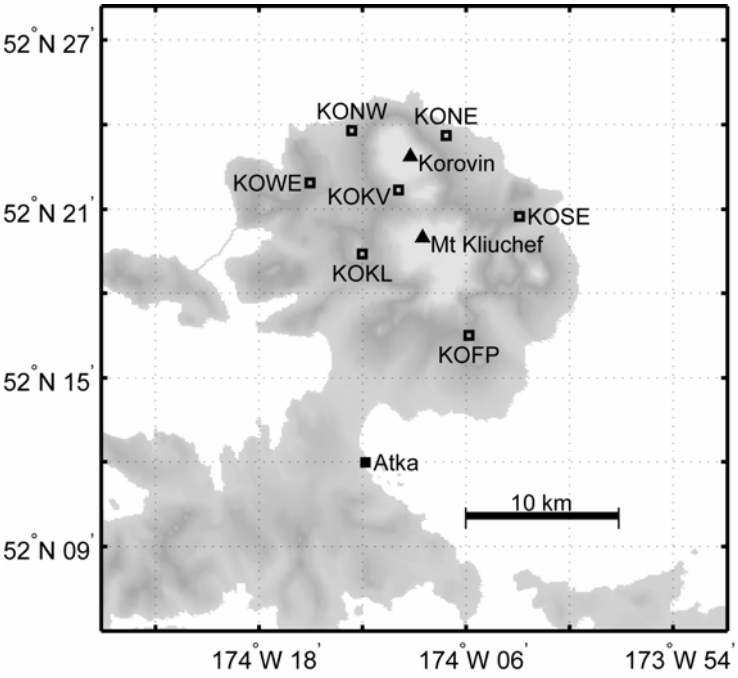

Figure C20. AVO seismograph stations near Korovin Volcano. Seismograph stations are shown by open squares. Closed triangles show volcanic centers.

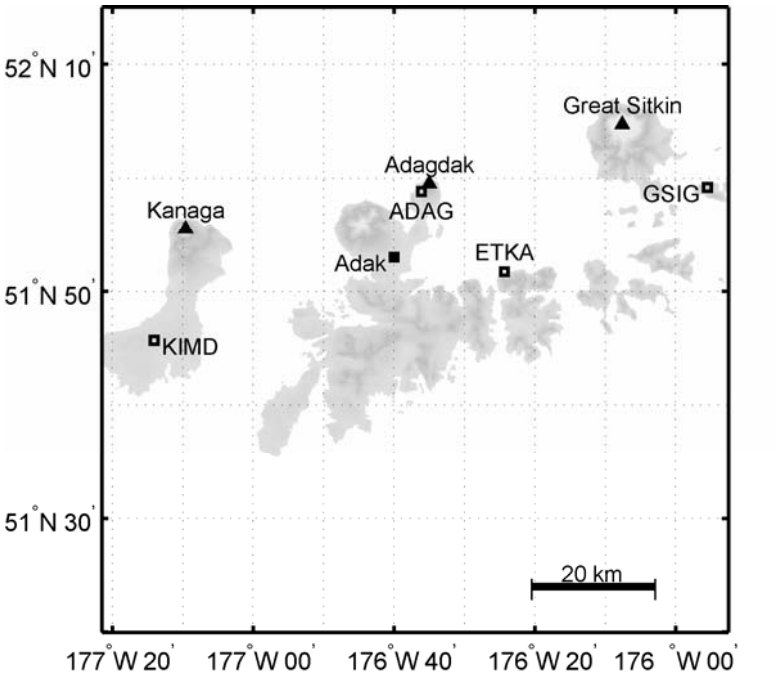

Figure C21. Regional AVO seismograph stations around Adak Island. Seismograph stations are shown by open squares. Closed triangles show volcanic centers.

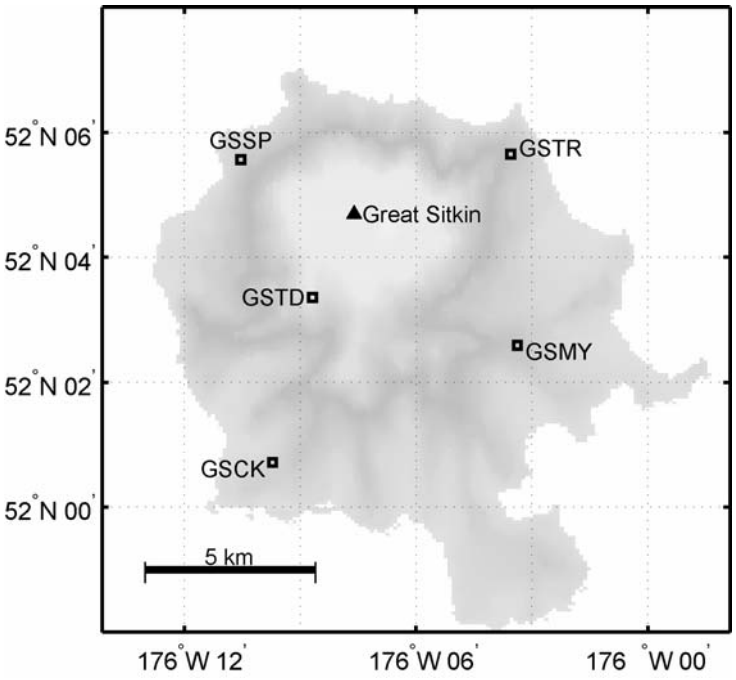

Figure C22. AVO seismograph stations near Great Sitkin Volcano. Seismograph stations are shown by open squares. Closed triangles show volcanic centers.

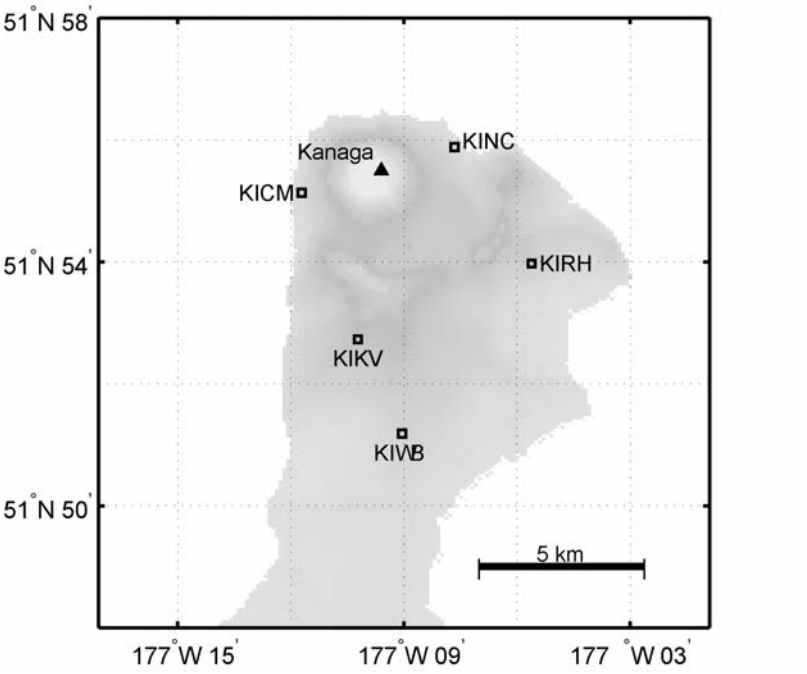

Figure C23. AVO seismograph stations near Kanaga Volcano. Seismograph stations are shown by open squares. Closed triangles show volcanic centers.

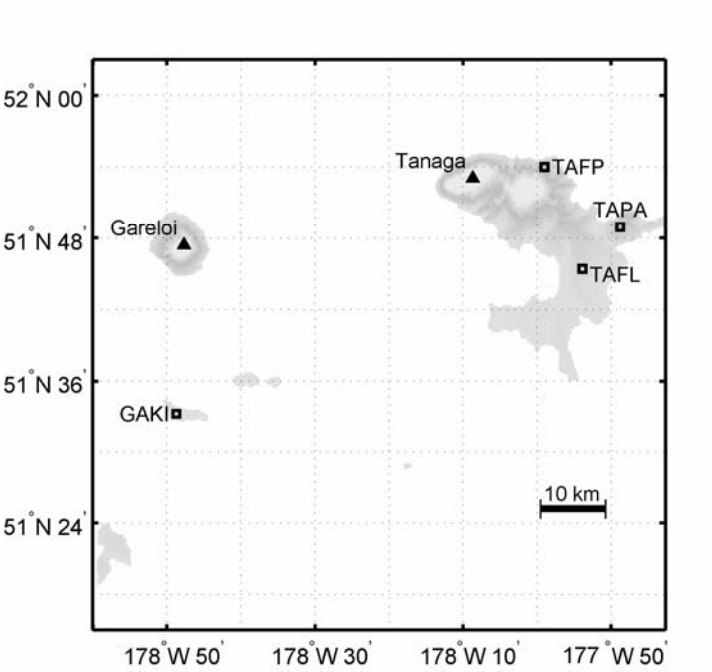

Figure C24. Regional AVO seismograph stations around Tanaga Volcano and Mount Gareloi. Seismograph stations are shown by open squares. Closed triangles show volcanic centers.

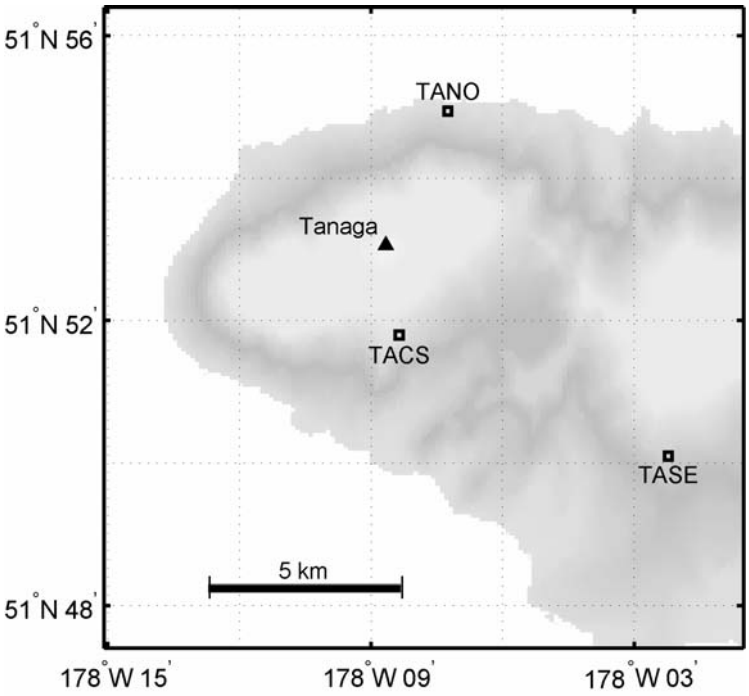

Figure C25. AVO seismograph stations near Tanaga Volcano. Seismograph stations are shown by open squares. Closed triangles show volcanic centers.

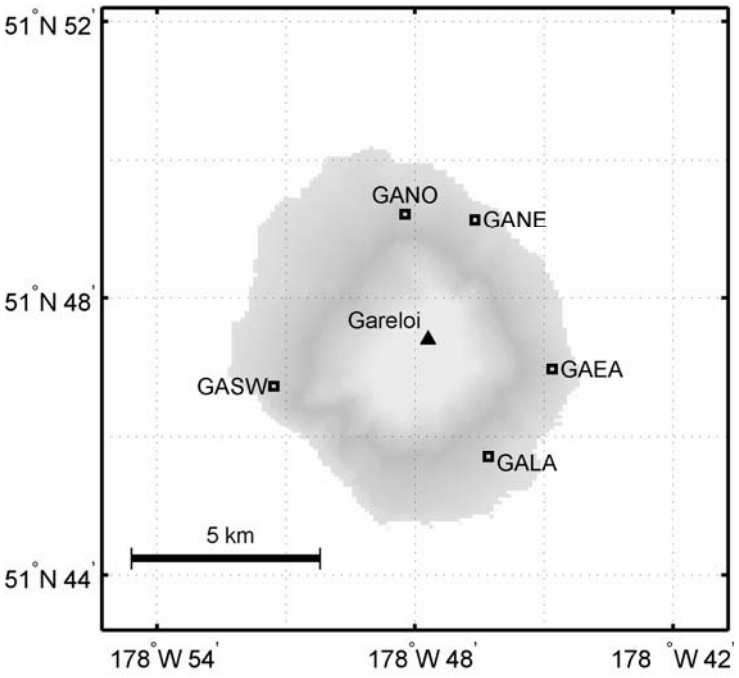

Figure C26. AVO seismograph stations near Mount Gareloi. Seismograph stations are shown by open squares. Closed triangles show volcanic centers.

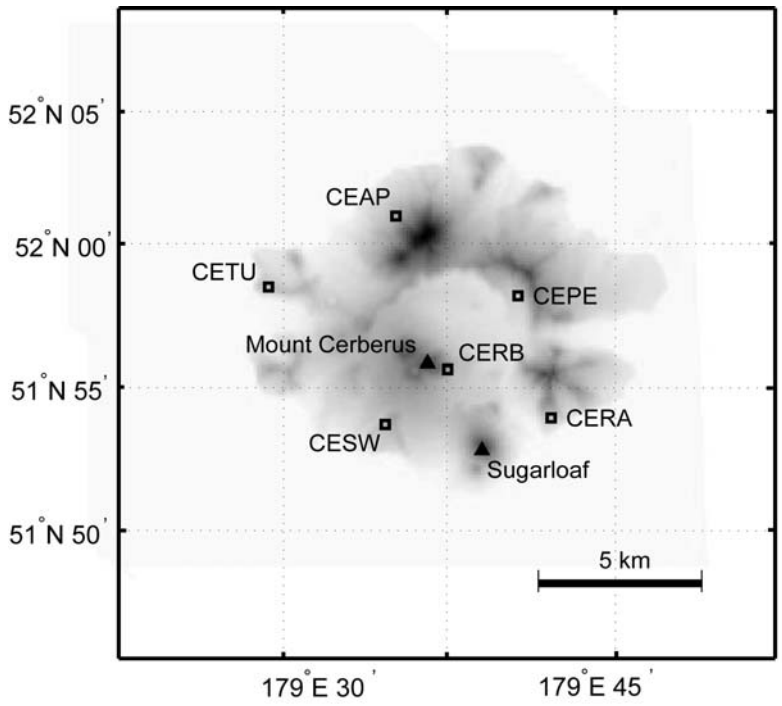

Figure C27. AVO seismograph stations on Semisopochnoi Island. Seismograph stations are shown by open squares. Closed triangles show volcanic centers.

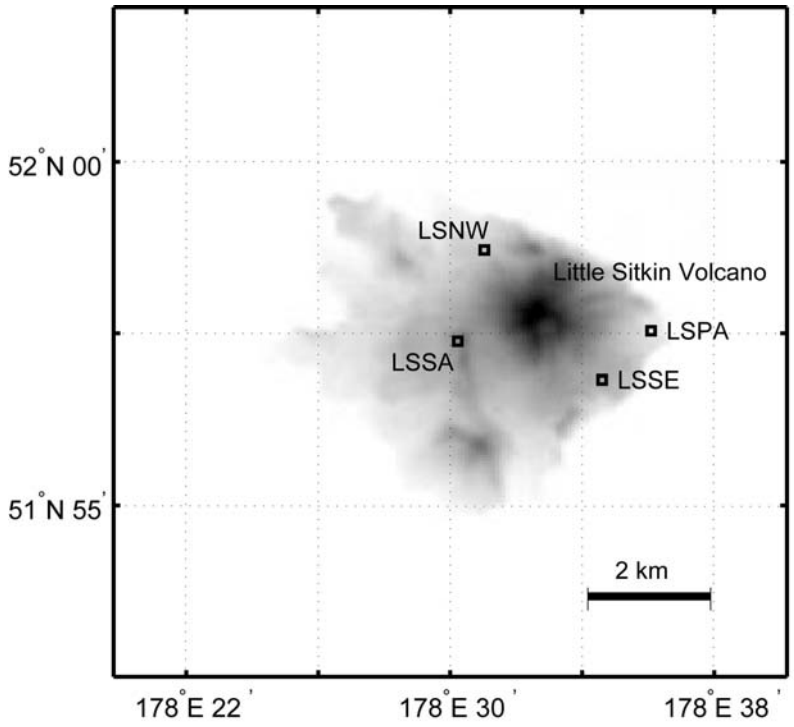

Figure C28. AVO seismograph stations on Little Sitkin Island. Seismograph stations are shown by open squares. Closed triangles show volcanic centers.

Appendix D: Operational status for AVO stations in 2005. A solid bar indicates periods of time a station was operational based on station use plots and weekly checks. Dashed vertical lines show the beginning/end of each month.

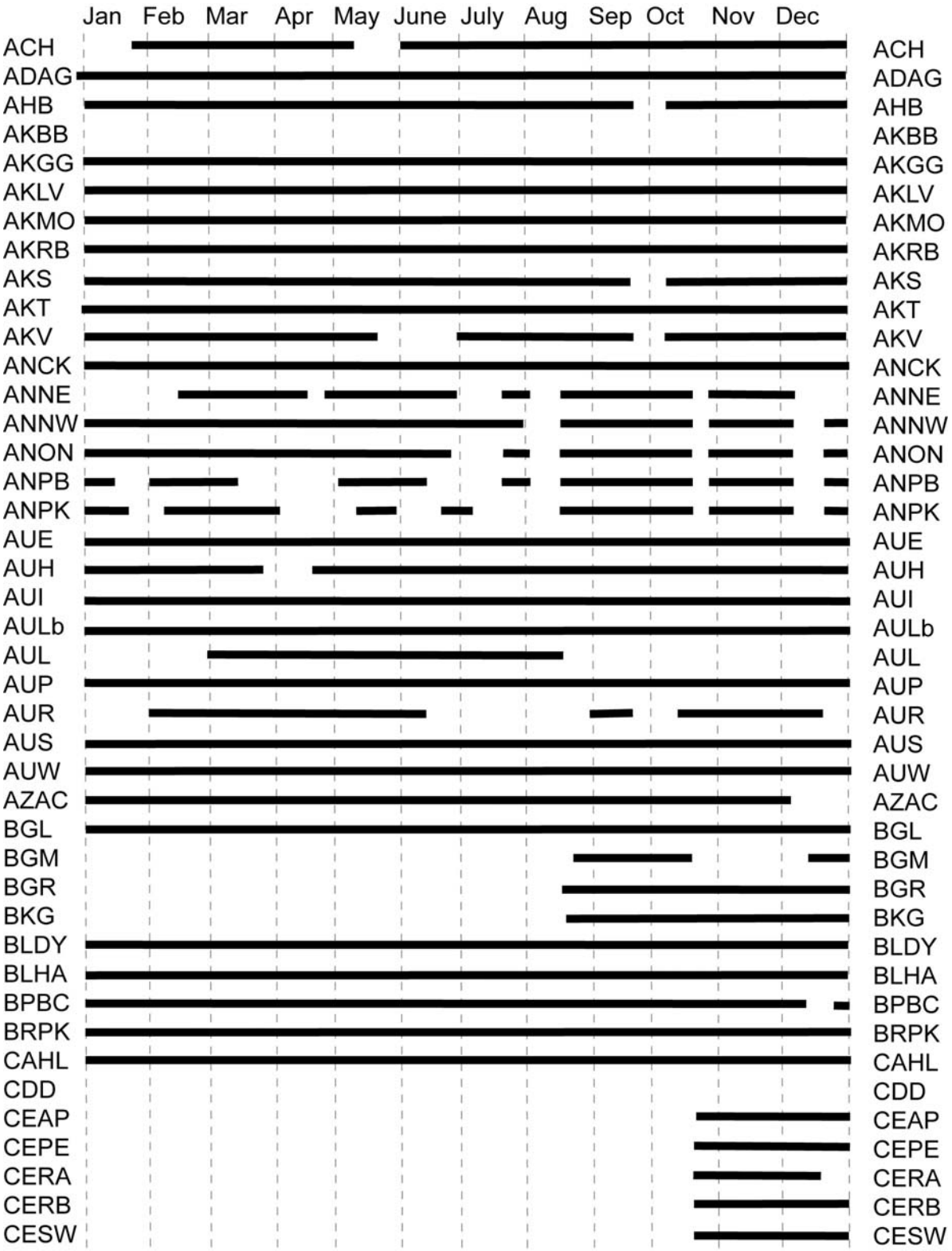

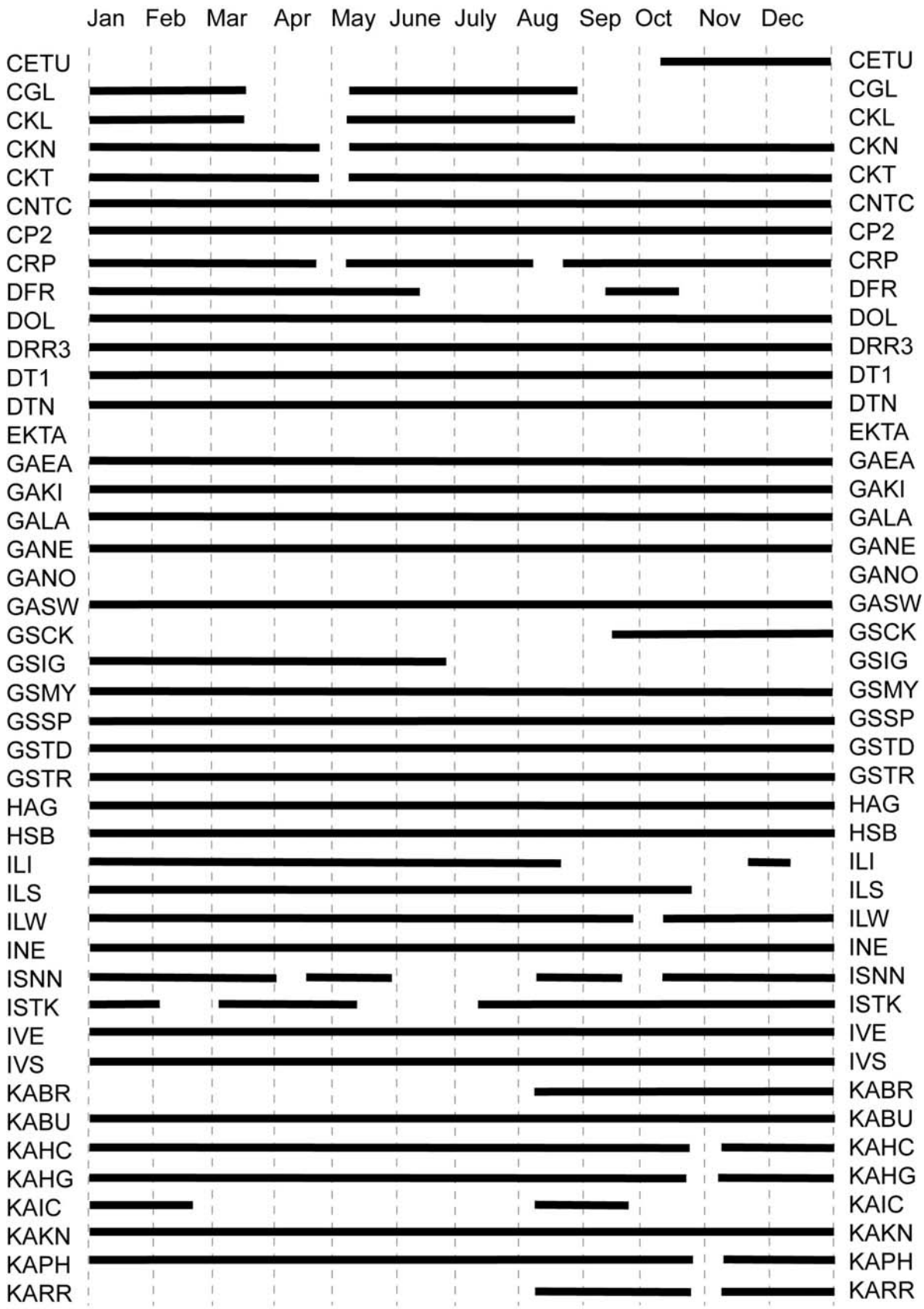
Jan
Feb
Mar
Apr
May
June
July
Aug
Sep
Oct
Nov
Dec
CETU
CGL
CKL
CKN
CKT
CNTC
CP2
CRP
DFR
DOL
DRR3
DT1
DTN
EKTA
GAEA
GAKI
GALA
GANE
GANO
GASW
GSCK
GSIG
GSMY
GSSP
GSTD
GSTR
HAG
HSB
ILI
ILS
ILW
INE
ISNN
ISTK
IVE
IVS
KABR
KABU
KAHC
KAHG
KAIC
KAKN
KAPH
KARR

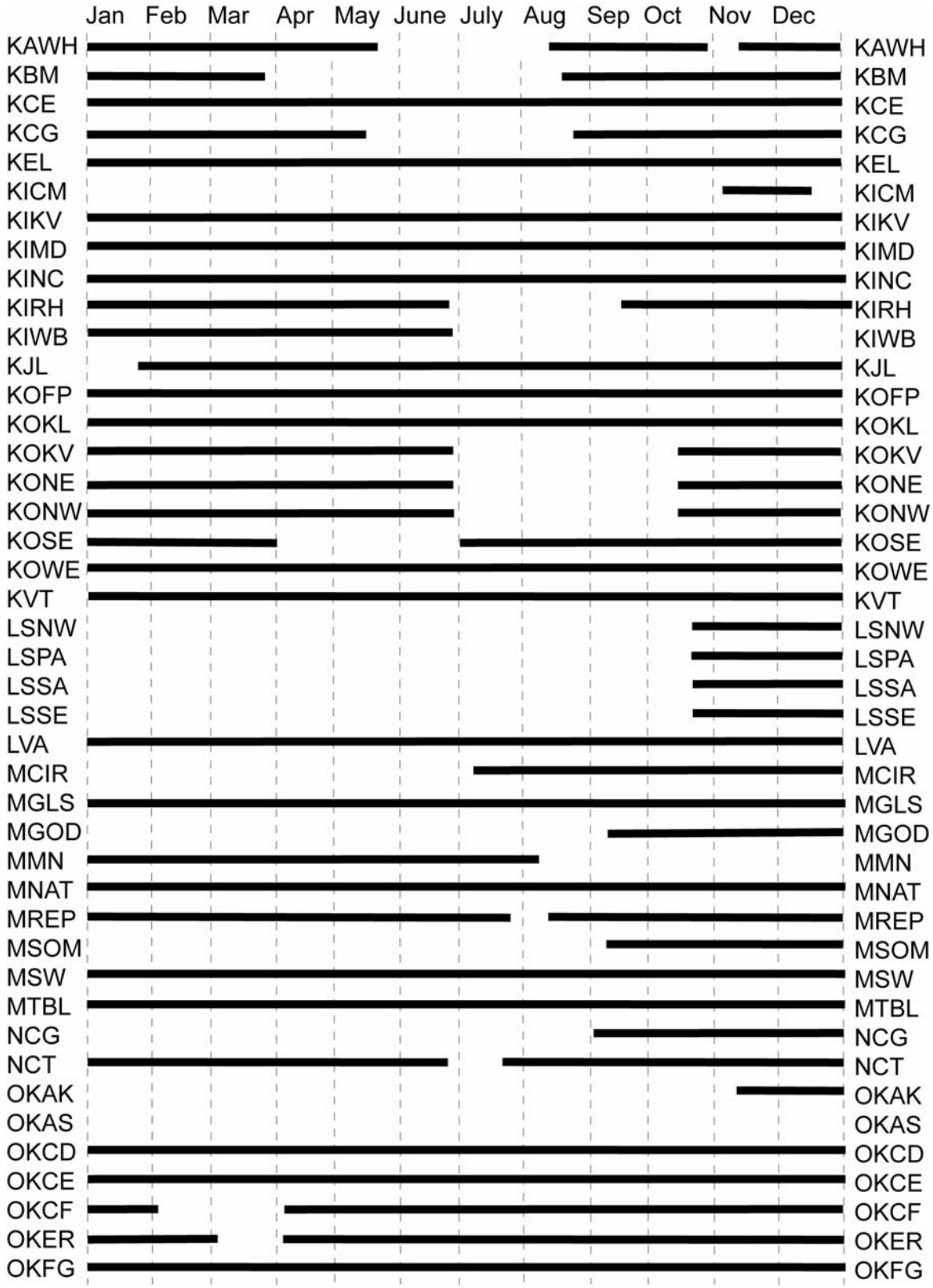
Jan
Feb
Mar
Apr
May
June
July
Aug
Sep
Oct
Nov
Dec
KAWH
KBM
KCE
KCG
KEL
KICM
KIKV
KIMD
KINC
KIRH
KIWB
KJL
KOFP
KOKL
KOKV
KONE
KONW
KOSE
KOWE
KVT
LSNW
LSPA
LSSA
LSSE
LVA
MCIR
MGLS
MGOD
MMN
MNAT
MREP
MSOM
MSW
MTBL
NCG
NCT
OKAK
OKAS
OKCD
OKCE
OKCF
OKER
OKFG

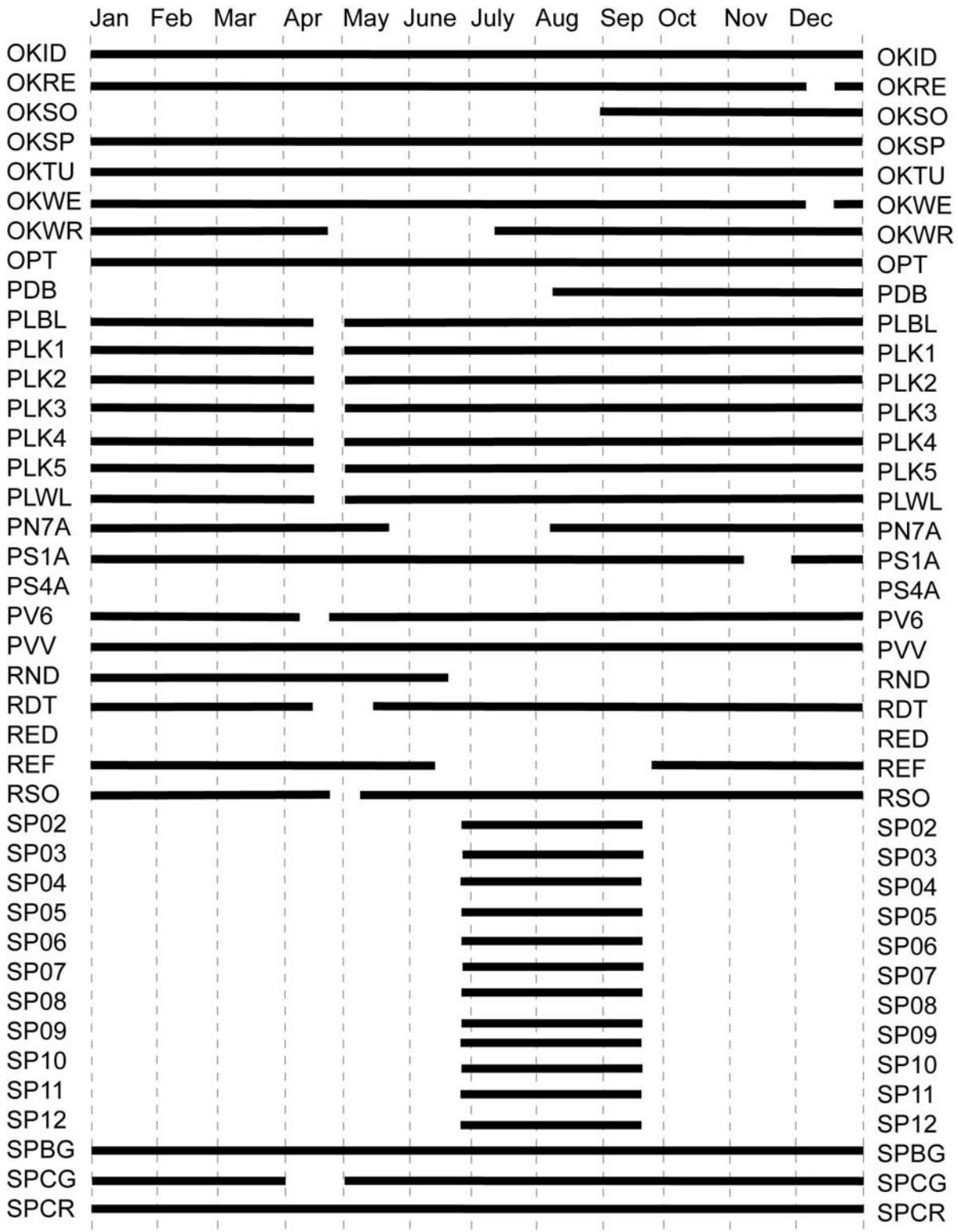
Jan
Feb
Mar
Apr
May
June
July
Aug
Sep
Oct
Nov
Dec
OKID
OKRE
OKSO
OKSP
OKTU
OKWE
OKWR
OPT
PDB
PLBL
PLK1
PLK2
PLK3
PLK4
PLK5
PLWL
PN7A
PS1A
PS4A
PV6
PVV
RND
RDT
RED
REF
RSO
SP02
SP03
SP04
SP05
SP06
SP07
SP08
SP09
SP10
SP11
SP12
SPBG
SPCG
SPCR

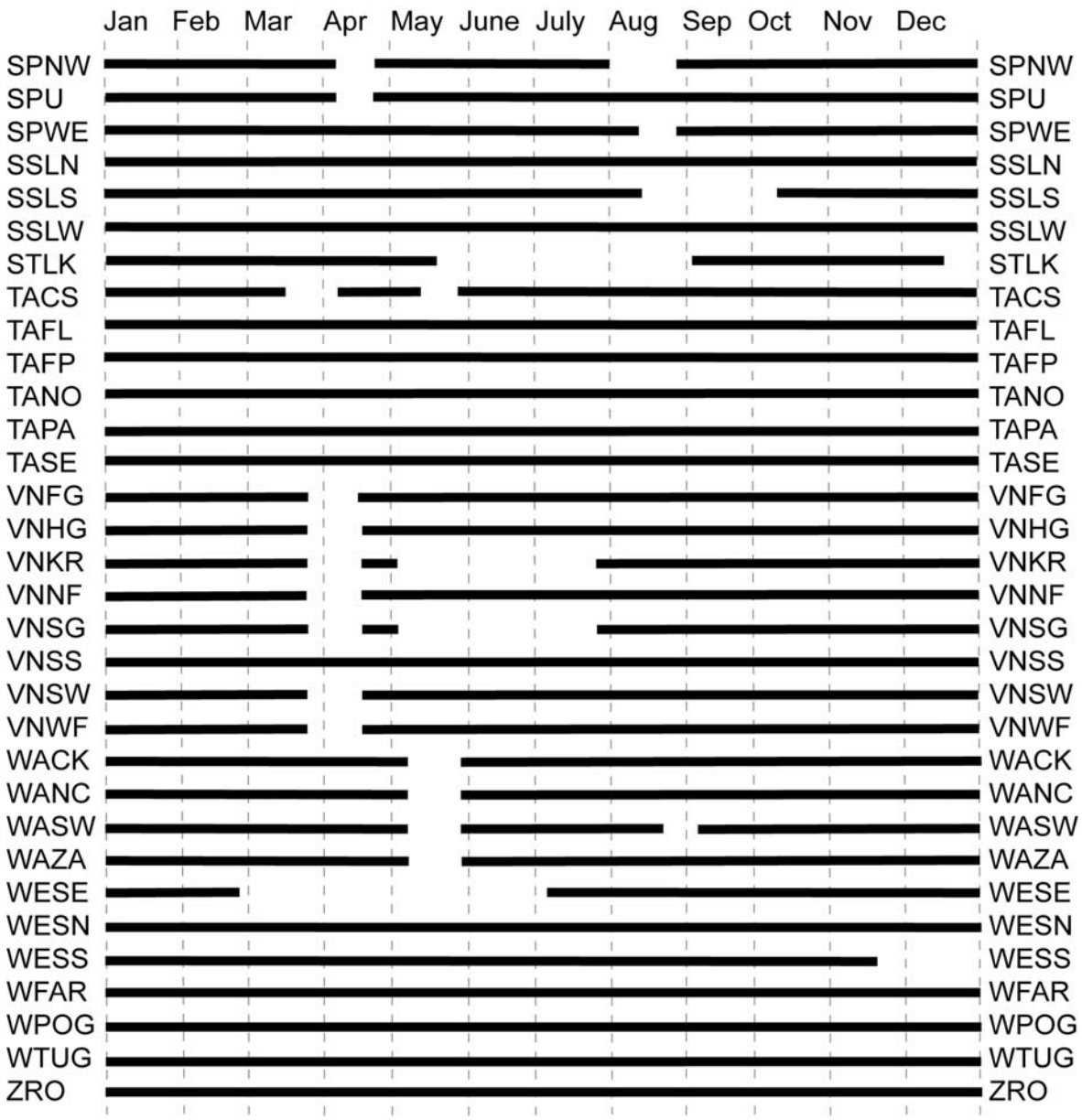
Jan
Feb
Mar
Apr
May
June
July
Aug
Sep
Oct
Nov
Dec
SPNW
SPU
SPWE
SSLN
SSLS
SSLW
STLK
TACS
TAFL
TAFP
TANO
TAPA
TASE
VNFG
VNHG
VNKR
VNNF
VNSG
VNSS
VNSW
VNWF
WACK
WANC
WASW
WAZA
WESE
WESN
WESS
WFAR
WPOG
WTUG
ZRO

Appendix E: Seismic velocity models used in locating the earthquakes described in this report. Following the name of each velocity model is a list of volcano subnetworks for which the model is used. Depths are referenced to sea level, with negative values reflecting height above sea level.

Cylindrical Model Parameters (Latitude and Longitude are the center of the model)

Velocity Model	Latitude (°N)	Longitude (°E)	Radius (km)	Top (km)	Bottom (km)
Spurr	61.60	-152.40	20	-3	50
Spurr	61.47	-152.33	20	-3	50
Spurr	61.33	-152.25	20	-3	50
Spurr	61.17	-152.35	20	-3	50
Spurr	61.00	-152.45	20	-3	50
Redoubt	60.83	-152.55	20	-3	50
Redoubt	60.66	-152.66	20	-3	50
Redoubt	60.49	-152.75	20	-3	50
Redoubt	60.34	-152.86	20	-3	50
Redoubt	60.19	-152.98	20	-3	50
Redoubt	59.87	-153.17	20	-3	50
Redoubt	59.70	-153.25	20	-3	50
Redoubt	59.53	-153.34	20	-3	50
Iliamna	60.03	-153.09	20	-3	50
Augustine	59.36	-153.42	20	-3	50
Katmai	58.17	-155.35	20	-3	50
Katmai	58.29	-154.86	20	-3	50
Katmai	58.35	-155.09	20	-3	50
Katmai	58.43	-154.38	20	-3	50
Veniaminof	56.18	-159.38	30	-3	50
Cold Bay	55.42	-161.89	20	-3	50
Cold Bay	55.18	-162.27	20	-3	50
Cold Bay	54.76	-163.97	30	-3	50
Westdahl	54.52	-164.65	20	-3	50
Akutan	54.15	-165.97	20	-3	50
Andreanof	52.08	-176.13	20	-3	50
Andreanof	51.93	-176.75	20	-3	50
Andreanof	51.92	-177.17	20	-3	50
Tanaga	51.89	-178.15	20	-3	50

Regional Velocity Model (for all areas south of 62.5°N not covered by a volcano specific model): Aniakchak, Gareloi, Korovin, Little Sitkin, Makushin, Okmok, Peulik, Semisopochnoi, and Wrangell (Fogleman and others, 1993).

Layer number	Vp (km/sec)	Top of layer (km)	Vp/Vs
1	5.3	-3.0	1.78
2	5.6	4.0	1.78
3	6.2	10.0	1.78
4	6.9	15.0	1.78
5	7.4	20.0	1.78
6	7.7	25.0	1.78
7	7.9	33.0	1.78
8	8.1	47.0	1.78
9	8.3	65.0	1.78

Akutan Velocity Model: Akutan (Power and others, 1996).

Layer number	Vp (km/sec)	Top of layer (km)	Vp/Vs
1	2.30 +0.37 km/sec for each km of depth	-3.0	1.80
2	6.30	7.0	1.80

Andreanof Velocity model: Great Sitkin, and Kanaga (Toth and Kisslinger, 1984).

Layer number	Vp (km/sec)	Top of layer (km)	Vp/Vs
1	3.50	-3.0	1.73
2	3.88	-2.8	1.73
3	4.25	-2.6	1.73
4	4.62	-2.4	1.73
5	5.00	-2.2	1.73
6	5.50	-2.0	1.73
7	5.62	-1.0	1.73
8	5.74	0.0	1.73
9	5.86	1.0	1.73
10	5.98	2.0	1.73
11	6.10	3.0	1.73
12	6.60	4.0	1.73
13	6.68	5.0	1.73
14	6.80	8.0	1.73
15	6.92	11.0	1.73
16	7.04	14.0	1.73
17	7.16	17.0	1.73
18	7.28	20.0	1.73
19	7.85	23.0	1.73
20	8.05	37.0	1.73

Augustine Velocity Model: Augustine (Power, 1988).

Layer number	Vp (km/sec)	Top of layer (km)	Vp/Vs
1	2.3	-3.0	1.80
2	2.6	-0.7	1.80
3	3.4	0.0	1.80
4	5.1	1.0	1.80
5	6.3	9.0	1.78
6	8.0	44.0	1.78

Cold Bay Velocity Model: Dutton, Pavlof, and Shishaldin (McNutt and Jacob, 1986).

Layer number	Vp (km/sec)	Top of layer (km)	Vp/Vs
1	3.05	-3.00	1.78
2	3.44	0.00	1.78
3	5.56	1.79	1.78
4	6.06	3.65	1.78
5	6.72	10.18	1.78
6	7.61	22.63	1.78
7	7.90	38.51	1.78

Iliamna Velocity model: Iliamna (Roman and others, 2001) .

Layer number	Vp (km/sec)	Top of layer (km)	Vp/Vs
1	4.8	-3.0	1.78
2	6.1	-1.6	1.78
3	6.2	1.7	1.78
4	6.3	2.9	1.78
5	6.4	3.1	1.78
6	7.1	16.5	1.78

Katmai Velocity Model: Katmai (Searcy, 2003).

Layer number	Vp (km/sec)	Top of layer (km)	Vp/Vs
1	5.05	-3.0	1.78
2	5.10	1.0	1.78
3	5.41	2.0	1.78
4	5.49	3.0	1.78
5	5.65	4.0	1.78
6	5.67	5.0	1.78
7	5.69	6.0	1.78
8	5.76	7.0	1.78
9	5.80	8.0	1.78
10	6.00	9.0	1.78
11	6.04	10.0	1.78
12	6.08	12.0	1.78
13	6.30	15.0	1.78
14	6.73	20.0	1.78
15	7.54	25.0	1.78
16	7.78	33.0	1.78

Redoubt Velocity Model: Redoubt (Lahr and others, 1994) .

Layer number	Vp (km/sec)	Top of layer (km)	Vp/Vs
1	2.90	-3.0	1.80
2	5.10	-1.7	1.80
3	6.40	1.5	1.72
4	7.00	17.0	1.78

Spurr Velocity Model: Spurr (Jolly and others, 1994).

Layer number	Vp (km/sec)	Top of layer (km)	Vp/Vs
1	5.1	-3.00	1.81
2	5.5	-2.00	1.81
3	6.3	5.25	1.74
4	7.2	27.25	1.78

Tanaga Velocity Model: Tanaga (Power, personal communication, 2005) .

Layer number	Vp (km/sec)	Top of layer (km)	Vp/Vs
1	4.0	-3.0	1.78
2	4.5	-1.2	1.78
3	5.0	0.0	1.78
4	5.6	4.0	1.78
5	6.9	10.0	1.78
6	7.2	15.0	1.78
7	7.8	20.0	1.78
8	8.1	33.0	1.78

Veniaminof Velocity Model: Veniaminof (Sánchez, 2005) .

Layer number	Vp (km/sec)	Top of layer (km)	Vp/Vs
1	4.82	-3.0	1.73
2	5.23	4.0	1.88
3	5.23	10.0	1.38
4	6.49	15.0	1.65
5	6.52	20.0	1.51
6	8.18	25.0	1.89
7	8.21	33.0	1.90
8	8.21	47.0	1.80
9	8.30	65.0	1.78

Westdahl Velocity Model: Westdahl (Dixon and others, 2005).

Layer number	Vp (km/sec)	Top of layer (km)	Vp/Vs
1	3.03	-3.0	1.71
2	3.18	0.0	1.71
3	5.03	2.0	1.71
4	5.70	8.0	1.71
5	6.30	10.0	1.71
6	6.82	16.0	1.71
7	7.17	26.0	1.71
8	8.16	38.0	1.71

Appendix F: Maps showing the location of volcanic zones modeled using multiple cylinders. Volcanic centers, modeled by a single cylinder, are not shown.

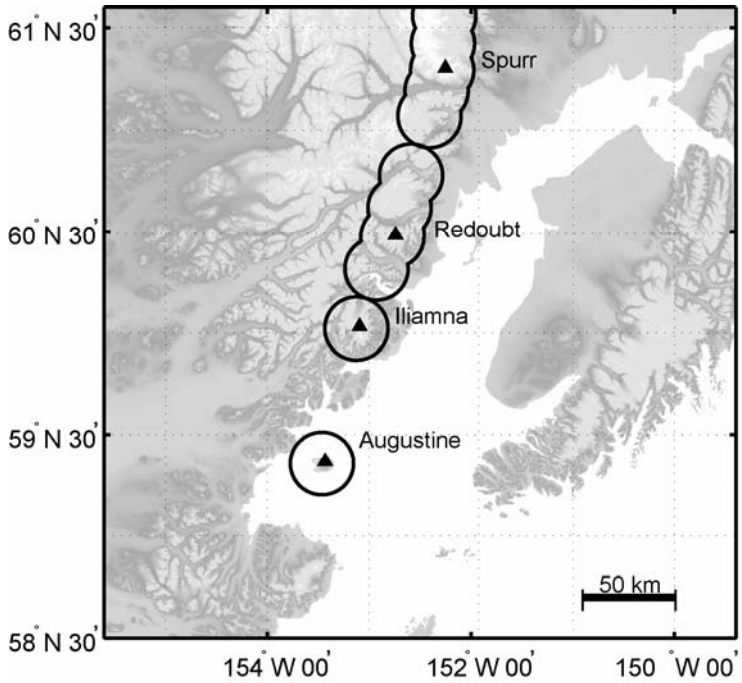

Figure F1. Volcanic zones for the Cook Inlet Volcanoes. Five overlapping cylinders model the Spurr volcanic zone. Four overlapping cylinders model the Redoubt volcanic zone. Single cylinders model the Iliamna and Augustine volcanic zones.

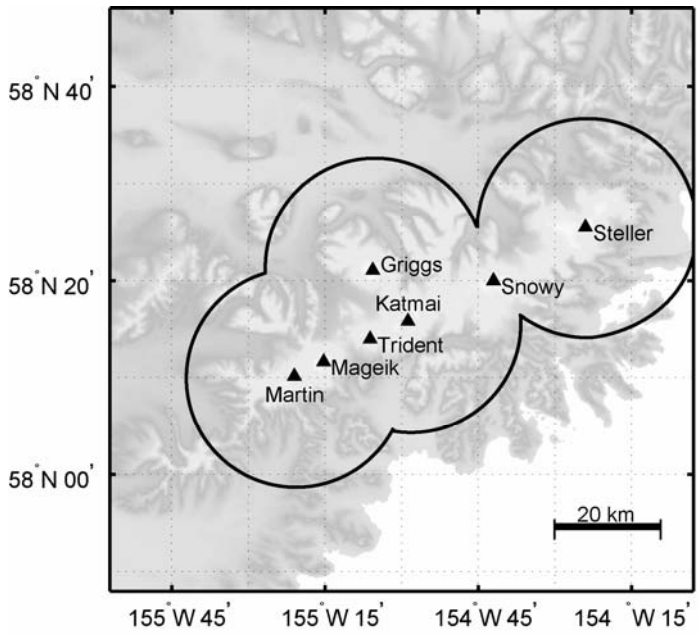

Figure F2. Volcanic zone for the Katmai volcanic cluster. The volcanic zone is modeled using four cylinders centered on Mount Martin, Mount Katmai, Mount Griggs and Mount Steller.

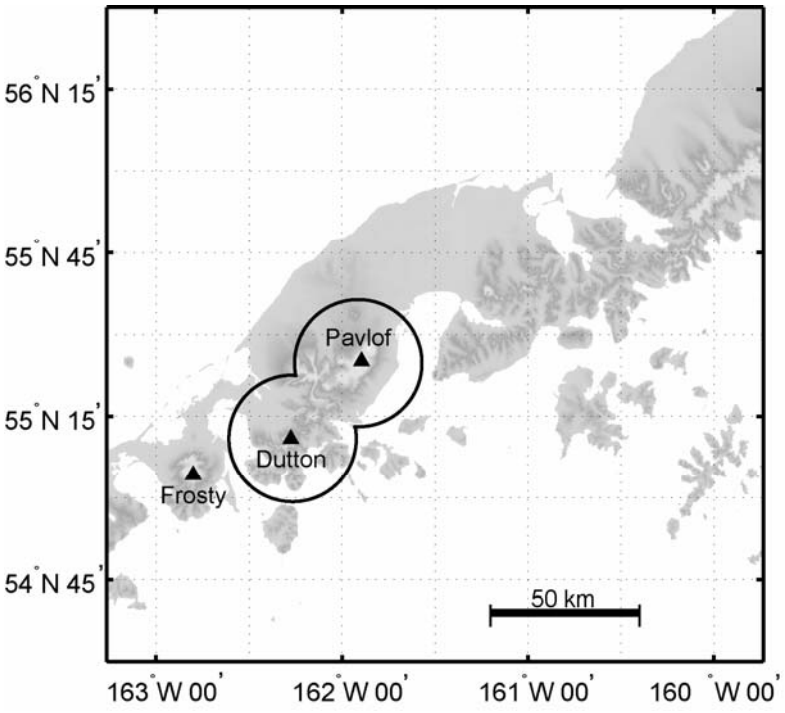

Figure F3. Volcanic zones for Mount Veniaminof Dutton. The volcanic zone is modeled using a single cylinder.

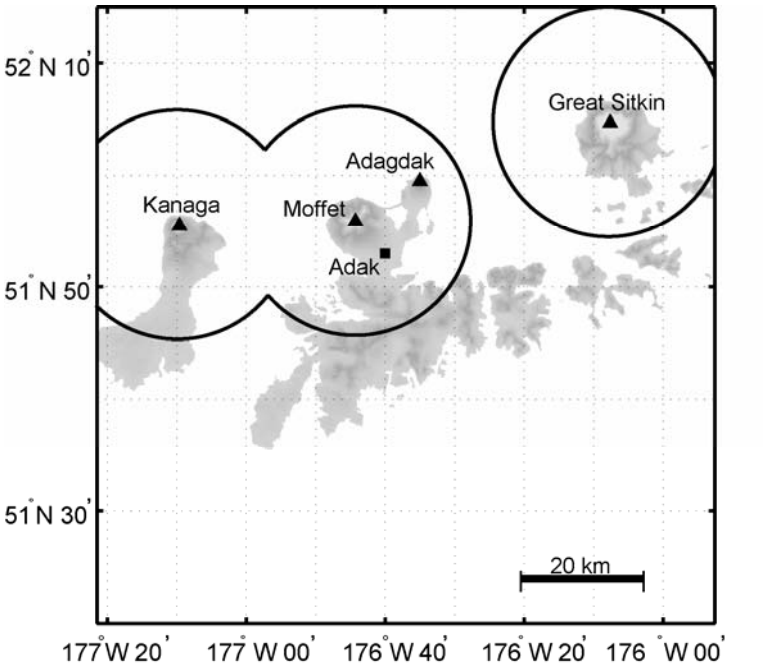

Figure F4. Volcanic zones in the Adak region. The volcanic zones are modeled using cylinders centered on Kanaga Volcano, Mount Moffet, and Great Sitkin Volcano.

Appendix G: Previous AVO Earthquake Catalogs.

1989-90: Power, J. A., G. D. March, J. C. Lahr, A. D. Jolly, and G. R. Cruse (1993). Catalog of earthquake hypocenters at Redoubt Volcano and Mount Spurr, Alaska: October 12, 1989-December 31, 1990, *U.S. Geol. Surv. Open-File Rept., 93-685-A*, 57 p.

1991-93: Jolly, A. D., J. A. Power, S. D. Stihler, L. N. Rao, G. Davidson, J. Paskievitch, S. Estes, J. C. Lahr (1996). Catalog of earthquake hypocenters for Augustine, Redoubt, Iliamna, and Mount Spurr Volcanoes, Alaska: January 1, 1991 – December 31, 1993, *U.S. Geol. Surv. Open-File Rept. 96-70*, 90 p.

1994-99: Jolly, A. D., S. D. Stihler, J. A. Power, J. C. Lahr, J. Paskievitch, G., Tytgat, S. Estes, A. B. Lockhart, S. C. Moran, S. R. McNutt, and W. R. Hammond (2001). Catalog of earthquake hypocenters at Alaskan Volcanoes: January 1, 1994 – December 31, 1999, *U.S. Geol. Surv. Open-File Rept. t 01-189*, 202 p.

2000-01: Dixon, J. P, S. D. Stihler, J. A. Power, G. Tytgat, S. Estes, S. C. Moran, J. Paskievitch, and S. R. McNutt (2002). Catalog of Earthquake Hypocenters at Alaska Volcanoes: January 1, 2000 – December 31, 2001, *U.S. Geol. Surv. Open-File Rept. 02-342*, 56 p.

2002: Dixon, J. P., S. D. Stihler, J. A. Power, G. Tytgat, S. C. Moran, J. J. Sánchez, S. Estes, S. R. McNutt and J. Paskievitch (2003). Catalog of Earthquake Hypocenters at Alaska Volcanoes: January 1 – December 31, 2002, *U.S. Geol. Surv. Open-File Rept. 03-267*, 58 p.

2003: Dixon, J. P., S. D. Stihler, J. A. Power, G. Tytgat, S. C. Moran, J. J. Sánchez, S. Estes, S. R. McNutt, and J. Paskievitch (2004). Catalog of Earthquake Hypocenters at Alaska Volcanoes: January 1 – December 31, 2003, *U.S. Geol. Surv. Open-File Rept. 2004-1234*, 59 p.

2004: Dixon, J. P., S. D. Stihler, J. A. Power, G. Tytgat, S. Estes, S. Prejean, J. J. Sánchez, R. Sanches, S. R. McNutt, and J. Paskievitch (2005). Catalog of Earthquake Hypocenters at Alaskan Volcanoes: January 1 through December 31, 2004, *U.S. Geol. Surv. Open-File Rept. 2005-1312*, 74 p.

Appendix H: Selected AVO papers published in 2005

De Angelis, S. and S. R. McNutt (2005). Degassing and hydrothermal activity at Mt. Spurr, Alaska during the summer of 2004 inferred from the complex frequencies of long-period events, *Geophys. Res. Lett.*, **32**, L12312, Doi: 10.1029/2005GL022618.

Lu, Z., C. Wicks, O. Kwoun, J. A. Power, D. Dzurisin (2005). Surface deformation associated with the March 1996 earthquake swarm at Akutan Island, Alaska, revealed by C-band ERS and L-band radar interferometry, *Can. J. Remote Sensing*, **31**, 7-20.

McNutt, S. R. (2005). A Review of Volcanic Seismology. *Ann. Rev. Earth Planet. Sci.*, **33**, 461-491 doi: 10.1146/annurev.earth.33.092203.122459.

West, M., J. J. Sánchez, and S. R. McNutt (2005). Periodically-triggered seismicity at Mt. Wrangell volcano following the Sumatra-Andaman Islands earthquake, *Science*, **308**, 1144-1146.